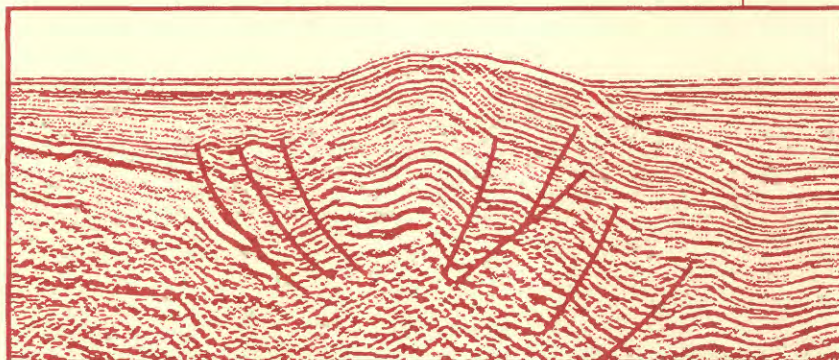


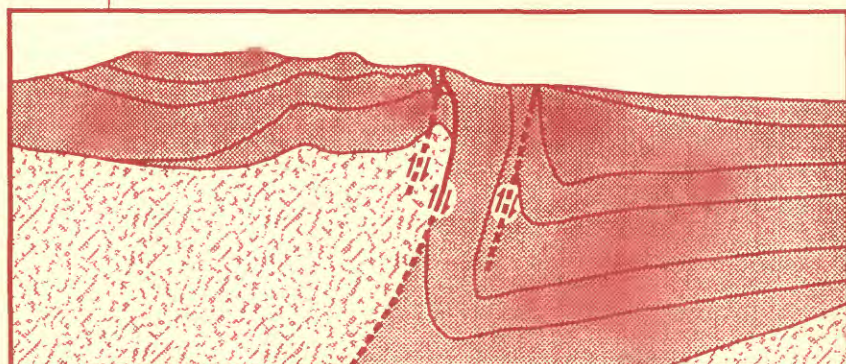
# Volcanic Rocks of the Santa Maria Province, California

## Age and Tectonic Inferences from a Condensed(?) Succession of Upper Cretaceous, Paleocene, and Eocene Strata, Big Pine Mountain Area, Santa Barbara County, California

Bulletin 1995–R, S



Geophysical section offshore Santa Maria basin



Geologic section onshore Santa Maria basin

---

## AVAILABILITY OF BOOKS AND MAPS OF THE U.S. GEOLOGICAL SURVEY

---

Instructions on ordering publications of the U.S. Geological Survey, along with prices of the last offerings, are given in the current-year issues of the monthly catalog "New Publications of the U.S. Geological Survey." Prices of available U.S. Geological Survey publications released prior to the current year are listed in the most recent annual "Price and Availability List." Publications that may be listed in various U.S. Geological Survey catalogs (**see back inside cover**) but not listed in the most recent annual "Price and Availability List" may no longer be available.

Reports released through the NTIS may be obtained by writing to the National Technical Information Service, U.S. Department of Commerce, Springfield, VA 22161; please include NTIS report number with inquiry.

Order U.S. Geological Survey publications **by mail** or **over the counter** from the offices listed below.

### BY MAIL

#### Books

Professional Papers, Bulletins, Water-Supply Papers, Techniques of Water-Resources Investigations Reports, Circulars, publications of general interest (such as leaflets, pamphlets, booklets), single copies of Earthquakes & Volcanoes, Preliminary Determination of Epicenters, and some miscellaneous reports, including some of the foregoing series that have gone out of print at the Superintendent of Documents, are obtainable by mail from

U.S. Geological Survey, Information Services  
Box 25286, Federal Center  
Denver, CO 80225

Subscriptions to periodicals (Earthquakes & Volcanoes and Preliminary Determination of Epicenters) can be obtained **ONLY** from the

Superintendent of Documents  
Government Printing Office  
Washington, DC 20402

(Check or money order must be payable to Superintendent of Documents.)

#### Maps

For maps, address mail orders to

U.S. Geological Survey, Information Services  
Box 25286, Federal Center  
Denver, CO 80225

Residents of Alaska may order maps from

U.S. Geological Survey  
Earth Science Information Center  
101 Twelfth Ave., Box 12  
Fairbanks, AK 99701

### OVER THE COUNTER

#### Books and Maps

Books and maps of the U.S. Geological Survey are available over the counter at the following U.S. Geological Survey offices, all of which are authorized agents of the Superintendent of Documents.

- **ANCHORAGE, Alaska**—Rm. 101, 4230 University Dr.
- **LAKEWOOD, Colorado**—Federal Center, Bldg. 810
- **MENLO PARK, California**—Bldg. 3, Rm. 3128, 345 Middlefield Rd.
- **RESTON, Virginia**—USGS National Center, Rm. 1C402, 12201 Sunrise Valley Dr.
- **SALT LAKE CITY, Utah**—Federal Bldg., Rm. 8105, 125 South State St.
- **SPOKANE, Washington**—U.S. Post Office Bldg., Rm. 135, West 904 Riverside Ave.
- **WASHINGTON, D.C.**—Main Interior Bldg., Rm. 2650, 18th and C Sts., NW.

#### Maps Only

Maps may be purchased over the counter at the following U.S. Geological Survey offices:

- **FAIRBANKS, Alaska**—New Federal Bldg, 101 Twelfth Ave.
- **ROLLA, Missouri**—1400 Independence Rd.
- **STENNIS SPACE CENTER, Mississippi**—Bldg. 3101

# Volcanic Rocks of the Santa Maria Province, California

By RONALD B. COLE and RICHARD G. STANLEY

# Age and Tectonic Inferences from a Condensed(?) Succession of Upper Cretaceous, Paleocene, and Eocene Strata, Big Pine Mountain Area, Santa Barbara County, California

By JOHN G. VEDDER, RICHARD G. STANLEY, HUGH  
McLEAN, MARY LOU COTTON, MARK V. FILEWICZ, and  
DAVID R. VORK

Chapters R and S are issued as a single volume  
and are not available separately

U.S. GEOLOGICAL SURVEY BULLETIN 1995

EVOLUTION OF SEDIMENTARY BASINS/ONSHORE OIL AND GAS INVESTIGATIONS—  
SANTA MARIA PROVINCE

Edited by Margaret A. Keller

U.S. DEPARTMENT OF THE INTERIOR  
BRUCE BABBITT, Secretary



U.S. GEOLOGICAL SURVEY  
Thomas J. Casadevall, Acting Director

Any use of trade, product, or firm names  
in this publication is for descriptive purposes only  
and does not imply endorsement by the U.S. Government

UNITED STATES GOVERNMENT PRINTING OFFICE, WASHINGTON: 1998

---

For sale by  
U.S. Geological Survey  
Information Services  
Box 25286  
Denver Federal Center  
Denver, CO 80225

#### Library of Congress Cataloging in Publication Data

Volcanic rocks of the Santa Maria Province, California/by Ronald B. Cole and Richard G. Stanley. Age and tectonic inferences from a condensed(?) succession of Upper Cretaceous, Paleocene, and Eocene strata, Big Pine Mountain area, Santa Barbara County, California/by John G. Vedder...[et al.]. p. cm. — U.S. Geological Survey bulletin ; 1995)

(Evolution of sedimentary basins/onshore oil and gas investigations—Santa Maria Province; ch. R, S)

“Chapters R and S are issued as a single volume and are not available separately.”

Includes bibliographical references.

Supt. of Docs. no.: I 19.3:1995-R, S.

1. Rocks, Igneous—California—Santa Maria Basin. 2. Geology, Stratigraphic—Tertiary. 3. Geology—California—Santa Maria Basin. 4. Santa Maria Basin (Calif.) 5. Mudstone—California—Big Pine Mountain Region. I. Stanley, Richard G. II. Vedder, John G. III. Title. IV. Title: Age and tectonic inferences from a condensed(?) succession of Upper Cretaceous, Paleocene, and Eocene strata, Big Pine Mountain area, Santa Barbara County, California. V. Series. VI. Series: Evolution of sedimentary basins/onshore oil and gas investigations— Santa Maria Province ; ch. R, S.

QE75.B9 no. 1995-R, S  
[QE461]

557.3s—dc21  
[552'.2'097949]

97-48362  
CIP

Chapter R

# Volcanic Rocks of the Santa Maria Province, California

By RONALD B. COLE and RICHARD G. STANLEY

U.S. GEOLOGICAL SURVEY BULLETIN 1995

EVOLUTION OF SEDIMENTARY BASINS/ONSHORE OIL AND GAS INVESTIGATIONS—  
SANTA MARIA PROVINCE

Edited by Margaret A. Keller

# CONTENTS

Abstract **R1**

Introduction **R1**

Acknowledgements **R3**

Stratigraphy, ages, and descriptions of volcanic rocks **R3**

Tranquillon Volcanics of Dibblee (1950) **R3**

Unnamed basaltic andesite of Santa Rosa Creek **R6**

Unnamed lower Miocene tuffs of the Santa Barbara coast **R7**

Tuff deposits in the Lospe Formation near Point Sal **R7**

Sill near Point Sal **R10**

Obispo Formation and related rocks **R11**

Unnamed volcanic rocks of the Catway Road area **R13**

Unnamed volcanic rocks of the Lopez Mountain area **R14**

Morro Rock–Islay Hill complex **R14**

Cambria Felsite **R14**

Unnamed volcanic rocks of upper Pine Creek **R14**

Subsurface volcanic rocks (onshore and offshore) **R15**

Other occurrences of volcanic rocks **R15**

Geochemistry of volcanic rocks **R16**

Volcanic source areas and paleogeography **R19**

Relations of volcanism to regional tectonic events **R22**

Conclusions **R24**

References cited **R25**

Appendixes—

1. Data, interpretations, and assumptions used to construct the stratigraphic chart for middle Tertiary volcanic units in the Santa Maria province (fig. 2) **R29**
2. Compilation of available major element and selected trace element data for volcanic rocks of the Santa Maria area **R31**
3. Subsurface data used to construct lower Miocene volcanic thickness map of figure 15 **R34**

## FIGURES

1. Map of the Santa Maria province **R2**
2. Stratigraphic chart for middle Tertiary volcanic units in the Santa Maria province **R4**
3. Schematic stratigraphic column of the Tranquillon Volcanics of Dibblee (1950) near Tranquillon Mountain **R6**
4. Photographs of the Tranquillon Volcanics of Dibblee (1950) in its type area near Tranquillon Mountain **R6**
5. Unnamed basaltic andesite near Santa Rosa Creek in an outcrop about 25 km east of Tranquillon Mountain **R7**
6. Schematic composite stratigraphic section of the Lospe Formation in its type area near Point Sal **R8**
7. Photographs of tuff deposits in the Lospe Formation in its type area near Point Sal. **R9**
8. Composite stratigraphy of subaqueous tuffs in the upper member of the Lospe Formation that were deposited as reworked ash from high-density turbidity flows **R10**

9. Photomicrograph under cross-polarized light of trachybasalt sill that intrudes the Point Sal Formation near Point Sal **R11**
10. Representative stratigraphic columns of the Obispo Formation drawn from original field data of this study combined with data reported by Schneider and Fisher (1996) **R11**
11. Photographs of the Obispo Formation **R12**
12. Catway volcanics in the Catway Road area **R13**
13. Photomicrograph of unnamed basalt at Lopez Mountain under cross-polarized light **R14**
14. Photographs of intrusion at Morro Rock **R15**
15. Thickness map of lower Miocene volcanic rocks in part of the Santa Maria province **R16**
16. Silica ( $\text{SiO}_2$ ) versus total alkalis ( $\text{Na}_2\text{O} + \text{K}_2\text{O}$ ) for Santa Maria province volcanic rocks showing lithologic classifications of LeBas and others (1986) **R17**
17. Silica ( $\text{SiO}_2$ ) versus titanium ( $\text{TiO}_2$ ), magnesium ( $\text{MgO}$ ), sodium ( $\text{Na}_2\text{O}$ ), and potassium ( $\text{K}_2\text{O}$ ) for volcanic units in the Santa Maria province **R18**
18. Samarium (Sm) versus hafnium (Hf) variation diagram for selected 20-16 Ma volcanic units in the Santa Maria province **R19**
19. Lanthanum (La) versus samarium (Sm), ytterbium (Yb), and niobium (Nb) for selected 20-16 Ma volcanic units in the Santa Maria province **R20**
20. Early Miocene paleogeographic reconstruction for the Santa Maria province and simplified model of block rotations and zones of crustal extension **R23**

#### TABLE

1. Compilation of available radiometric ages for volcanic rocks in and around the Santa Maria province **R5**



# Volcanic Rocks of the Santa Maria Province, California

By Ronald B. Cole<sup>1</sup> and Richard G. Stanley

## ABSTRACT

Volcanic and intrusive rocks within the Santa Maria province of central California comprise two age groups (28-23 Ma and 20-16 Ma) that record at least two separate episodes of crustal extension or transtension. These episodes occurred during a transition from a convergent to a transform plate boundary in western California as segments of the Farallon-Pacific spreading ridge intersected the continental margin in the vicinity of the Santa Maria province. The source for the volcanic and intrusive rocks included basaltic upper-mantle-derived magmas (similar to mid-ocean ridge basalt magmas) that melted and assimilated silicic crustal rocks to form a bimodal igneous suite.

Santa Maria province volcanic units include subaerial and subaqueous acidic pyroclastic flow deposits, pyroclastic fallout deposits, basaltic breccias, volcanoclastic turbidites, and various basaltic flows. Felsic and mafic intrusive rocks are also present within the Santa Maria province. Based on a combination of surface and subsurface data, the thickness of lower Miocene volcanic rocks ranges from zero in much of the central Santa Maria province (including the Santa Maria basin) to more than 4,900 feet (1,490 meters) in places along the margins. Major eruptive centers identified on the basis of volcanic facies, thickness of volcanic units, paleoflow data, and paleobathymetry were most likely present in the northern and southern parts of the Santa Maria province along the Santa Maria River and Santa Ynez River Faults, respectively. These eruptive centers probably coincided with zones of extension that resulted from clockwise rotation of the western Transverse Ranges and slivering of the Santa Maria basin by northwest-trending faults. Eruptive centers for Santa Maria volcanism may also have been along the Hosgri Fault Zone in the present offshore Santa Maria basin, where reported lower Miocene volcanic rocks in the subsurface locally exceed 900 feet (274 meters) in thickness.

## INTRODUCTION

The Santa Maria province of central California contains several middle Tertiary volcanic units that provide

regional and local stratigraphic marker horizons in petroliferous sedimentary basins, including the onshore and offshore Santa Maria basins (fig. 1). Volcanism and coeval basin development in the Santa Maria province were coincident with a transition from convergent to transform plate boundaries along western California as segments of the Farallon-Pacific spreading ridge intersected North America (Atwater, 1970, 1989). This paper summarizes and combines existing data with new information on the stratigraphy, distribution, depositional histories, geochemistry, and tectonic implications of Santa Maria province volcanic units. This information is important for understanding the relations between middle Tertiary volcanic events, basin development, and tectonism in west-central California.

Volcanic rocks have long been recognized and mapped within the Santa Maria province (for example, Woodring and Bramlette, 1950; Dibblee, 1950, 1966, 1988a,b, 1989; Hall and Corbató, 1967; Vedder and others, 1967, 1994; Hall, 1973, 1978, 1982; Ernst and Hall, 1974; Hall and others, 1979; McLean, 1994). Within this area more than a dozen separate volcanic units have been identified, with exposures that range from small outcrops of tens to hundreds of square meters to regional outcrop belts extending for tens of kilometers (fig. 1). The volcanic units, some of which are not yet formally named, include a wide array of mafic and felsic lavas and pyroclastic deposits that are interbedded with nonmarine and marine sedimentary rocks. The volcanic rocks overall preserve a history of diverse eruption styles and deposition around several eruptive centers within the Santa Maria province. Hall and others (1966), Fisher (1977), and Surdam and Hall (1984) discuss aspects of the Obispo Formation, one of the larger volcanic units in the region, which includes a diverse assemblage of mafic to felsic pyroclastic deposits and lavas. Recently in another paper of this bulletin, Schneider and Fisher (1996) interpret thick pyroclastic units of the Obispo Formation as submarine deposits of remobilized ash. The work of Robyn (1979, 1980) represents the first focused analysis of felsic pyroclastic rocks at Tranquillon Mountain, which we believe is in the vicinity of an important eruptive center that existed in the southern portion of the Santa Maria province. Cole and Stanley (1994) interpret felsic tuffs in the Lospe Formation as the deposits of pyroclastic flows and subaqueous sediment gravity flows of

<sup>1</sup>Department of Geology, Allegheny College, Meadville, PA 16335.

Manuscript approved for publication January 13, 1998

reworked ash that was probably derived from eruptions in the vicinity of Tranquillon Mountain. In addition, several smaller, less well exposed volcanic units within the Santa Maria province have been described elsewhere (for ex-

ample, Ballance and others, 1983; Vedder and others, 1991; McLean, 1994; Hornafius, 1994). This paper provides the first coherent summary of information on Santa Maria province volcanic rocks that allows for new inter-

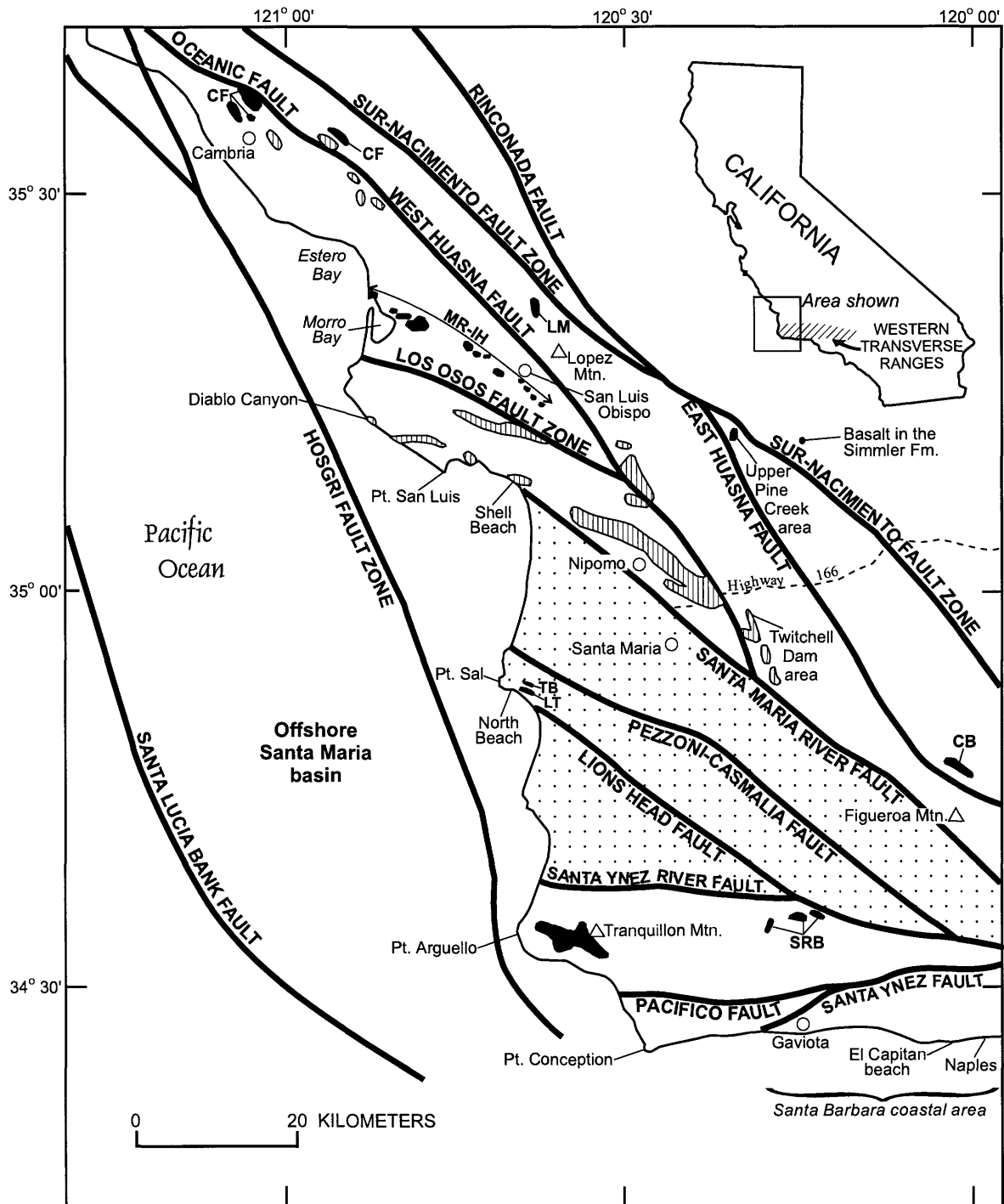


**Figure 1.** Map of the Santa Maria province showing outcrop locations of middle Tertiary igneous rocks (Obispo Formation represented by vertical lines; other units shaded black), major faults, the onshore Santa Maria basin (stippled), and the offshore Santa Maria basin. Abbreviations: CB, Catway volcanics; CF, Cambria Felsite; LT, tuffs in the Lospe Formation; MR-IH, Morro Rock-Islay Hill complex; SRB, basaltic andesite near Santa Rosa Creek; TB, sill at Point Sal. Map compiled from Jennings (1958, 1959) and Pacific Gas and Electric Company (1988).

pretations of a regional history of volcanism in the Santa Maria province.

Although volcanism was integral in the geologic history of the Santa Maria province, previous work that addressed the origin and tectonic significance of volcanic rocks in the Santa Maria province is sparse. Dickinson and Snyder (1979) proposed one of the first regional tectonic models in which volcanism that occurred in the Santa Maria province was attributed to a northwest-migrating asthenospheric slab window that formed in conjunction with the Mendocino Triple Junction. In a different interpretation, Hall (1981a) proposed that some of the Santa Maria province volcanic rocks were erupted into a continental marine environment along a leaky transform fault that was associated with the intersection of the Farallon-Pacific spreading ridge with western California. Since this earlier work, we have gained more and better stratigraphic and radiometric age control as well as geochemical data on these volcanic rocks. With these new data, which are described in this paper, we are able to offer alternative tectonic models to explain the origin of Santa Maria volcanism in relation to ridge-trench interactions (Cole and Basu, 1992, 1995; McCrory and others, 1995) and the ensuing transtension and block rotations that occurred during development of the Santa Maria basin (Hornafius and other, 1986; Stanley and others, 1996).

## ACKNOWLEDGMENTS

This research was supported in part by grants from the American Chemical Society–Petroleum Research Fund and the Geological Society of America. We thank J.G. Vedder, K.J. Bird, Hugh McLean, and M.A. Keller for their informative reviews. We also benefited from discussions with J.G. Vedder, Hugh McLean, K.J. Bird, R.V. Fisher, M.A. Keller, A.R. Basu, J.L. Schneider, and P.W. Weigand. We thank the U.S. Air Force for access to outcrops located on Vandenberg Air Force Base and Maurice Twitchell for allowing access to private land. N.A. Frambes provided assistance in manuscript preparation.

## STRATIGRAPHY, AGES, AND DESCRIPTIONS OF VOLCANIC UNITS

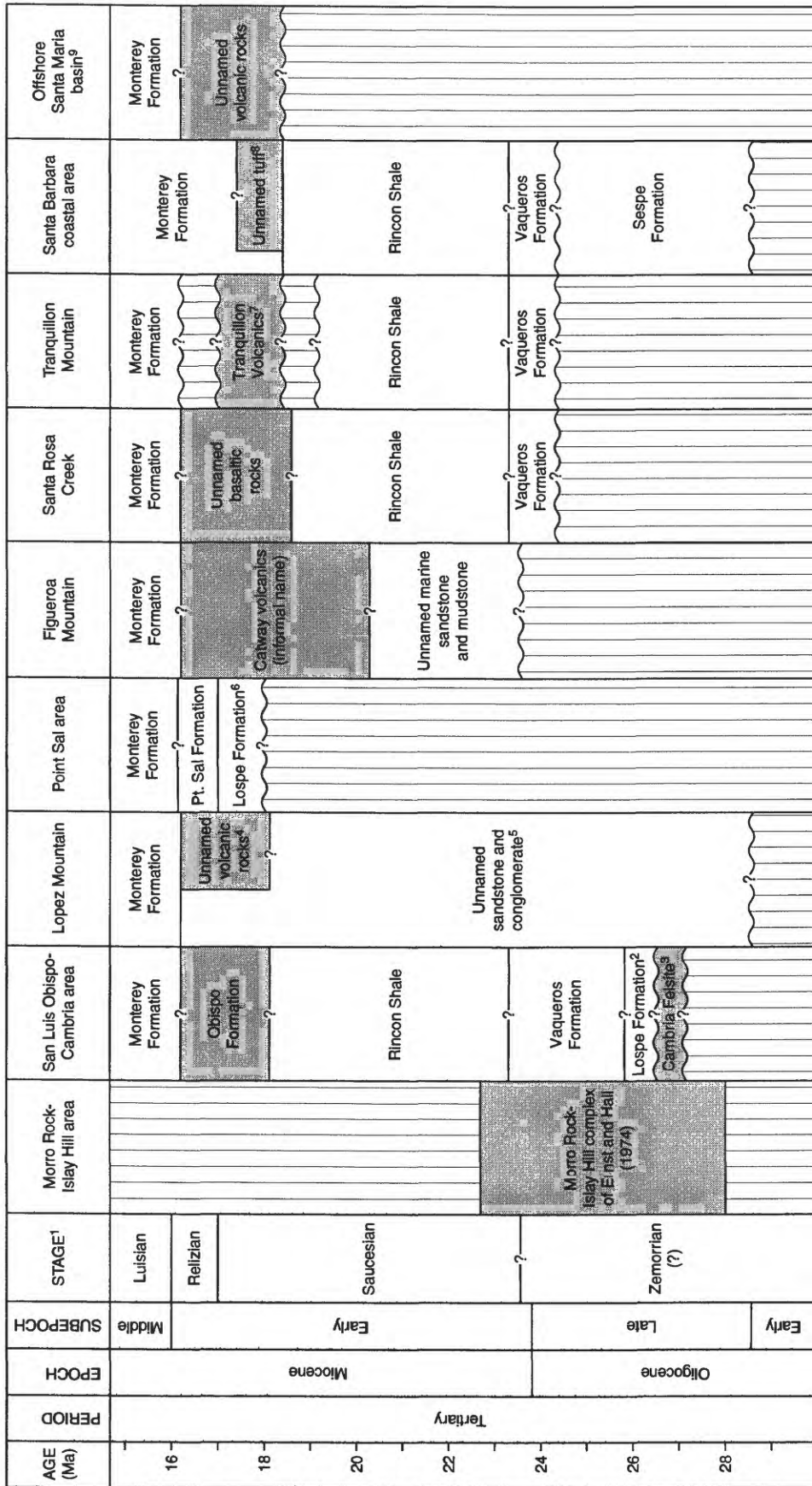
Volcanic rocks in the Santa Maria province range in age from late Oligocene to early Miocene (fig. 2, table 1, app. 1). On the basis of available radiometric dates there appear to be two age groups of Santa Maria volcanic rocks. An older group exhibits radiometric ages ranging from  $28.0 \pm 1.0$  to  $22.7 \pm 0.9$  Ma (29.0 to 21.9 Ma including the range of reported errors; table 1); we refer to the age range of this group as about 28 to 23 Ma. A younger group exhibits radiometric ages ranging from  $20.3 \pm 1.6$  to  $15.7 \pm 0.9$

Ma (21.9 to 14.7 Ma including the range of reported errors; table 1); we refer to the age range of this group as about 20 to 16 Ma. Within these two groups are several major volcanic units, which are described below in terms of local stratigraphy, ages, thicknesses, petrographic characteristics, and possible origins.

## Tranquillon Volcanics of Dibblee (1950)

Volcanic rocks on and near Tranquillon Mountain were mapped and described by Dibblee (1950) as “1200 feet of rhyolite, agglomerate, and ash exposed on Tranquillon Mountain ridge and vicinity.” Dibblee (1950) designated these rocks the Tranquillon Volcanics and proposed a type section along a ridge between Tranquillon Mountain and Point Arguello (fig. 1). Based on measured sections and detailed stratigraphic analyses by Robyn (1980), combined with our field investigation, these rocks consist of up to 150 m of nonwelded and welded rhyolitic tuff and lapilli tuff and minor basalt (figs. 3, 4). The tuff and lapilli tuff most likely formed by combinations of pyroclastic flows and pyroclastic fallout (Robyn, 1980; Cole and others, 1991a). Detailed petrographic characteristics of the type Tranquillon volcanic rocks are given by Robyn (1979, 1980). In general these deposits consist of 60–90 percent glass shards, 15–40 percent pumice, 5–15 percent crystals, and less than 5 percent sedimentary lithic fragments. Vitric components are in places diagenetically altered to analcime and clinoptilolite and also have devitrified to potassium feldspar and quartz (cristobalite) (Robyn, 1980). The welded-tuff intervals are defined by a eutaxitic texture where pumice grains and other glass shards are flattened and aligned parallel to bedding (fig. 4A). These flattened pumice grains and glass shards are commonly bent and deformed around crystals. Crystal components include mostly euhedral to subhedral quartz and sanidine with minor amounts of albite (less than 5 percent). Many crystals show smooth and embayed boundaries.

In the vicinity of Tranquillon Mountain, the Tranquillon Volcanics unconformably overlie the Rincon Shale (Dibblee, 1950) and are unconformably overlain by the Monterey Formation (fig. 2; Dibblee, 1950, 1988b). Near Tranquillon Mountain the lower 30 cm of the Tranquillon Volcanics is a pebble-granule conglomerate composed mainly of dolomite clasts and abundant robust, shallow marine invertebrate fossils. The dolomite clasts are probably recycled dolomite concretions derived from the underlying Rincon Shale (Stanley and others, 1996). The fossils include *Turritella ocoyana topangensis* Merriam, *Turritella temblorensis* Wiedey, and *Spondylus perrini* Wiedey, all of which are representative of the uppermost “Vaqueros” or “Temblor” molluscan “Stages” (early Miocene) (J.G. Vedder, oral commun., 1987; Stanley and others, 1996). A single sample of welded tuff from



<sup>1</sup>Modified from Kleinpell (1938, 1980).  
<sup>2</sup>Lospe Formation of Hall (1974), Hall and Prior (1975), and Hall and others (1979); Lospe Formation(?) of Ernst and Hall (1974).  
<sup>3</sup>Cambria Felsite of Ernst and Hall (1974).  
<sup>4</sup>Unnamed volcanic rocks of McLean (1994, map units Tv1 and Tv1).  
<sup>5</sup>Unnamed sandstone and conglomerate of McLean (1994, map unit Tsc).  
<sup>6</sup>Type Lospe Formation (Wissler and Dreyer, 1943, p.237); consists of sedimentary and minor volcanic rocks discussed in text.  
<sup>7</sup>Tranquillon Volcanics of Dibblee (1950).  
<sup>8</sup>Called by various informal names including "Bentonite Bed" (Kleinpell and Weaver, 1963, p. 11), Tranquillon bentonite (Hornatius, 1994, p. 52), Tranquillon tuff (Hornatius, 1994, p. 52), and Summerland rhyolite tuff (Turner, 1970, p. 118).  
<sup>9</sup>After McCulloch (1989).

**Figure 2.** Stratigraphic chart for middle Tertiary volcanic units (gray shaded areas) in the Santa Maria province. Vertical lines represent missing time along unconformities. Data, interpretations, and assumptions used in constructing this chart are given in appendix 1.

**Table 1.** Compilation of available radiometric ages for volcanic rocks in and around the Santa Maria province.

Volcanic unit	Age (Ma) <sup>1</sup>	Method	Mineral	References
Tranquillon Volcanics of Dibblee (1950)	17.80 ± 0.05	<sup>40</sup> Ar/ <sup>39</sup> Ar	sanidine	Stanley and others (1996)
Unnamed basaltic andesite of Santa Rosa Creek	17.4 ± 1.2	<sup>40</sup> K/ <sup>40</sup> Ar	whole rock	Turner (1970)
Unnamed lower Miocene tuffs of the Santa Barbara coast: Summerland rhyolite tuff (informal name)	17.2 ± 0.5	<sup>40</sup> K/ <sup>40</sup> Ar	plagioclase	Turner (1970)
	16.5 ± 0.6	--- do ---	--- do ---	--- do ---
Tuff near base of Monterey Formation at Naples	18.42 ± 0.06	<sup>40</sup> Ar/ <sup>39</sup> Ar	sanidine	Stanley and others (1996)
Tuff deposits in the Lospe Formation near Point Sal	17.70 ± 0.02	<sup>40</sup> Ar/ <sup>39</sup> Ar	sanidine	Stanley and others (1996)
	17.39 ± 0.06	--- do ---	plagioclase	--- do ---
Obispo Formation	15.7 ± 0.9 to 16.9 ± 1.2	<sup>40</sup> K/ <sup>40</sup> Ar	plagioclase	Turner (1970)
Unnamed volcanic rocks of the Catway Road area	17.2 ± 2.5	<sup>40</sup> K/ <sup>40</sup> Ar	?	Hall (1981a)
	20.3 ± 1.6	--- do ---	?	--- do ---
	18.8 ± 1.5	--- do ---	plagioclase	Vedder and others (1994)
Unnamed volcanic rocks of the Lopez Mountain area	17.0 ± 0.5	<sup>40</sup> K/ <sup>40</sup> Ar	plagioclase	McLean (1994)
Morro Rock-Islay Hill complex	27.1 ± 0.8	<sup>40</sup> K/ <sup>40</sup> Ar	biotite	Turner (1968)
	25.6 ± 1.2	--- do ---	plagioclase	--- do ---
	22.7 ± 0.9	--- do ---	plagioclase	--- do ---
	27.2 ± 0.8	--- do ---	sanidine	--- do ---
	28.0 ± 1.0	--- do ---	biotite	Buckley (1986)
	26.0 ± 0.8	--- do ---	biotite	--- do ---
	25.1 ± 0.8	--- do ---	whole rock	--- do ---
Cambria Felsite	27 to 26.5	<sup>40</sup> Ar/ <sup>39</sup> Ar	?	unpublished data; J.D. Obradovich, oral commun. (1994); M.E. Tennyson and M.A. Keller, oral commun. (1994); M.A. Mason and C.C. Swisher, oral commun. (1990)
Unnamed volcanic rocks of upper Pine Creek	26.6 ± 0.5	<sup>40</sup> K/ <sup>40</sup> Ar	plagioclase	Vedder and others (1991)
Unnamed basalt at Hell's Half Acre (about 9 km southeast of Figueroa Mountain)	18.5 ± 2.0	<sup>40</sup> K/ <sup>40</sup> Ar	whole rock	Fritsche and Thomas (1990)
Basalt in the lower part of the Simmler Formation about 30 km northeast of Nipomo	23.4 ± 0.8	<sup>40</sup> K/ <sup>40</sup> Ar	whole rock	Ballance and others (1983)
	22.9 ± 0.7	--- do ---	--- do ---	--- do ---

<sup>1</sup>K/Ar ages from Turner (1968, 1970) and Hall (1981a) corrected using methods described in Dalrymple (1979).

near the top of Tranquillon Mountain yielded an  $^{40}\text{Ar}/^{39}\text{Ar}$  age of  $17.80 \pm 0.05$  Ma on sanidine (Stanley and others, 1996). These ages are consistent with other biostratigraphic data that constrain the Tranquillon volcanic rocks as early Miocene (Dibblee, 1950). Based on differences between the Tranquillon volcanic rocks and tuffs in the Obispo Formation in major element chemistry, stratigraphy, and depositional settings, Robyn (1979, 1980) suggested that these

two volcanic units are separate and were erupted from separate sources on opposite sides of the Santa Maria basin. We agree with Robyn (1979, 1980) and discuss possible volcanic sources and paleogeography more fully in a later section.

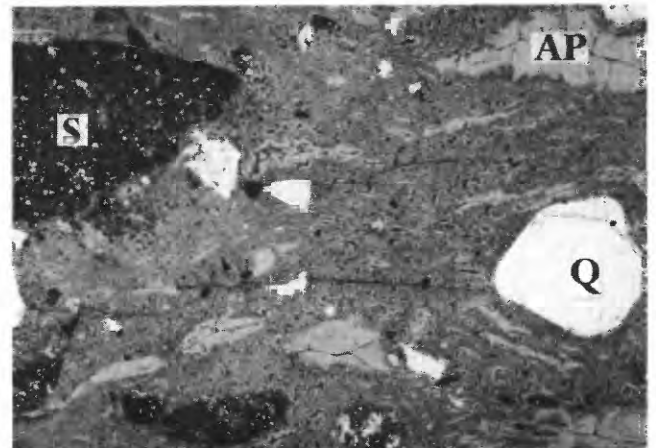
### Unnamed Basaltic Andesite of Santa Rosa Creek

Basaltic rocks mapped as Tranquillon Volcanic Formation by Dibblee (1988a) crop out about 25 km east of Tranquillon Mountain near Santa Rosa Creek (fig. 1; Dibblee, 1950, 1988a). This deposit consists of basaltic andesite breccia of unknown thickness that stratigraphically overlies the Rincon Shale and underlies the Monterey Formation (Dibblee, 1950, 1988a; figs. 2, 5). The unit includes blocks of aphanitic basaltic andesite that consist of very fine grained plagioclase laths in pilotaxitic texture. Minor amounts of brown glass and iron-titanium oxides are present between the plagioclase laths. Some small blocks of mudstone, perhaps derived from the underlying Rincon Shale, are incorporated into the basaltic andesite breccia. Mudstone along with sand- to pebble-sized basaltic andesite fragments form a matrix between the coarser blocks. A radiometric date for this basalt from Turner (1970), cor-

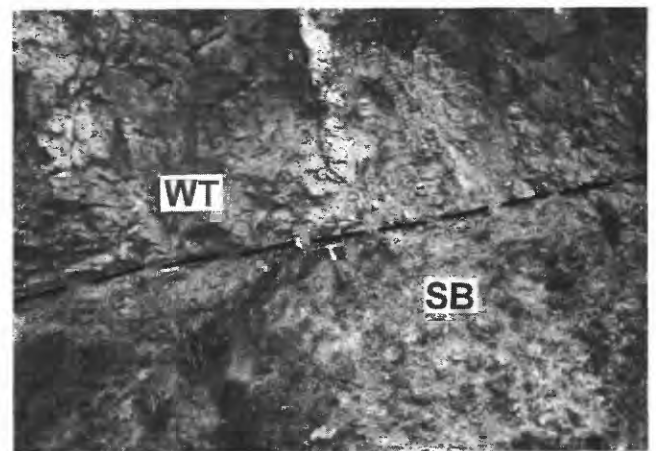
EPOCH	UNIT	LITHOLOGY	THICKNESS (IN METERS)	DESCRIPTION
Miocene	Monterey Fm.	[Horizontal dashes]		
	Tranquillon Volcanics	[Diagonal dashes]	11-27	White to pink and yellow nonwelded tuff
		[Wavy lines]	4-28	White to pink-white and yellow-white welded tuff and lapilli tuff
		[Diagonal dashes]	5-16	White to white-green nonwelded tuff
		[Wavy lines]	8-15	Gray to brown welded pumice lapilli tuff
		[Wavy lines]	4-9	Black welded vitric tuff
		[Diagonal dashes]	1-5	White to yellow bentonite
		[Small circles]	0.3	Pebble-granule conglomerate with clasts of dolomite and robust fossils (see text for details)
	Rincon Shale	[Horizontal dashes]		

**Figure 3.** Schematic stratigraphic column of the Tranquillon Volcanics of Dibblee (1950) near Tranquillon Mountain. Modified from Robyn (1980).

**Figure 4.** Photographs of the Tranquillon Volcanics of Dibblee (1950) in its type area near Tranquillon Mountain. *A*, Photomicrograph of welded rhyolite lapilli tuff. Note eutaxitic texture where glass shards are deformed around crystal fragments. Abbreviations: Q, quartz; AP, altered pumice; S, sedimentary lithic fragment. Field of view is 6 mm across. *B*, Massive spheroidal “bomb” bed (SB; fallout deposit) overlain by a welded lapilli tuff (WT; pyroclastic flow deposit). Contact is shown as dashed line. Hammer is 27 cm long.



*A*



*B*

rected with the methods of Dalrymple (1979), is  $17.4 \pm 1.2$  Ma, which is about the same age as the rhyolitic volcanic rocks at Tranquillon Mountain.

The blocky and angular nature of basaltic andesite clasts in this deposit as well as the close-fitting fabric of the clasts suggest that this volcanic unit may have been a subaqueous lava flow that was rapidly quenched and shattered by water. This origin is consistent with the marine depositional setting implied by the nonvolcanic marine deposits that underlie and overlie the basaltic andesite breccia. It is likely that these breccias were derived from a nearby source because of the close-fitting clast fabric, which suggests minimal, if any, postdepositional transport.

### Unnamed Lower Miocene Tuffs of the Santa Barbara Coast

A thin tuff bed was mapped by Dibblee (1966) within the lowest part of the Monterey Formation along the coast near Santa Barbara (fig. 1), directly above the contact between the Monterey and the overlying Rincon Shale (fig. 2). Biostratigraphic data from the Rincon Shale and the Monterey Formation (Dibblee, 1950, 1966; Kleinpell and Weaver, 1963; Turner, 1970; DePaolo and Finger, 1991; Stanley and others, 1992b, 1994) constrain the age of this tuff to early Miocene (upper part of the Saucesian Stage of Kleinpell, 1938). This tuff, locally and informally known as the Tranquillon bentonite and (or) Tranquillon tuff (Hornafius, 1994, p. 52) and the Summerland rhyolite tuff (Turner, 1970, p. 118), is an important stratigraphic marker because it appears to occur at about the same stratigraphic level as the Tranquillon Volcanics of Dibblee (1950). At one site near the town of Summerland (about 75 km east of Point Conception) this tuff is 1.8 m thick and yields radiometric dates of  $16.5 \pm 0.6$  and  $17.2 \pm 0.5$  Ma (Turner, 1970, corrected using methods of Dalrymple, 1979). A sample of altered tuff from near the base of the Monterey Formation in a sea-cliff exposure near Naples yielded a single crystal laser fusion  $^{40}\text{Ar}/^{39}\text{Ar}$  age of  $18.42 \pm 0.06$  Ma (Stanley and others, 1996). At a site about 40 km west of Santa Barbara, a tuff in the same stratigraphic position is described by Stanley and others (1992b) as a 70-cm-thick weathered, soft, poorly exposed, apparently felsic tuff.

Hornafius (1994) also describes two other related sets of tuff beds within strata of the Monterey Formation that are assigned to the Upper Saucesian Stage of Kleinpell (1938). One tuff, sample NB440 of group 1c (Hornafius, 1994, p. 52), includes a dacite vitric tuff about 440 ft (134 m) above the base of the Monterey Formation at Naples (fig. 1). This tuff is chemically similar to acidic tuffs of the Obispo Formation (Hornafius, 1994; app. 2). Another set, group 2 (Hornafius, 1994, p. 52, 57), includes three separate tuff beds at about 151 ft (46 m), 288 ft (87.8 m), and 400 ft (121.9 m) above the base of the

Monterey Formation at Naples and a tuff bed at about 250 ft (76.2 m) above the base of the Monterey Formation at El Capitan Beach. The group 2 tuffs include intermediate compositions (basaltic andesite-andesite) and dacite (Hornafius, 1994, table 1b; app. 2).

The absence of tuff beds in the Rincon Shale beneath the Tranquillon tuff at El Capitan Beach led Hornafius (1994) to suggest that the Tranquillon tuff represents the oldest Miocene volcanic ash in the Santa Barbara coastal area. The Tranquillon tuff is also the thickest lower Miocene ash deposit in the area, reaching up to 60 ft (18.3 m) offshore near Gaviota and thinning eastward to about 5 ft (1.5 m) in the offshore near Santa Barbara (Hornafius, 1994). This thickness variation may represent thinning away from a volcanic source that could have been located toward the west at Tranquillon Mountain, as suggested by Dibblee (1950) and Hornafius (1994). Overall, the lower Miocene tuff layers of the Santa Barbara coast generally decrease in thickness with increasing stratigraphic height within the Monterey Formation (Hornafius, 1994, p. 45). This pattern could reflect a decrease in the volume of ash due to waning explosive volcanism through lower Miocene time in the Santa Maria province. The origin of thin Middle Miocene (Luisian) ash beds in the Monterey Formation in this area is uncertain, but they could have been the ash fallout deposits from volcanic sources outside of the Santa Maria province (Hornafius, 1994).

### Tuff Deposits in the Lospe Formation Near Point Sal

The Lospe Formation near Point Sal is an 800-m-thick interval of nonmarine to shallow marine sedimentary rocks

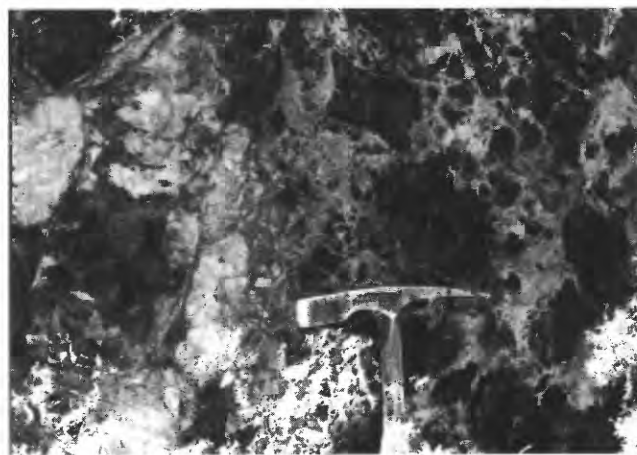


**Figure 5.** Unnamed basaltic andesite near Santa Rosa Creek in an outcrop about 25 km east of Tranquillon Mountain. Dark clasts are blocks of aphanitic basaltic andesite. Light clasts are blocks of mudstone, probably derived from the underlying Rincon Shale. Matrix material between clasts consists of mudstone and sand- to pebble-sized basaltic andesite fragments.

with interbedded volcanic rocks (Woodring and Bramlette, 1950; Stanley and others, 1990, 1991; Johnson and Stanley, 1994). The Lospe Formation records initial subsidence of the onshore Santa Maria basin (Stanley and others, 1992a, 1996; McCrory and others, 1995). The lower member of the Lospe Formation is about 210 m thick and consists of alluvial fan and fan-delta deposits (Johnson and Stanley,

1994), whereas the upper member consists of about 600 m of interbedded turbidite sandstone and mudstone that were deposited in a lake (Stanley and others, 1990). Interbedded with the deposits of both members are several rhyolite and dacite tuffs (figs. 6, 7). These tuff deposits include 15-cm to 6-m-thick intervals in the alluvial-fan and fan-delta deposits of the lower member of the Lospe Formation, and up to 20-m-thick deposits in the lacustrine deposits of the upper member. The nonvolcanic deposits of the Lospe Formation provide a basis for interpreting depositional environments of the interbedded tuffs; those tuffs in the lower member of the Lospe Formation are most probably sub-aerial, whereas those in the upper member are most likely subaqueous lacustrine deposits.

The tuffs within the lower, conglomeratic member of the Lospe Formation are variable in composition and include vitric, lithic, and crystal tuffs. Several thin- to medium-bedded (15-30 cm thick) lithic-rich tuffs are interbedded with streamflow conglomerate and sandstone and may represent reworked volcanoclastic deposits (fig. 7A). Thicker tuff intervals range from 1.5 to 6 meters thick and consist mostly of vitric shards with few lithic fragments derived from the Jurassic Point Sal ophiolite of Hopson and Frano (1977) (fig. 7B). These thicker tuffs are massive with inverse grading at the bases of beds and exhibit alignment of elongate clasts parallel to bedding. These tuffs were most likely deposited by subaerial pyroclastic flows (Cole and others, 1991a; Cole and Stanley, 1994).

Most tuff deposits in the upper member of the Lospe Formation are vitric-rich and consist of 95-98 percent vitric shards (cusped fragments and pumice) and 2-5 percent crystals (quartz and plagioclase) (fig. 7C) (Cole and Stanley, 1994). These tuff deposits exhibit repetitive and predictable stratigraphic and sedimentologic characteristics that are illustrated by a composite unit shown in figure 8. The tuffs in the upper member can be attributed to deposition of reworked ash in the form of high-density turbidity flows (fig. 8) (Cole and others, 1991a; Cole and Stanley, 1994). Individual turbidite intervals range from 2 to 12 m thick and are amalgamated to form mappable tuff horizons that are up to 20 m thick (fig. 7D).

One tuff in the upper member of the Lospe Formation consists of a 65-cm-thick cross-bedded crystal- and vitric-tuff bed (figs. 7E, 7F). Restored paleoflow direction based on the dip direction of large-scale foresets is toward the northeast, suggesting flow from the southwest. This cross-bedded tuff is interbedded with lacustrine mudstone and presumably represents subaqueous reworking by unidirectional currents. Very limited exposure precludes a detailed interpretation for the origin of this tuff bed.

Single-crystal  $^{40}\text{Ar}/^{39}\text{Ar}$  analyses of sanidine from two nonwelded tuffs in the Lospe Formation yield ages of  $17.70 \pm 0.02$  and  $17.39 \pm 0.06$  Ma (Stanley and others,

PERIOD	EPOCH	UNIT	LITHOLOGY	THICKNESS (IN METERS)	DESCRIPTION	
TERTIARY	Miocene	Point Sal Formation			Marine deposits	
				25-30	Trachybasalt sill	
					Marine deposits	
		Lospe Formation	Upper member		15-30	Shallow marine deposits
					200-600	Lacustrine deposits
Lospe Formation	Lower member		180-210	Fan delta and alluvial fan deposits		
JURASSIC		Point Sal Ophiolite		?	(of Hopson and Frano, 1977)	

EXPLANATION

	Mostly shale, siltstone, and fine sandstone		Rhyolite and dacite tuff
	Mostly sandstone and conglomerate		Unconformity

Figure 6. Schematic composite stratigraphic section of the Lospe Formation in its type area near Point Sal. Generalized from Stanley and others (1991, 1996).

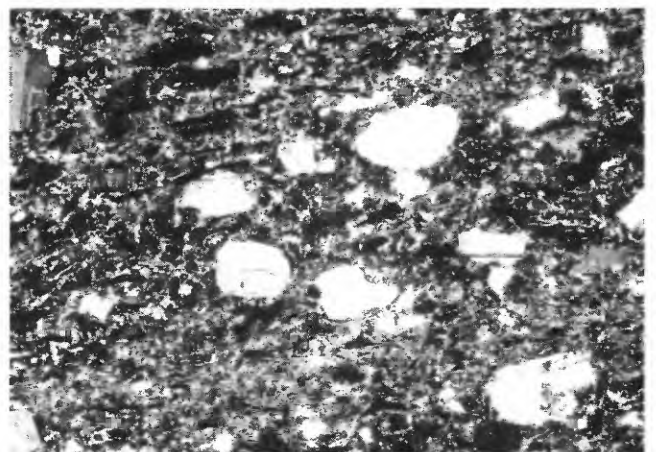
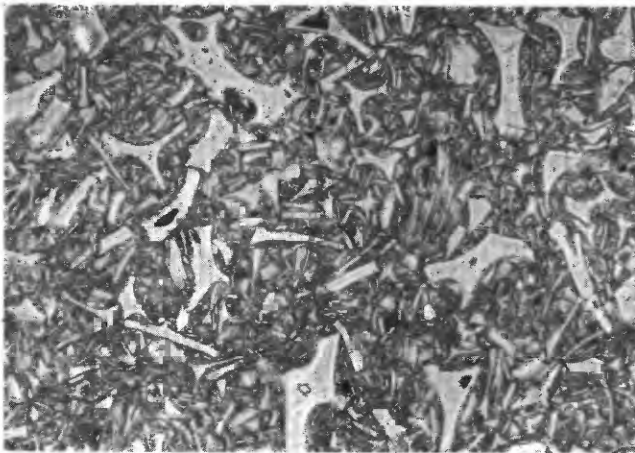
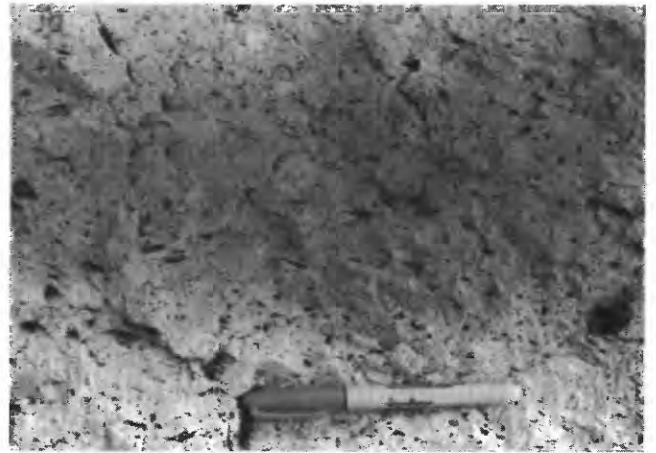
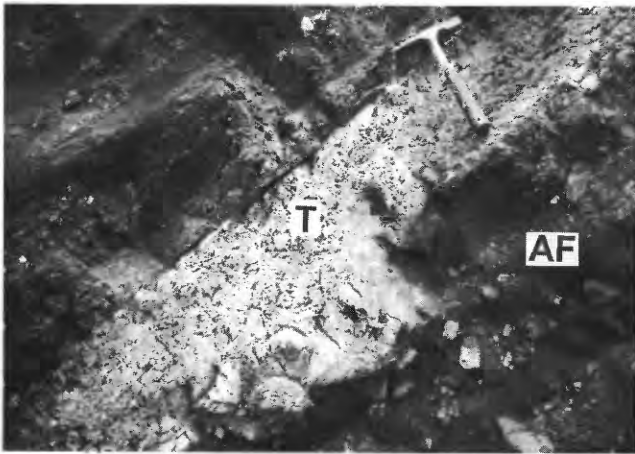


**Figure 7.** Photographs of tuff deposits in the Lospe Formation in its type area near Point Sal. *A*, Thin reworked vitric-lithic tuff (T) interbedded with alluvial-fan deposits (AF) in the lower member of the Lospe Formation. *B*, Subaerial pyroclastic flow deposit of the lower member of the Lospe Formation. Lapilli-sized clasts are fragments of Point Sal ophiolite. *C*, Photomicrograph of subaqueous vitric tuff in the upper member of the Lospe Formation under plane-polarized light. Note the cusped and bladed shapes of vitric shards; field of view is 3 mm across. *D*, Subaqueous vitric tuff interbedded with shale and fine-grained sandstone of the upper member of the Lospe Formation. Tuff unit is 20 m thick. Arrows point to intervals of the tuff deposit that are planar or thin bedded. *E*, Cross-bedded vitric-crystal tuff in the upper member of the Lospe Formation exposed at Point Sal. *F*, Photomicrograph of vitric-crystal tuff in the upper member of the Lospe Formation under cross-polarized light. Crystals of subrounded to subangular plagioclase are aligned with their long axes parallel to bedding. The plagioclase grains are set in a finer grained matrix of vitric shards (dark grains). Field of view is 3 mm across.

1996). These dates are for tuff samples from 30 m and 210 m above the base of the Lospe Formation at North Beach, respectively. These ages plus the presence of early Miocene palynomorphs and benthic foraminifers in the upper member of the Lospe Formation indicate a late early Miocene age for the volcanism that was the source of the tuffs in the Lospe Formation. Locations of possible eruptive sources for these tuffs include the Tranquillon Mountain area to the south, regions now located in the offshore Santa Maria basin to the south and west, and possibly regions north of Point San Luis (fig. 1). A more detailed discussion of potential eruptive centers and the potential source(s) of volcanoclastic rocks in the Santa Maria province is given in a later section.

### Sill Near Point Sal

A trachybasalt sill is present within the lower part of the Point Sal Formation in the vicinity of Point Sal (fig. 1) (Dibblee, 1989). This intrusive unit is about 25-30 m thick and consists of plagioclase, pyroxene, and altered olivine (iddingsite) (fig. 9). Parts of the unit are coarsely crystalline and can be considered a diabase. Portions of the matrix material between crystals exhibit axiolitic and fibrous textures. This sill intrudes the lower part of the Point Sal Formation, which contains benthic foraminifers of the lower Miocene Relizian Stage (Woodring and Bramlette, 1950); therefore, the sill is of early Miocene age or younger (fig. 2). This

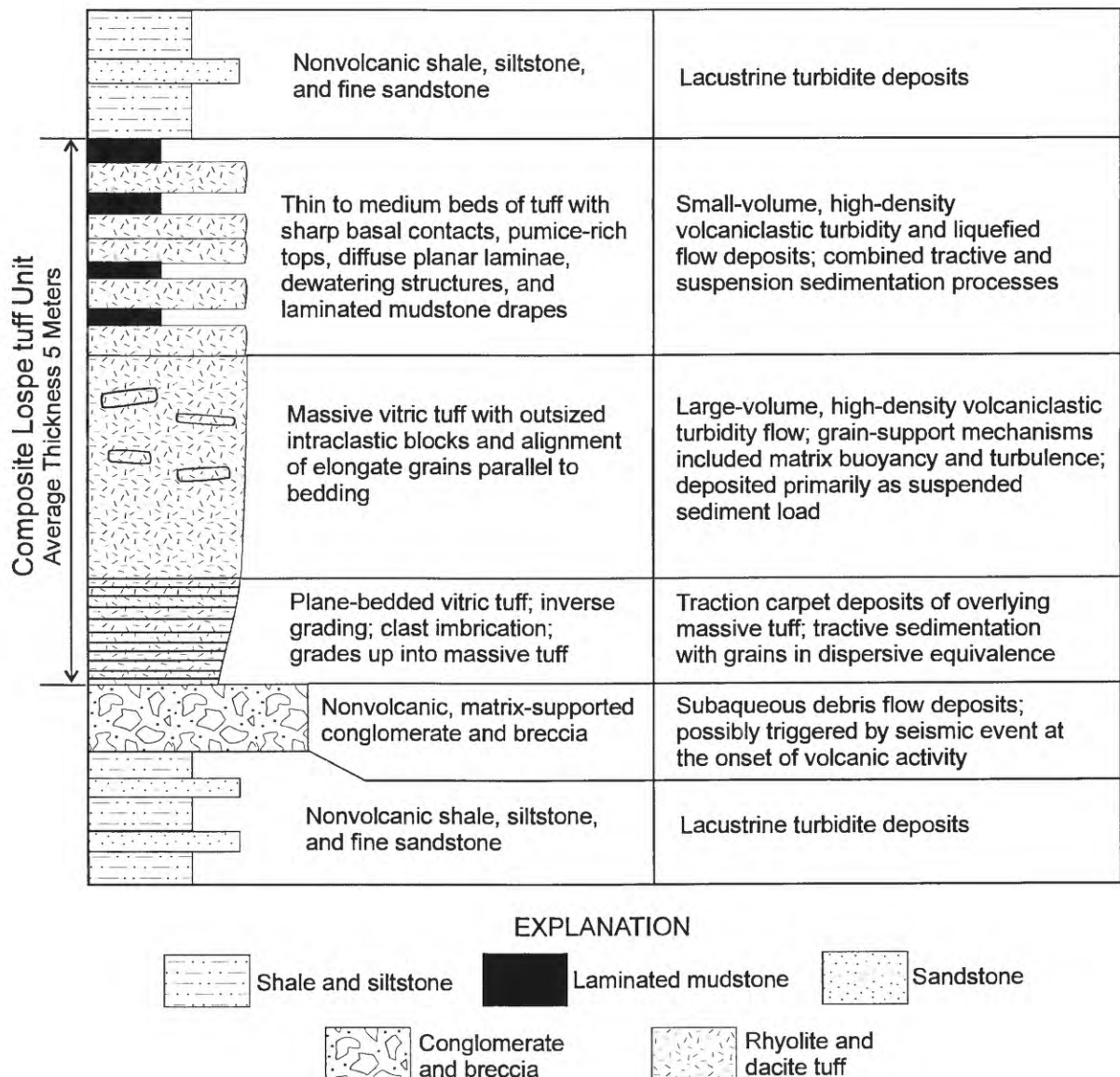


**Figure 8.** Composite stratigraphy of subaqueous tuffs in the upper member of the Lospe Formation that were deposited as reworked ash from high-density turbidity flows. Modified from Cole and Stanley (1994).

basaltic intrusive represents a magmatic pulse that was younger than that which formed the tuffs in the Lospe Formation, also found in the region of Point Sal.

## Obispo Formation and Related Rocks

The Obispo Formation is a widespread and thick volcanic unit that outcrops in a northwest-southeast-trending zone from north of Estero Bay to near Santa Maria (fig. 1). The Obispo Formation consists of up to 1,500 m of rhyolite, dacite, and andesite tuff and lapilli tuff; basalt and andesite lava flows and intrusives; basaltic hyaloclastite and breccias; volcanoclastic sandstones; and tuffaceous shales (Hall and Corbató, 1967; Fisher, 1977; Hall and others, 1979; Hall, 1981b; Surdam and Hall, 1984; Schneider and Fisher, 1996; fig. 10). The Obispo Formation conformably overlies the Rincon Shale and is overlain conformably by the Monterey Formation (fig. 2; Hall and Corbató, 1967). Radiometric dates obtained from acidic tuffs in the lower part of the Obispo Formation range from  $15.7 \pm 0.9$  to  $16.9 \pm 1.2$  Ma (Turner, 1970, corrected with methods of Dalrymple, 1979).

Nonwelded, white acidic vitric tuff and pumice lapilli tuff, some of the most common lithologies in the Obispo Formation (figs. 11A-D), were deposited mostly as high-density sediment gravity flows and turbidity flows of remobilized ash in a marine setting (Fisher, 1977; Schneider and Fisher, 1996). Schneider and Fisher (1996) estimate the volume of these deposits to be between 250 and 450 km<sup>3</sup>. These deposits can be subdivided into thick, massive, poorly sorted intervals and well-bedded intervals (Schneider and Fisher, 1996; fig. 10). Massive tuff and lapilli-tuff intervals are well exposed in the seacliffs at Shell Beach and were likely deposited as mass flows of remobilized pyroclastic detritus (Schneider and Fisher, 1996). Several types of soft-sediment deformation, including asymmetric slump folds, load casts, and folded rip-up clasts, are present along the base of the upper massive tuff unit at Shell Beach (fig. 11A). Imbrication of rip-up clasts, slump fold vergence, and soft-sediment glide plane orientations reveal an east to northeast direction of paleoflow for this unit (Schneider and Fisher, 1996). Well-bedded acidic tuff intervals are exposed in areas east of Shell Beach in the vicinity of San Luis Obispo (along Highway 101) and Twitchell Dam and were most likely deposited as turbidites of reworked ash (fig. 11D) (Fisher, 1977; Schneider and Fisher, 1996). These intervals contain normally graded beds, ripple laminations, rare flute casts, burrowed horizons, and interbedded shales. On the basis of flute casts, ripple foresets, and pebble imbrication (total  $n=46$ ), Schneider and Fisher (1996) report east to northeast paleoflow for the well-bedded tuff interval at Twitchell Dam. The well-bedded tuff intervals may represent distal, lateral equivalents to the massive tuff intervals (fig. 10); collectively these deposits could have originated from subaerial pyroclastic flows that entered the sea, from submarine-erupted pyroclastic flows that mixed with water, or as large slumps from

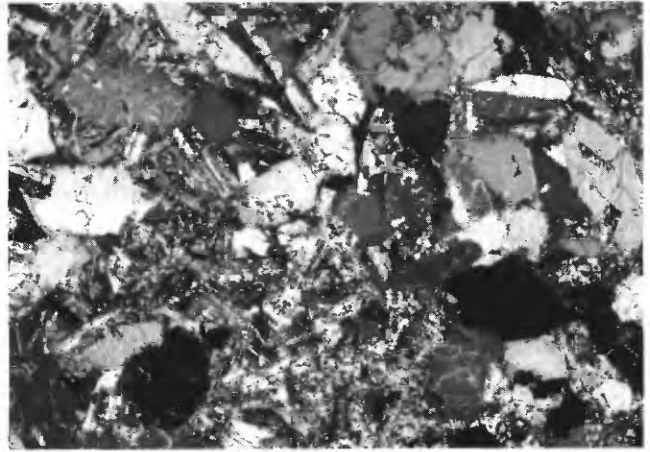


**Figure 9.** Photomicrograph under cross-polarized light of trachybasalt sill that intrudes the Point Sal Formation near Point Sal. Subophitic texture with plagioclase laths partially enclosed by clinopyroxene. Some alteration of plagioclase is present in the lower center of the photomicrograph. Field of view is 6 mm across.

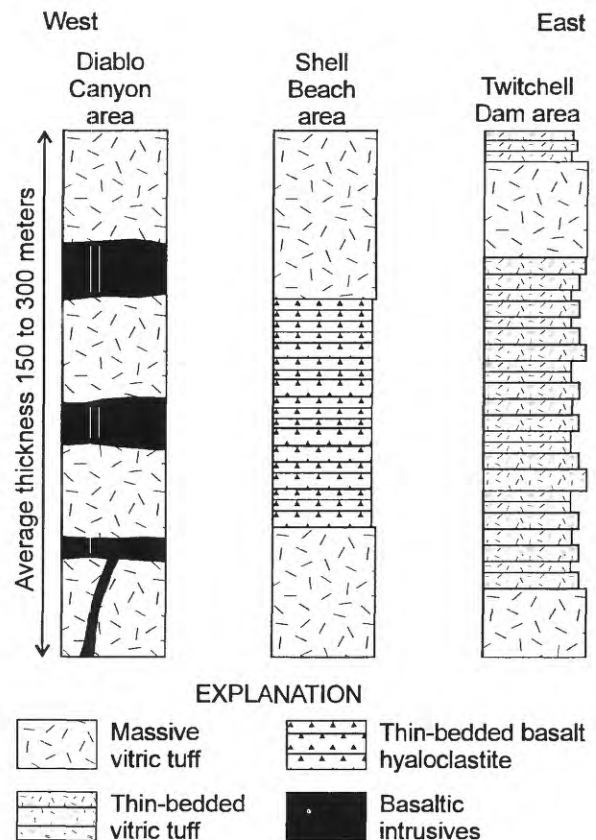
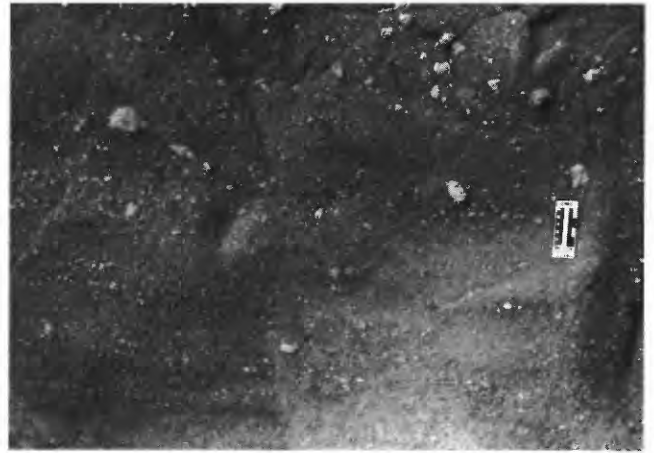


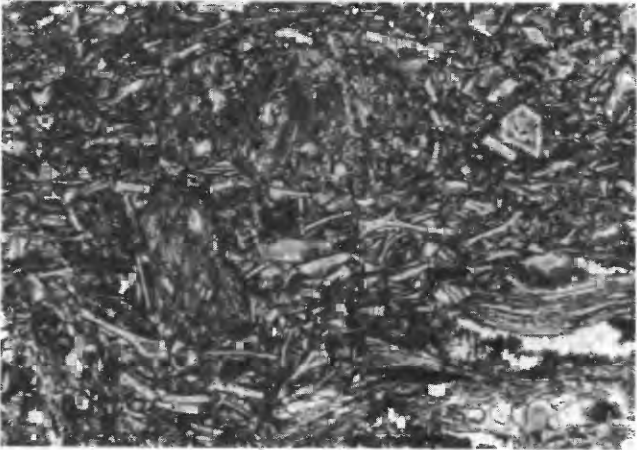
**Figure 10.** Representative stratigraphic columns of the Obispo Formation drawn from original field data of this study combined with data reported by Schneider and Fisher (1996). Intrusive basaltic rocks are more prevalent in the western exposures of the Obispo Formation (Surdam and Hall, 1984; Schneider and Fisher, 1996). These intrusive and related extrusive basalts were most likely reworked to form the basaltic hyaloclastite turbidites at Shell Beach. Reworked acidic tuff beds near Twitchell Dam were probably deposited from turbidites, which may also have been derived from the west (Schneider and Fisher, 1996).



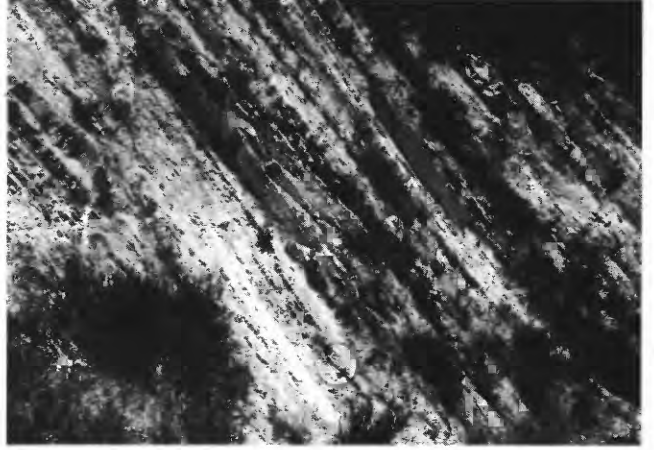
A



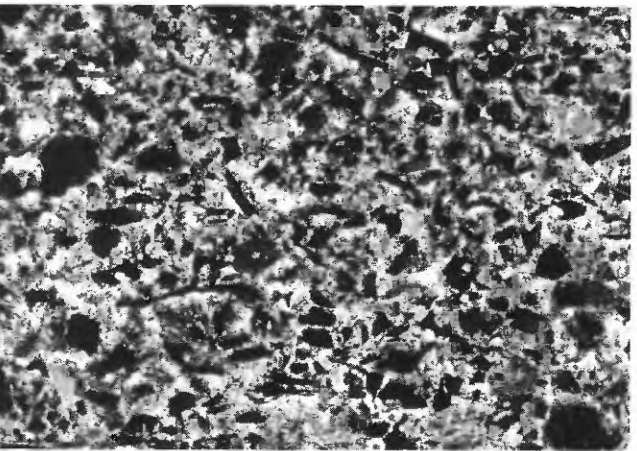
B



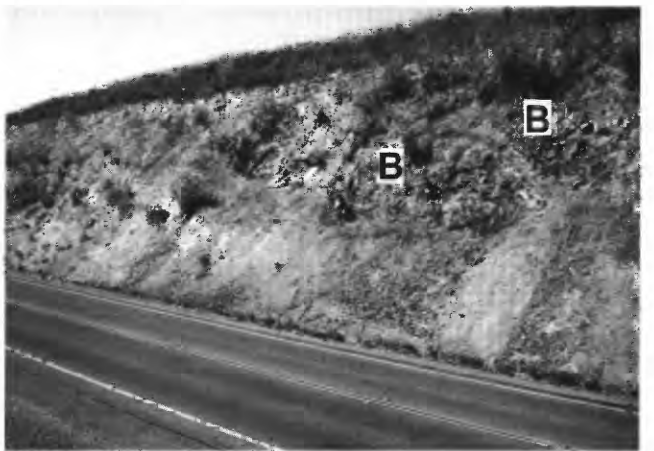
C



D

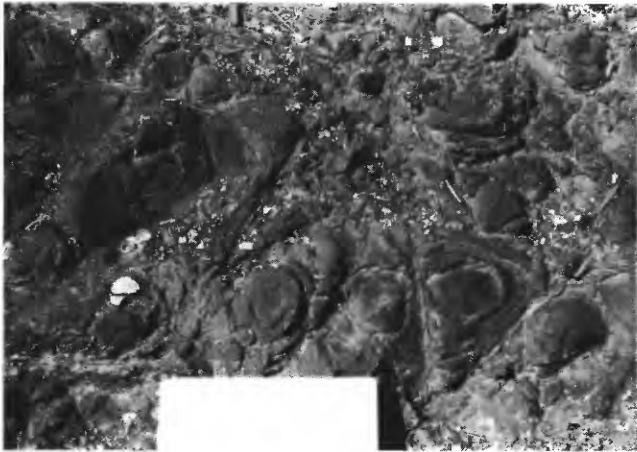


E



F

**Figure 11.** Photographs of the Obispo Formation. *A*, Massive, light-colored vitric-pumice lapilli tuff at Shell Beach with large, dark-colored, soft-sediment deformed shale blocks. The shale blocks were most likely eroded from the underlying Rincon Shale by subaqueous pyroclastic flows from which the tuffs were deposited. *B*, Massive to planar-bedded pumice-lapilli tuff at Shell Beach. These are most likely subaqueous pyroclastic flow deposits. *C*, Photomicrograph of vitric lapilli tuff at Shell Beach under plane-polarized light. Note the bladed vitric shards and the pumice lapilli in the upper center of the photomicrograph. Field of view is 6 mm across. *D*, Thin-bedded vitric tuff near Twitchell Dam. These most likely are turbidite deposits of vitric ash that was reworked from the west. *E*, Photomicrograph of basaltic hyaloclastite turbidite deposits at Shell Beach under cross-polarized light. Dark blocky grains are basalt glass; matrix is calcite cement. A few subangular to subrounded plagioclase grains are present. Field of view is 6 mm across. *F*, Outcrop of basalt (*B*; dark intervals) interbedded with the lower part of the Monterey Formation (light intervals) along the north side of Highway 166 about 4.5 km east of Santa Maria. *G*, Pillow basalt with spheroidal weathering interbedded with the lower part of the Monterey Formation along Highway 166. Clipboard shown for scale is 14 in. long. *H*, Photomicrograph of basalt from outcrop in figure 11 *G* under crossed-polarized light. This rock exhibits intersertal and subophitic textures where plagioclase laths are partially contained within dark, iron-rich glass and clinopyroxene. Field of view is 3 mm across.



G  
Figure 11. Continued

the subaqueous flanks of a silicic volcano (Schneider and Fisher, 1996).

Welded acidic tuff in the Obispo Formation is reported by Schneider and Fisher (1996) as a 5- to 10-m-thick and 4-km-wide interval that is interbedded with volcanoclastic sedimentary rocks, breccias, and basaltic lava flows in the Nipomo area. The bounding marine sedimentary deposits imply subaqueous deposition of the welded tuff with emplacement temperatures estimated from thermal remanant magnetism to have been in the 450-550 °C range (Schneider and Fisher, 1996). Anisotropy of magnetic susceptibility reveals a possible north-east-southwest (020-035°) paleoflow lineation in this unit (Schneider and Fisher, 1996).

Interbedded with the acidic tuffs in the Shell Beach and Nipomo areas are beds of basaltic hyaloclastite and basaltic turbidite sandstones (figs. 10, 11E) (Schneider and Fisher, 1996). Aphanitic basalt flows, pillow basalts, and possible sills within the upper part of the Obispo Formation (Hall, 1978) are exposed in roadcuts along Highway 166 in the Twitchell Dam area (figs. 1, 11F, 11G). These basalt units exhibit



H

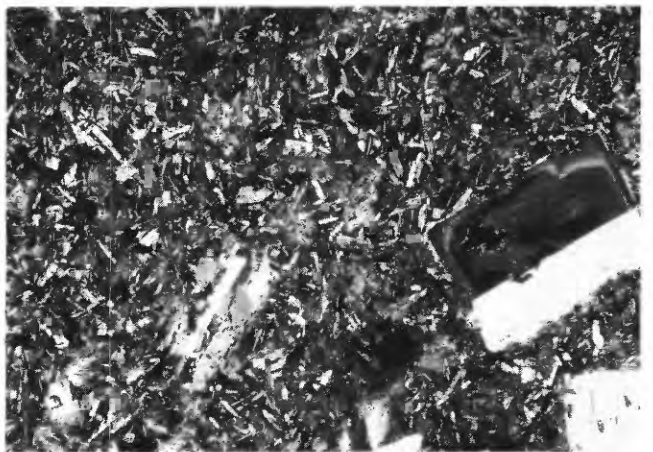
subophitic, hyaloophitic, and intersertal textures with clinopyroxene and laths of plagioclase in a dark matrix of iron-rich glass (fig. 11H).

### Unnamed Volcanic Rocks of the Catway Road Area

Basalt is present in the vicinity of Catway Road in a 3-km<sup>2</sup> area north of Figueroa Mountain in the San Rafael Mountains (fig. 1). Some outcrops display pillow structures (fig. 12A), but basaltic dikes, tuffs, and breccias also are present. Modal mineralogy includes olivine, clinopyroxene, and plagioclase where some of the plagioclase is present as coarser grained phenocrysts (fig. 12B). This basalt unit, informally referred to as the Catway volcanics, overlies unnamed sandstone, shale, and minor basaltic tuff and breccia that locally contain *Turritella ocoyana* Conrad var., suggesting that these rocks fall within the early Miocene Saucasian and(or) Relizian Stages (J.G. Vedder, oral commun., 1993; fig. 2). Overlying



A



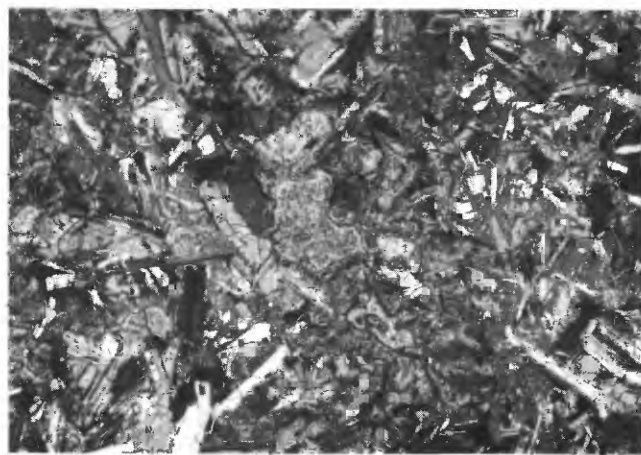
B

Figure 12. Catway volcanics in the Catway Road area. A, Outcrop of pillow basalt. B, Photomicrograph under cross-polarized light showing intersertal and hyalopilitic texture where phenocrysts of plagioclase are contained in a finer groundmass of olivine, clinopyroxene, and plagioclase laths. Some plagioclase phenocrysts are zoned. Field of view is 3 mm across.

the Catway volcanics is the Monterey Formation, which is biostratigraphically dated as Relizian and (or) Luisian in this area (J.G. Vedder, oral commun., 1993; fig. 2). The contact between the Catway volcanics and Monterey Formation is not exposed, but it may be erosional because interbeds of sandstone in the Monterey Formation contain basalt fragments. Published radiometric ages for the Catway volcanics include  $17.2\pm 2.5$  Ma and  $20.3\pm 1.6$  Ma (Hall, 1981a, corrected with methods of Dalrymple, 1979) and  $18.8\pm 1.5$  Ma (Vedder and others, 1994). Stratigraphic position of these samples is unknown, owing to poor exposures and complicated structure. Hall (1981b) originally mapped this interval as part of the Temblor Formation. We elect to use an informal designation and unnamed status for these rocks because the name "Temblor" is more commonly applied only to units on the northeast side of the San Andreas fault.

### Unnamed Volcanic Rocks of the Lopez Mountain Area

Near Lopez Mountain in the Santa Lucia Range (fig. 1), a poorly exposed and unnamed sequence of light-gray vitric tuff and basaltic andesite rests unconformably on Cretaceous and Jurassic sedimentary rocks. The tuff is well bedded and appears to grade upward into shales of the Miocene Monterey Formation, which in this area yields microfossil assemblages ranging in age from Saucian to Mohnian (McLean, 1994). The tuff is crystal poor and could not be dated, but a sample of interbedded basaltic rock yielded a K-Ar age on plagioclase of  $17.0\pm 0.5$  Ma (McLean, 1994). The basaltic flows are approximately 25 m thick, and the exposed thickness of the tuff is about 20 m (McLean, 1994). The basalt exhibits ophitic to subophitic textures in which plagioclase laths are enclosed by



**Figure 13.** Photomicrograph of unnamed basalt at Lopez Mountain under cross-polarized light. Plagioclase laths are partially to completely enclosed by clinopyroxene to form a subophitic to ophitic texture. Olivine, partially altered to clay minerals, is present in the center of the photomicrograph. Field of view is 3 mm across.

clinopyroxene (fig. 13). Altered olivine is present and appears to be exclusive of the ophitic minerals, suggesting that the olivine may have had a separate crystallization history.

### Morro Rock-Islay Hill Complex

The informally named Morro Rock-Islay Hill complex of Ernst and Hall (1974) is a 25-km-long chain of dacite, trachyte, and rhyolite volcanic necks, plugs, lava domes, and dikes that extends southeast from Morro Bay (figs. 1, 14A) (Ernst and Hall, 1974; Buckley, 1986). These rocks intrude mélangé and metamorphic rocks of the Franciscan Complex, and occur along a linear trend of about N. 55° W. This alignment implies that intrusion was fault controlled (Greenhaus and Cox, 1979). Radiometric dates for these intrusive rocks range from  $22.7\pm 0.9$  to  $28\pm 1.0$  Ma (fig. 2, table 1; Turner, 1968; Buckley, 1986). Detailed petrographic descriptions for the Morro Rock-Islay Hill complex are given by Ernst and Hall (1974) and Buckley (1986). In general, these rocks consist mostly of glassy matrix and plagioclase phenocrysts with minor amounts of quartz, biotite, hornblende, and iron oxides (fig. 14B). One potential extrusive equivalent to the Morro Rock-Islay Hill complex is the Cambria Felsite.

### Cambria Felsite

The Cambria Felsite was first named and described by Ernst and Hall (1974). This unit consists of about 115 m of rhyolite-dacite crystalline felsite and poorly exposed tuff in the region north of Estero Bay (fig. 1; Ernst and Hall, 1974). The Cambria Felsite unconformably overlies Jurassic and Cretaceous rocks of the Franciscan Complex and is unconformably overlain by late Oligocene nonmarine sedimentary rocks of the Lospe(?) Formation of Ernst and Hall (1974) (fig. 2). Mineralogically the Cambria Felsite consists of plagioclase, quartz, biotite, and iron oxides in a fine glassy matrix. Unpublished  $^{40}\text{Ar}/^{39}\text{Ar}$  isotopic data from the Cambria Felsite suggest an age of about 27 to 26.5 Ma (J.D. Obradovich, oral commun., 1994; M.E. Tennyson and M.A. Keller, oral commun., 1994; M.A. Mason and C.C. Swisher, oral commun., 1990).

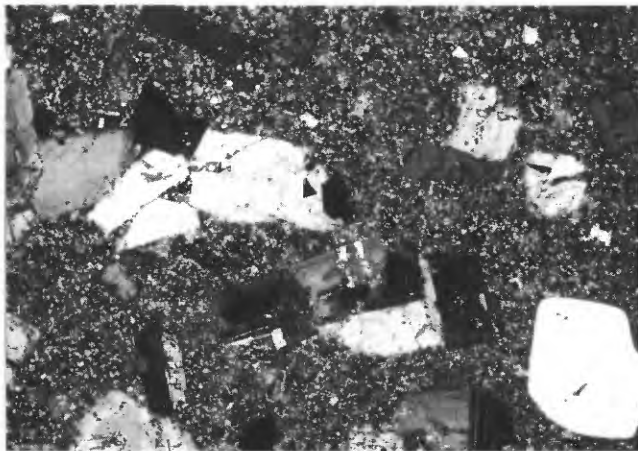
### Unnamed Volcanic Rocks of Upper Pine Creek

Several small patches of unnamed basaltic andesite were mapped by Hall and Corbató (1967) and Vedder and others (1991) in the upper Pine Creek area (fig. 1). The outcrops are very poor, and it is unclear whether the basaltic andesites are intrusive or extrusive. Hall and Corbató (1967) originally assigned these rocks to the Obispo Formation but a K-Ar age on plagioclase of  $26.6\pm 0.5$  Ma (Vedder and others, 1991) implies that this unnamed basaltic andesite unit is older than rocks of the Obispo Formation. Thin sections show that these rocks consist of lath-shaped phenocrysts of plagioclase in a groundmass of strongly flow-

oriented (trachytic) plagioclase microlites, with subordinate amounts of augite and opaque oxides. The volcanic rocks of upper Pine Creek are about the same age as the Morro Rock–Islay Hill complex but do not fall along the same structural trend. They may instead represent a localized volcanic center that is genetically related to the Sur-Nacimiento Fault Zone (Vedder and others, 1991).

### Subsurface Volcanic Rocks (Onshore and Offshore)

The Santa Maria province contains large oil and gas reserves and has been explored extensively with well and seismic data (Hall, 1982; Ogle, 1984; Crain and others, 1985; Fischer, 1987; McCulloch, 1987; Dunham and others, 1991; McIntosh and others, 1991; Meltzer and Levander, 1991). By combining this published information with unpublished well-



B

**Figure 14.** Photographs of intrusion at Morro Rock. *A*, Morro Rock at Morro Bay. This outcrop may be the remnant of a volcanic plug. *B*, Photomicrograph of Morro Rock under cross-polarized light. Porphyritic texture with rounded quartz, euhedral and zoned plagioclase, and euhedral to subhedral biotite in a glassy groundmass. Some plagioclase phenocrysts are clumped together and form a glomeroporphyritic texture. Field of view is 3 mm across.

log data (K.J. Bird, oral commun., 1991) and surface data, a regional thickness map for volcanic rocks in the Santa Maria province has been constructed (fig. 15). The sources of data for this map are listed in appendix 3. Because available data from wells is very sparse, figure 15 shows only limited onshore trends and information only for the southern portion of the offshore Santa Maria basin. These results are therefore tentative and should be treated as preliminary.

The precise age of volcanic rocks in the subsurface Santa Maria province is poorly constrained. Subsurface volcanic rocks onshore are found overlying the upper Oligocene part of the Vaqueros Formation or the lower Miocene Rincon Shale, or are interbedded with the lower Miocene Lospe Formation, and are overlain by the middle Miocene Monterey Formation (Hall, 1982; Tennyson and others, 1991; Stanley and others, 1996). Examination of exploratory well logs along with available seismic interpretations show that the subsurface volcanic rocks in the southern offshore Santa Maria basin unconformably overlie Jurassic and (or) Cretaceous rocks and are overlain by either the lower Miocene Point Sal Formation or the lower and middle Miocene Monterey Formation (Crain and others, 1985; Meltzer and Levander, 1991; K.J. Bird, oral commun., 1991). Therefore, the offshore subsurface volcanic rocks have a potential age range between Cretaceous and lower Miocene. Because these stratigraphic relations are similar to the stratigraphic relations of exposed and radiometrically dated onshore Santa Maria province 20–16 Ma volcanic rocks, we tentatively refer to the subsurface volcanic rocks as lower Miocene.

In general, the thickness patterns of lower Miocene volcanic rocks follow the major structural trends within the Santa Maria province (fig. 15). For example, linear zones of thick volcanic deposits are parallel to the Santa Ynez River and Los Osos Faults and are present along the Hosgri Fault (fig. 15). Available seismic data suggest that the offshore volcanic rocks thicken across several small, northwest-trending normal faults that were active during early Miocene time (McCulloch, 1987; McIntosh and others, 1991; Meltzer and Levander, 1991; K.J. Bird, oral commun., 1991).

### Other Occurrences of Volcanic Rocks

Several other occurrences of volcanic rocks are not shown on figure 2 because their stratigraphic relations are poorly known or because they occur just outside the Santa Maria province. About 15 km southeast of Lopez Mountain (fig. 1), recent mapping by Hugh McLean (oral commun., 1995) has revealed small patches of basaltic rocks that interfinger with and are overlain by shallow-marine sandstone of the lower Miocene Vaqueros Formation, which in this area contains the marine gastropod *Turritella inezana* and is overlain by Rincon Shale containing calcareous nannofossils of the earliest Miocene CN1 and (or) CN2 zones. Small undated basaltic dikes that intrude Cretaceous and lower(?) Miocene strata occur at scattered localities in the San Rafael Mountains east, north-

east, and north of Figueroa Mountain and along the Sisquoc and Cuyama Rivers east of Santa Maria (Vedder and others, 1967; Hall and Corbató, 1967; J.G. Vedder, oral commun., 1995). At Hell's Half Acre, about 9 km southeast of Figueroa Mountain and east of the edge of the map in figure 1, Fritsche and Thomas (1990) found a lens of basalt that yielded a whole-rock potassium-argon age of  $18.5 \pm 2.0$  Ma (table 1). About 3 km northeast of the Sur-Nacimiento fault and 25 km northeast of Nipomo (fig. 1), a basalt flow in the lower part of the Oligocene and lower Miocene Simmler Formation yielded whole-rock potassium-argon ages of  $23.4 \pm 0.8$  and  $22.9 \pm 0.7$  Ma (table 1; Ballance and others, 1983).

## GEOCHEMISTRY OF VOLCANIC ROCKS

Several studies provide information on the geochemical characteristics of some of the volcanic rocks in the Santa Maria province (Ernst and Hall, 1974; Robyn, 1980; Weigand, 1982; Buckley, 1986; Cole and others, 1991b; Cole and Basu, 1992, 1995; Hornafius, 1994; app. 2). Available data on major element chemistry show that the Santa Maria province volcanic rocks generally comprise a bimodal suite with basalt and basaltic andesite as a basic end-member and rhyolite, dacite, and trachyte forming an acidic end-member (fig. 16). Intermediate compositions (for example, andesites) are notably sparse from the available sample set.

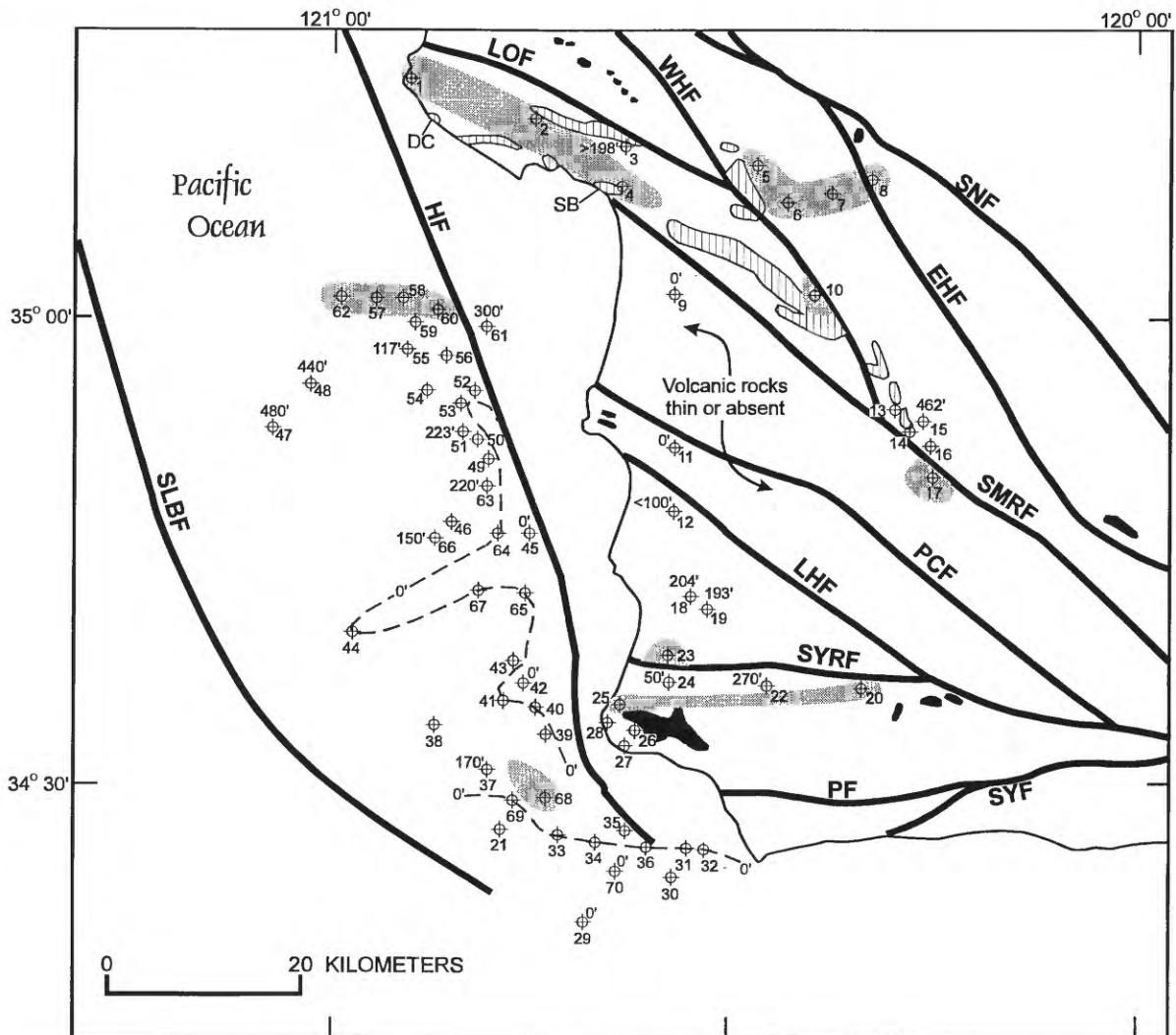
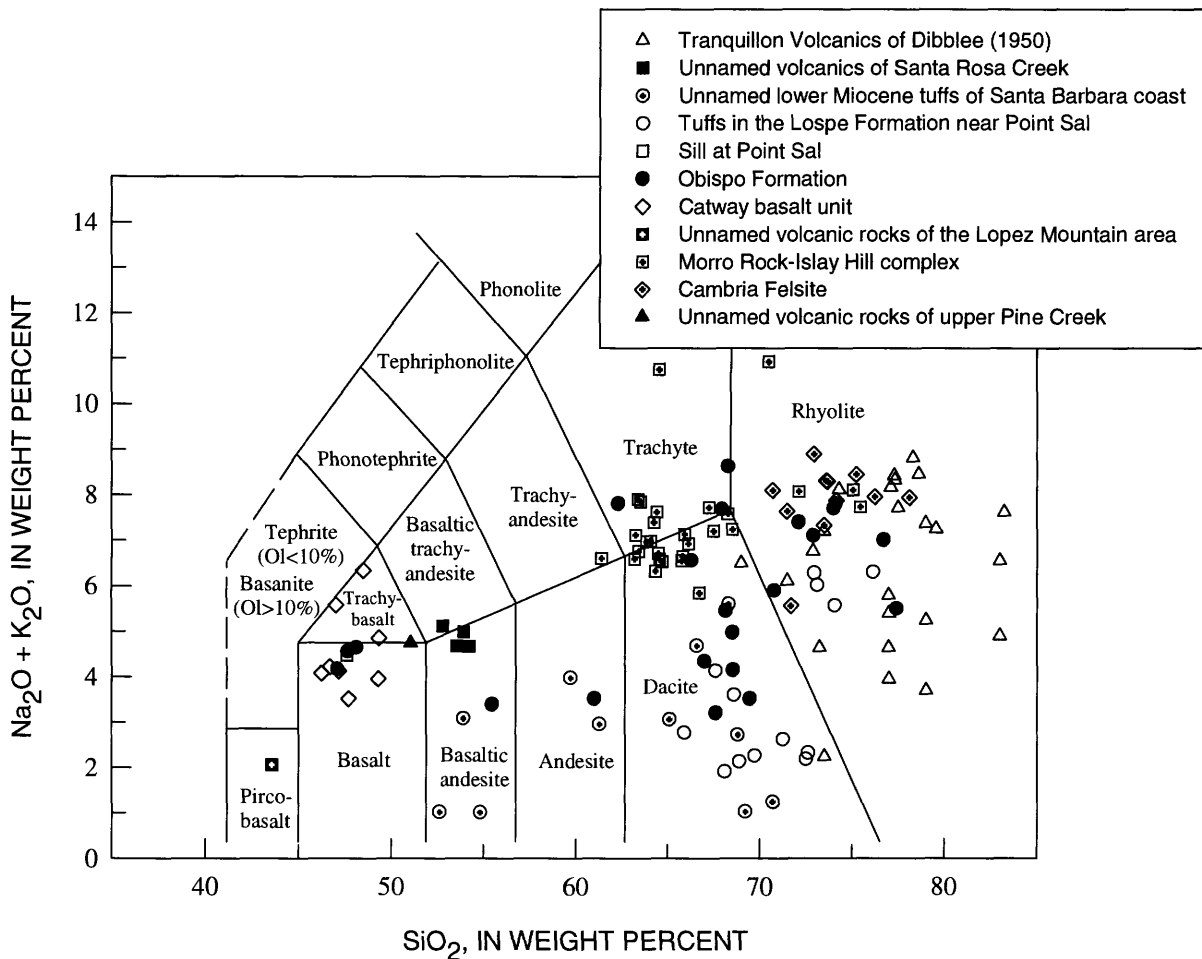


**Figure 15.** Thickness map of lower Miocene volcanic rocks in part of the Santa Maria province. Gray shading represents zones where volcanic rock thickness is 500 ft (152 m) or more. Dashed line represents a contour of zero thickness for volcanic rocks. Numbered points represent wells or outcrops where the thickness of volcanic units was available. Data for these points are listed in appendix 3. Outcrop patterns of volcanic rocks are as shown in figure 1. Abbreviations: DC, Diablo Canyon area; SB, Shell Beach; SMRF, Santa Maria River Fault; SNF, Sur-Nacimiento Fault; EHF, East Huasna Fault; WHF, West Huasna Fault; LHF, Lions Head Fault; SYRF, Santa Ynez River Fault; PF, Pacifico Fault; SYF, Santa Ynez Fault; HF, Hosgri Fault; LOF, Los Osos Fault; PCF, Pezzoni-Casmalia Fault; SLBF, Santa Lucia Bank Fault.

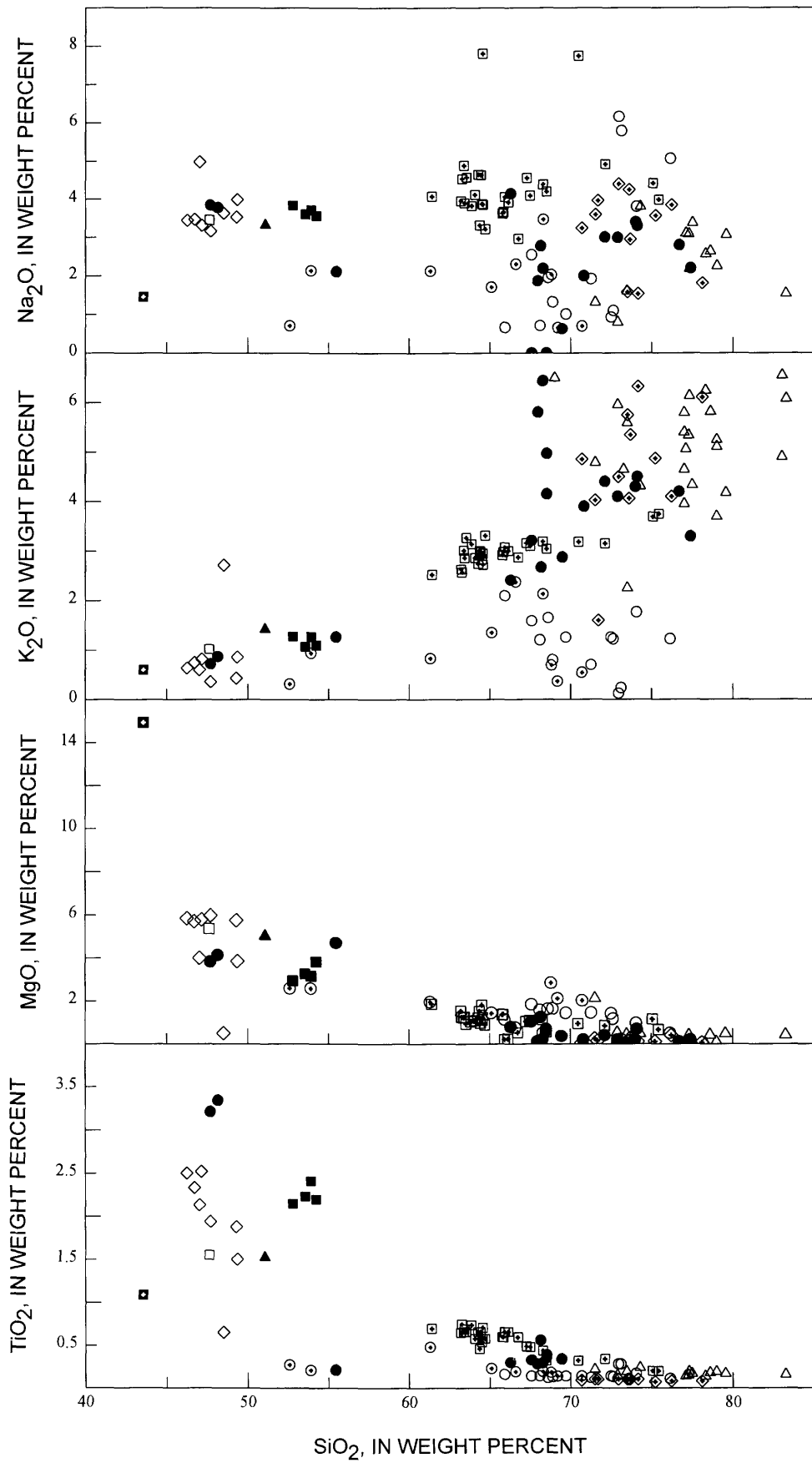
Variations of some major oxides with respect to  $\text{SiO}_2$  are shown in figure 17. No apparent geochemical differences exist between the 20-16 and 28-23 Ma volcanic suites. The coherent trends among these elements suggest that the suites of Santa Maria province volcanic rocks may have had a similar petrogenetic history. The trend of decreasing  $\text{MgO}$  and  $\text{TiO}_2$  with increasing  $\text{SiO}_2$  may have been a result of fractional crystallization of olivine, pyroxene, and ilmenite (Wilson, 1989). The increase of  $\text{K}_2\text{O}$  with increasing  $\text{SiO}_2$  could possibly be attributed to assimilation of high-K crust by basaltic magmas (Watson, 1982). In addition, the  $\text{Na}_2\text{O}$  contents of a suite of rocks produced by crustal contamination may be expected to remain relatively constant with respect to  $\text{K}_2\text{O}$  (Watson, 1982). Although there is considerable variation in  $\text{Na}_2\text{O}$  content among just the acidic volcanic rocks, the average  $\text{Na}_2\text{O}$  content among the combined basic and acidic end-members is a narrow range between 3 and 5 weight percent (fig. 17). These variations suggest that combinations of fractional crystallization and crustal assimilation were important during the petrogenetic history of the Santa Maria province volcanic rocks.

Available Nd- and Sr-isotopic and trace element data support the variations of major element chemistry and indicate that the bimodal suite of Santa Maria volcanic rocks evolved by combinations of assimilation and fractional crystallization (Cole and Basu, 1992, 1995). Initial ratios of  $^{87}\text{Sr}/^{86}\text{Sr}$  range between 0.702575 and 0.711308, and initial  $\epsilon_{\text{Nd}}$  values range between +9.3 and -3.2 (Cole and Basu, 1992, 1995). These data indicate that the source of basaltic magma for Santa Maria volcanism included suboceanic mantle similar to the source of mid-ocean ridge basalt. This basaltic source underwent some fractionation and also melted local enriched crustal rocks to form acidic magmas, resulting in the bimodal suite of Santa Maria province volcanic rocks (Cole and Basu, 1992, 1995). The presence of modal olivine, clinopyroxene, and plagioclase in Santa Maria province basalt samples indicates that these rocks are tholeiitic basalt, which is consistent with derivation from mid-ocean ridge type magma.

Limited trace element data are available and have been compiled for some of the Santa Maria province volcanic rocks (app. 2). Because these data are from different sources in which



**Figure 16.** Silica ( $\text{SiO}_2$ ) versus total alkalis ( $\text{Na}_2\text{O} + \text{K}_2\text{O}$ ) for Santa Maria province volcanic rocks showing lithologic classifications of LeBas and others (1986). Data as shown in appendix 2 are compiled from Ernst and Hall (1974), Robyn (1980), Weigand (1982), Buckley (1986), Cole and Basu (1992, 1995), and Hornafius (1994).



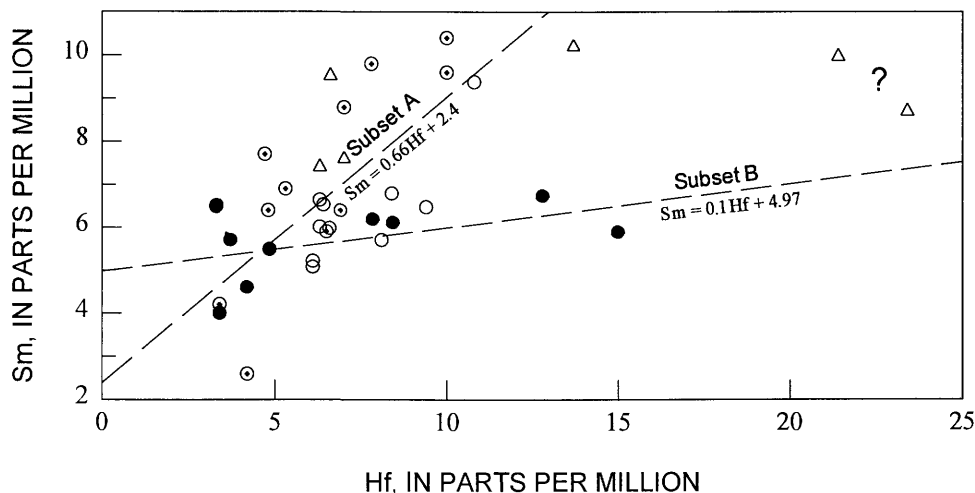


**Figure 18.** Samarium (Sm) versus hafnium (Hf) variation diagram for selected 20-16 Ma volcanic units in the Santa Maria province. Data as shown in appendix 2 are compiled from Hornafius (1994) and Cole and Basu (1995), and include new data for tuffs in the Lospe Formation. Symbols of volcanic units are the same as in figure 16. Dashed lines are best-fit linear regression lines for subsets A and B of the 20-16 Ma volcanic rocks, as labelled. The equation for each line is also shown. Note that subsets A and B are defined by different correlation lines that may represent eruption of each subset from separate magmatic suites.

measurements were made by different methods, rigorous quantitative petrogenetic modeling is not warranted. Nevertheless, simple qualitative observations of the compiled trace element data appear to be useful for recognizing possible correlations (comagmatic sets) among the 20-16 Ma acidic volcanic rocks. The 28-23 Ma volcanic rocks are not included in this discussion because very little trace element data are available for these rocks.

Two chemically distinct subsets among the 20-16 Ma acidic volcanic rocks are defined by comparing concentrations of incompatible elements (figs. 18, 19). Subset A includes the Tranquillon Volcanics of Dibblee (1950), tuffs in the Lospe Formation, and tuffs of the Santa Barbara coast; subset B includes rocks of the Obispo Formation. The variation of these subsets with respect to Sm and Hf are displayed in figure 18, where subset B is defined by a less steep correlation line. Subsets A and B are also distinguished by the variation of Nb and La (La/Nb = 3.03 and 2.0 for subsets A and B, respectively) and on the basis of their enrichment of light rare earth elements (LREE), where subset A exhibits greater LREE enrichment (for subset A, La/Yb = 12.14 and La/Sm = 5.52, but for subset B, La/Yb = 5.82 and La/Sm = 4.15; see fig. 19). Because Sm-Hf and La-Nb are incompatible element pairs that have similar bulk partition coefficients, the ratio of these element pairs is not expected to vary significantly during the course of fractional crystallization or partial melting of mantle-derived magmas (Bougault and others, 1980; Sun and

McDonough, 1989; Rollinson, 1993). These ratios would, however, be expected to vary as a result of magma mixing or crustal contamination. The variation of Hf/Sm and La/Nb between subsets A and B might therefore characterize a different contamination and (or) mixing history of suboceanic mantle-derived magmas (for example, Cole and Basu, 1995) that erupted separately to form the two subsets of volcanic rocks. The difference in LREE enrichment between subsets A and B could also be attributed to different contamination histories of suboceanic mantle-derived magma. Based upon these observations, we suggest that the volcanic rocks of subsets A and B were erupted from different volcanic centers within the Santa Maria province. In other words, we suggest that these geochemical variations reveal that the Tranquillon Volcanics of Dibblee (1950), tuffs in the Lospe Formation, and tuffs of the Santa Barbara coast were comagmatic and formed from one eruptive region, whereas the Obispo Formation volcanic rocks represent a separate comagmatic suite. As noted by Hornafius (1994), tuff samples NB440 and NB399 of the Santa Barbara coast appear to be chemically similar to the Obispo Formation and lie within subset B (fig. 19); these two tuffs could represent fallout deposits that were derived from the Obispo eruptive source.

## VOLCANIC SOURCE AREAS AND PALEOGEOGRAPHY

Available information on the distribution, thickness, stratigraphy, facies, and geochemical characteristics of the Santa Maria province volcanic rocks allow correlation of widely separated volcanic units and identification of possible

◀ **Figure 17.** Silica (SiO<sub>2</sub>) versus titanium (TiO<sub>2</sub>), magnesium (MgO), sodium (Na<sub>2</sub>O), and potassium (K<sub>2</sub>O) for volcanic units in the Santa Maria province. Data compiled from the same sources as in figure 16. Symbols of volcanic units are the same as in figure 16.

source areas for volcanism. This information can be combined with existing data on middle Tertiary sedimentary basin development and fault activity to test paleogeographic models and to relate episodes of volcanism to tectonic events.

Two episodes of Santa Maria province volcanism are recognized on the basis of the ages of the volcanic units. An older group of rocks ranges between about 28 and 23 Ma and includes the Morro Rock–Islay Hill complex, the Cambria Fel-

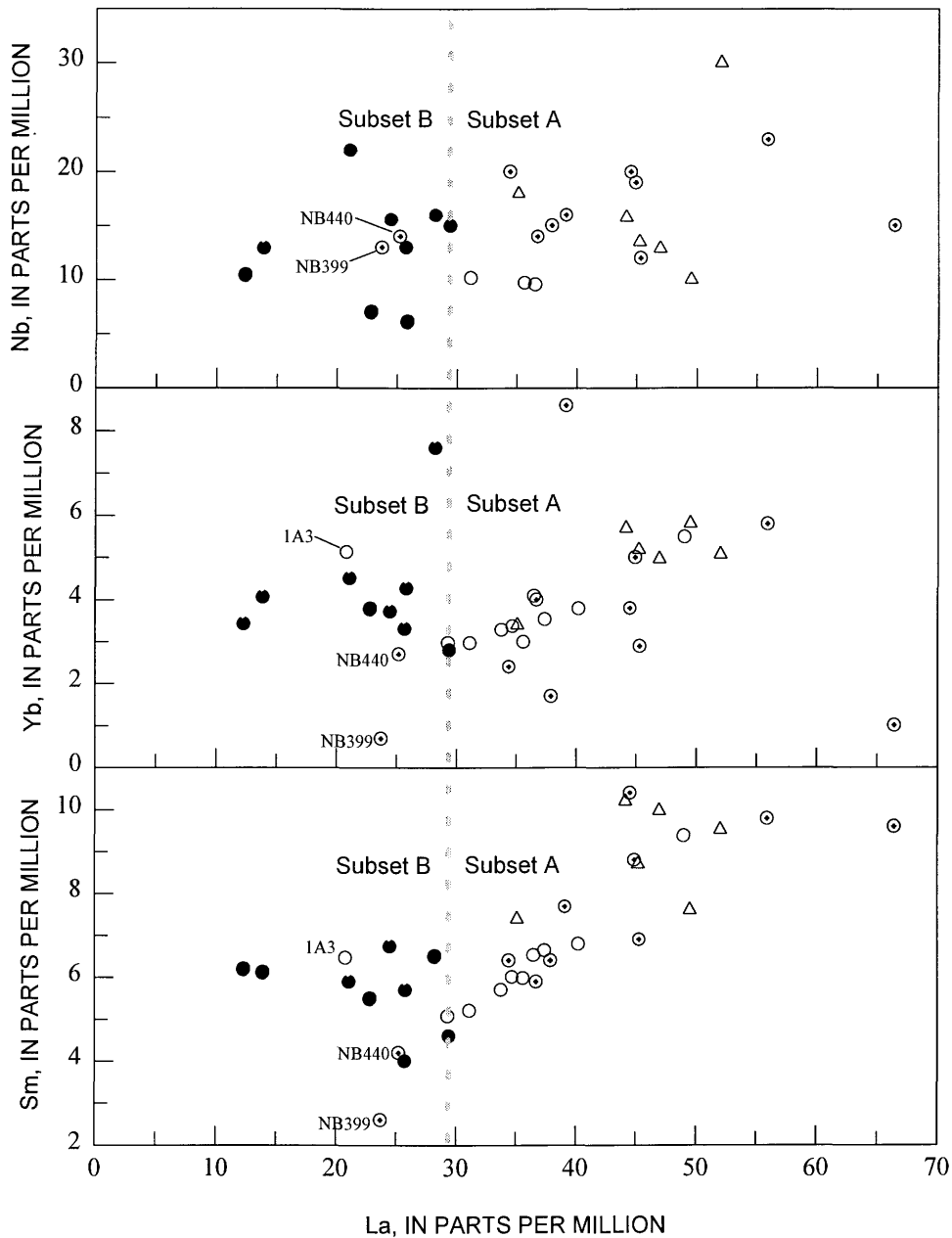


**Figure 19.** Lanthanum (La) versus samarium (Sm), ytterbium (Yb), and niobium (Nb) for selected 20-16 Ma volcanic units in the Santa Maria province. Data compiled from same sources as in figure 18. Symbols of volcanic units are the same as in figure 16. Gray dotted lines separate subsets A and B on the basis of their relative enrichment of La. Samples of subset A consistently show greater La/Nb, La/Yb, and La/Sm ratios than samples of subset B. In addition, samples of subset A appear to lie along different correlation lines than samples of subset B, especially for La-Yb and La-Sm. Samples NB440 and NB399 are from two unnamed tuffs of the Santa Barbara coast that appear to be chemically similar to the Obispo Formation and lie within subset B; all of the other unnamed tuffs of the Santa Barbara coast appear to be magmatically related to subset A. Sample 1A3, a tuff in the Lospe Formation near Point Sal, displays an anomalously low La concentration; the significance of this sample is uncertain.

site, and the unnamed volcanic rocks at upper Pine Creek. A younger group of rocks ranges between about 20 and 16 Ma and includes the Tranquillon Volcanics of Dibblee (1950), unnamed basaltic andesite of Santa Rosa Creek, Obispo Formation, tuffs in the Lospe Formation, unnamed lower Miocene tuffs of the Santa Barbara coast, the Catway volcanics, and the Lopez Mountain volcanic rocks. The poor age control on volcanic rocks in the offshore Santa Maria province does not allow them to be placed in the younger or older volcanic suite so we tentatively group them as lower Miocene.

The first episode of Santa Maria province volcanism (28–23 Ma) included the emplacement of the Morro Rock–Islay Hill complex and the Cambria Felsite. Based on the similar stratigraphic positions and the similar geochemical affinities of these two units, Ernst and Hall (1974) suggested that the Cambria Felsite was the extrusive equivalent of the Morro Rock–Islay Hill complex. The Cambria Felsite generally is more enriched in  $K_2O$  and  $SiO_2$  and less enriched in  $MgO$  than the intrusive rocks of the Morro Rock–Islay Hill complex (figs. 16, 17). This contrast in chemistry could indicate that the Cambria Felsite formed when high silica, K-rich crustal components were melted and assimilated by a magma that is partially preserved as the Morro Rock–Islay Hill intrusive rocks. Further field studies of the Cambria Felsite, including facies analysis and detailed thickness distributions, are required to determine the location(s) of the eruptive source area(s). Irrespective of the eruptive centers, the Morro Rock–Islay Hill complex and the Cambria Felsite range from somewhat older to about the same age as several other volcanic units and sedimentary basins that formed in central and southern California during the late Oligocene and early Miocene (Stanley, 1987, 1988; Atwater, 1989; Cole and Basu, 1995). These volcanic rocks were most likely erupted during regional extension or transtension along the continental margin during the initial transition from a subduction to a strike-slip plate boundary between the Pacific and North American plates (Atwater, 1970, 1989; Stanley, 1987, 1988; Severinghaus and Atwater, 1990).

Possible volcanic source areas for the second episode of middle Tertiary volcanism in the Santa Maria province (20–16 Ma) can be inferred by using thicknesses of volcanic units (assuming that volcanic units thicken toward their source), volcanoclastic facies, paleoflow data, relative abundance of intrusive rocks, and geochemical parameters. The Tranquillon Volcanics of Dibblee (1950) at Tranquillon Mountain include thick, welded lapilli tuffs that were most likely deposited from pyroclastic flows, and thick nonwelded tuffs and bomb-beds that probably represent fallout deposits (figs. 3, 4). These facies are typical of relatively proximal pyroclastic deposits (Smith, 1960; Fisher and Schmincke, 1984; Cas and Wright, 1987). In addition, the unconformity at the base of these volcanic rocks suggests that the region of Tranquillon Mountain had undergone uplift, possibly related to thermal doming near a volcanic source (Robyn, 1980). Volcanoclastic deposits that were distal equivalents to the type Tranquillon rocks would most likely be thinner and nonwelded. Such deposits may include the tuffs that are

interbedded in the Lospe Formation about 30 km north of Tranquillon Mountain (figs. 1, 6; Cole and others, 1991b) and most of the unnamed lower Miocene tuffs of the Santa Barbara coast. This hypothesis is consistent with available trace element data, which reveal that the rocks of these three areas most likely had a similar magmatic history (figs. 18, 19). In this hypothesis, the tuffs of the Lospe Formation would have been shed northward (in present and early Miocene time) by pyroclastic flows and subaqueous sediment gravity flows of reworked ash (Cole and Stanley, 1994). Northward-directed flow is corroborated by crossbeds in one tuff bed in the Lospe Formation. Sparse well data (for example, index numbers 23, 18, 19, and 12 on fig. 15 and in app. 3) between Tranquillon Mountain and the tuffs of the Lospe Formation suggest that there are volcanic rocks in the subsurface between the two units, which thin from south to north. This is consistent with the hypothesis that the tuffs in the Lospe Formation were derived from sources to the south. Most of the thin tuffs and bentonites exposed along the Santa Barbara coast, including the thickest and stratigraphically lowest tuff (for example, the Tranquillon tuff) probably represent deposits from small pyroclastic flows or airborne ash clouds that drifted southward and eastward away from the eruptive center near Tranquillon Mountain.

The source(s) for volcanoclastic rocks of the Obispo Formation was (were) probably different than the source of the volcanoclastic units to the south (for example, tuffs in the Lospe Formation and the Tranquillon volcanic rocks). Sparse well data (for example, index numbers 9 and 11) show an absence of subsurface volcanic rocks in the area between outcrops of the Obispo Formation and the tuffs in the Lospe Formation (fig. 15). The Obispo Formation as well as the unnamed volcanics of Santa Rosa Creek also display a different trace element composition than tuffs in the Lospe Formation and the Tranquillon Volcanics of Dibblee (1950) which suggests a different magmatic and eruptive history. Several lines of evidence indicate that an eruptive source area for the Obispo Formation was located in the offshore and (or) Diablo Canyon area west of the present Obispo Formation outcrop belt (Surdam and Hall, 1984; R.V. Fisher, oral commun., 1990; Schneider and Fisher, 1996; fig. 1). First, paleoflow data from tuffs in the Obispo Formation indicate transport from west to east (Surdam and Hall, 1984; Schneider and Fisher, 1996). Second, the thickest and more proximal pyroclastic facies of the Obispo Formation is exposed in the west (Shell Beach area) with thinner and more distal facies present eastward (Twitchell Dam area; Schneider and Fisher, 1996). Third, the concentration of mapped intrusive rocks is greatest at the northwestern end of the Obispo Formation exposures (Surdam and Hall, 1984; R.V. Fisher, oral commun., 1990). Finally, water depths during deposition of the Obispo Formation, based on faunal evidence, were more shallow to the west (50 m) and deeper to the east (>500 m; Surdam and Hall, 1984). Collectively, these data suggest that a topographically high volcanic source region was probably located west to northwest of the Obispo Formation outcrops in the present offshore Santa Maria basin. Based

upon a similarity in chemical composition with the Obispo Formation, it is possible that one or two of the unnamed tuffs of the Santa Barbara coast (for example, samples NB440 and NB399 of Hornafius, 1994; fig. 19) were formed from ash that drifted southward from an Obispo eruptive source.

The thickest preserved lower Miocene volcanic rocks in the Santa Maria province reach about 4,900 ft (1,479 m) along the Santa Maria River Fault (index number 17 on fig. 15). These thick subsurface volcanic rocks could represent either proximity to an eruptive center or ponding in a topographic low area along the south side of the fault. The source of these volcanic rocks could have been the eruption center that is inferred in the Diablo Canyon area and (or) offshore areas to the northwest. This hypothesis is consistent with the Santa Maria River Fault being active during early Miocene volcanism and bounding a structural depression to the south where thick intervals of volcanic rocks accumulated.

Eruptive centers for some Santa Maria province volcanic rocks could also have been situated along and (or) west of the Hosgri Fault in the present offshore Santa Maria basin, where there are thick accumulations of lower Miocene volcanic rocks (fig. 15). Such a volcanic center(s) could have been a source for the Obispo Formation, the tuffs in the Lospe Formation, the type Tranquillon volcanic rocks, and (or) the Summerland tuff unit. Available seismic data for the offshore Santa Maria basin show several examples where lower Miocene volcanic and nonvolcanic rocks thicken across steep-dipping faults, but the overlying Pliocene rocks are not crosscut by these faults (McCulloch, 1987; McIntosh and others, 1991; Meltzer and Levander, 1991; K.J. Bird, oral commun., 1991). This includes data for the San Gregorio-Hosgri Fault, which may have been a southwest-dipping normal fault during the early Miocene (McCulloch, 1987; McIntosh and others, 1991). These data suggest that the offshore region was undergoing an episode of synvolcanic and syndepositional extension during early Miocene time. Eruptive centers may have been concentrated along these faults in this region of extension.

Eruptive sources for the several 20 to 16 Ma Santa Maria province basalt flows and basaltic breccias are not as readily discerned as the acidic pyroclastic eruptive sources. The basaltic flows probably were not as far travelled as the acidic volcanoclastic deposits and therefore may be relatively close to their eruptive sources.

To better understand the 20-16 Ma episode of volcanism in the Santa Maria province, these volcanic rocks have been restored to their approximate early Miocene positions (fig. 20) using paleogeographic reconstructions based upon paleomagnetic studies (Hornafius, 1985; Hornafius and others, 1986; Luyendyk, 1991). These studies suggest that the present east-west-trending western Transverse Ranges were previously oriented north-south during the early Miocene, prior to 95° of post-early Miocene clockwise rotation. During rotation right-lateral slip, with displacements generally less than 10-20 km, probably occurred along several northwest-trending faults in the Santa Maria basin,

including the Lions Head and Santa Maria River Faults (Hornafius and others, 1986). These faults formed the boundaries between individual crustal blocks and probably had some component of extension as well as strike-slip (Hornafius, 1985; Luyendyk, 1991).

The models discussed above predict that zones of extension within the Santa Maria province would have been developed between individual rotating and nonrotating blocks in an overall transtensional regime. The thickest accumulations of onshore Santa Maria volcanic rocks and the postulated eruptive centers for these rocks seem to be coincident with those regions in which the greatest extension is predicted by these models (fig. 20). For example, the predicted source of the Obispo Formation is near the northwest corner of the Santa Maria province and coincides with a zone of predicted crustal extension between the Hosgri fault and the northwest-trending Santa Maria River and Los Osos Faults. In addition, the Tranquillon Volcanics are thickest along trend with the Santa Ynez River Fault, which may have been adjacent to several triangular zones of extension during block rotations (Hornafius, 1985; Luyendyk, 1991; fig. 20).

## RELATIONS OF VOLCANISM TO REGIONAL TECTONIC EVENTS

The bimodal geochemical character of volcanic rocks in the Santa Maria province is consistent with the regional trend of Tertiary bimodal volcanism that occurred in western California as Sierra Nevada arc magmatism ended and near-trench bimodal volcanism began (Christiansen and Lipman, 1972). This change in the nature of volcanism in western California most likely occurred in response to the transition from a convergent to a strike-slip plate boundary when segments of the Farallon-Pacific spreading ridge intersected western North America in the vicinity of southern California (Atwater, 1970; 1989; Christiansen and Lipman, 1972; Snyder and others, 1976; McCrory and others, 1995). We propose that the combination of oblique-slip or transtension between the Pacific and North American plates and the source of heat and upper mantle magmas supplied to the base of the continental margin by subducted segments of the Farallon-Pacific spreading ridge, resulted in the episodes of Santa Maria province volcanism. In this model, the Farallon-Pacific spreading-ridge segments provided basaltic magmas for Santa Maria volcanism, and the transtension along the continental margin caused zones of crustal thinning and faulting that provided conduits for magmas to reach the surface. Isotopic and geochemical data support this hypothesis because several Santa Maria province basalt samples retain mid-ocean ridge basalt signatures (Cole and Basu, 1992, 1995).

If this model is accurate, then the two episodes of volcanism imply two episodes of Farallon-Pacific spreading-ridge collision with western North America. Tectonic reconstructions by

McCroly and others (1995) reveal that a large segment of the Farallon-Pacific ridge stopped spreading by 24 Ma, and that this segment intersected the area between Point Arguello to near San Francisco, which embraces the area of 28-23 Ma volcanic rocks of central and southern California. A second ridge segment, the Pacific-Monterey segment, stopped spreading at about 19 Ma in

the vicinity of the central Santa Maria province (McCroly and others, 1995). Spatial and temporal correlations between spreading-ridge segments along the continental margin and palinspastically restored Santa Maria province volcanic rocks (as well as other similar-aged volcanic rocks in southern and central California; Stanley, 1987; Cole and Basu, 1995) are con-

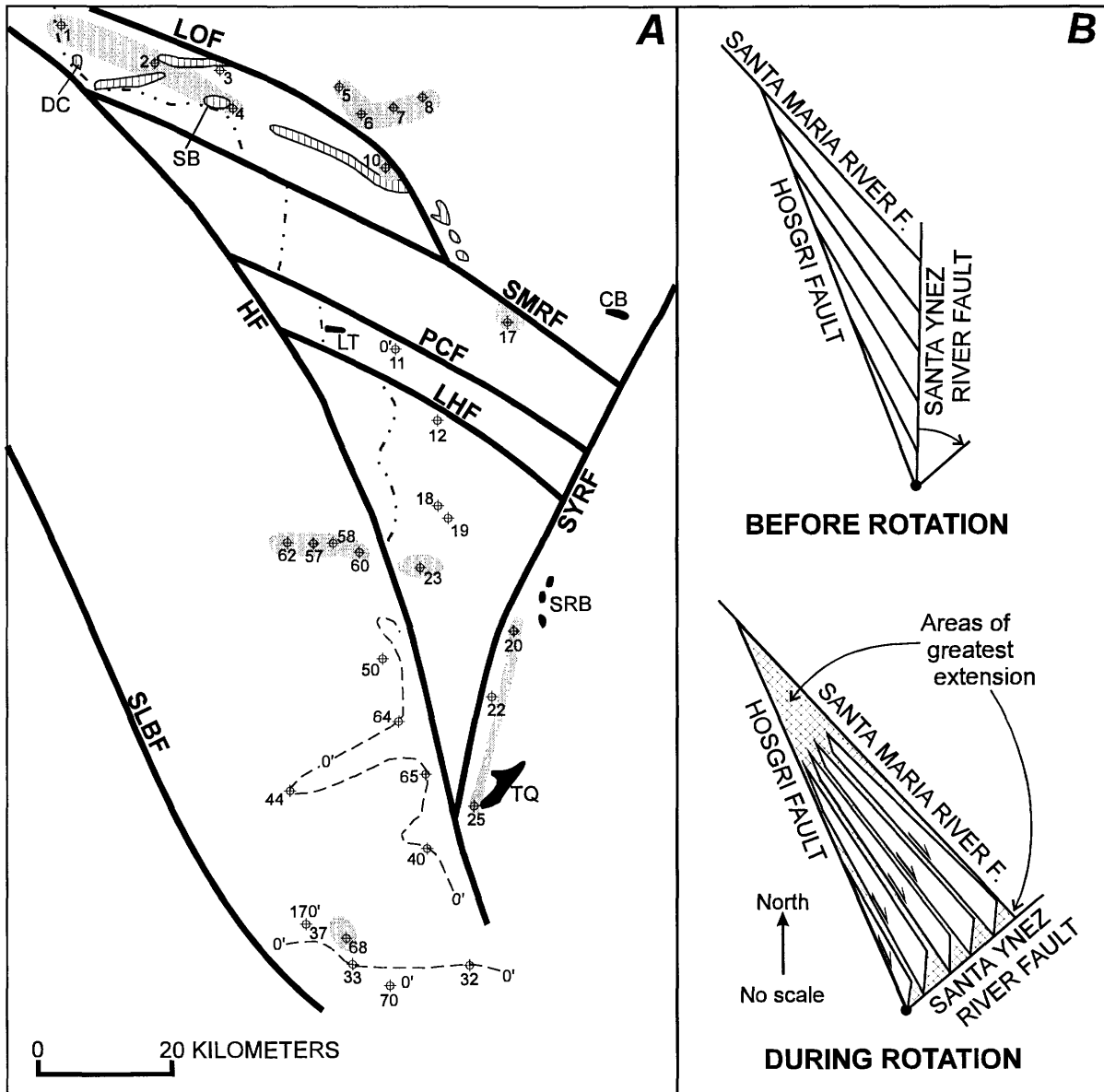


**Figure 20.** A, Early Miocene paleogeographic reconstruction for the Santa Maria province; restorations of Hornafius (1985), Hornafius and others (1986), and Luyendyk (1991). Volcanic thickness trends were adjusted from the present-day thickness map shown in figure 15. Representative thickness data points are shown for cross-reference with figure 15. Volcanic rocks in the offshore region are shown with 60 km of right-lateral displacement removed from the Hosgri Fault; this represents a median estimate for Hosgri Fault displacement. Total offset along the Hosgri Fault may have been as little as 5 km (Hamilton, 1982) or as much as 115 km (Graham and Dickinson, 1978a,b) or more (Graham and Peabody, 1981; Bachman and Abbott, 1988). Dashed-dotted lines represent restored modern coastline. Abbreviations: CB, Catway volcanics; LT, tuffs in the Lospe Formation; SRB, basalt near Santa Rosa Creek; TQ, Tranquillon Mountain; LOF, Los Osos Fault; SMRF, Santa Maria River Fault; PCF, Pezzoni-Casmalia Fault; LHF, Lions Head Fault; HF, Hosgri Fault; SYRF, Santa Ynez River Fault; SLBF, Santa Lucia Bank Fault; DC, Diablo Canyon area; SB, Shell Beach. B, Simplified model of block rotations and zones of crustal extension (cross-hatched) predicted in models of Hornafius (1985), Hornafius and others (1986), and Luyendyk (1991).

sistent with the model that volcanism occurred in response to spreading ridge-trench interactions. This model is also consistent with the slab window hypothesis in which upwelling asthenosphere fills a gap beneath western California following the demise of Farallon-Pacific spreading-ridge segments (Dickinson and Snyder, 1979; Severinghaus and Atwater, 1990).

Previous tectonic models have been suggested for Santa Maria province volcanism. In some respects our model is similar to a model proposed by Hall (1981a) that suggested that volcanism occurred along a leaky-transform fault that was a precursor to the San Andreas fault. The similarity between the two models is that each implies a mantle-derived magma source for volcanism. Our model, however, includes specific hypotheses that relate Santa Maria province volcanism to spreading ridge-trench interactions and discrete episodes of crustal extension and (or) transtension. Our model also differs from some previous models that suggest that volcanism in the Santa Maria province was a response to subduction-related processes (Crouch, 1978; Weigand, 1982). Isotopic and geochemical data reveal a bimodal magma source for Santa Maria province volcanic rocks where the basic end-member magmas were derived from upper mantle melts (similar to mid-ocean ridge basalt magma) as opposed to a melted subducted oceanic slab (Cole and Basu, 1992, 1995). In addition, based on radiometric ages for volcanic rocks described in this paper and paleomagnetic studies (for example, Hornafius and others, 1986; Luyendyk, 1991), we can infer that many of the Santa Maria province volcanic rocks were erupted in a transtensional regime during episodes of crustal block rotations when segments of the Farallon-Pacific spreading ridge were intersecting western California.

## CONCLUSIONS

The volcanic rocks of the Santa Maria province form important stratigraphic markers that are useful for surface and subsurface correlations and paleogeographic reconstructions in this petroleum-rich region. The Santa Maria volcanic units have distinctive lithologies that occupy discrete stratigraphic intervals. These volcanic units are, in some cases, laterally persistent and mappable for several to tens of kilometers.

Two separate age groups of volcanic rocks can be defined in the Santa Maria province on the basis of radiometric and biostratigraphic data. An older group of volcanic rocks that includes the Morro Rock–Islay Hill complex, the Cambria Felsite, and unnamed volcanic rocks of upper Pine Creek ranges from about 28 to 23 Ma. A younger group of volcanic rocks that includes the Obispo Formation, Tranquillon Volcanics of Dibblee (1950), tuffs in the Lospe Formation, and several other thin acidic tuffs and basaltic units ranges in age from about 20 to 16 Ma.

The vicinity of eruptive centers for Santa Maria volcanic units are determined by the thickness of volcanic units, volcanic facies, paleoflow data, the abundance of intrusive rocks, and geochemical data. Based upon their similar ages, compo-

sitional similarity, and close proximity, the Cambria Felsite may be the extrusive equivalent of the Morro Rock–Islay Hill complex. This relation is not well defined and can be tested by more detailed facies analysis of the Cambria Felsite.

Among the younger volcanic units, the Tranquillon Volcanics of Dibblee (1950) most likely represent proximal remnants of the southern Santa Maria province volcanic centers. This volcanic source may have shed ash as pyroclastic flows northward into the Santa Maria basin to form the tuffs within the Lospe Formation; this same eruptive source may also have formed ash clouds or small pyroclastic flows that transported ash to the south and east to form most of the unnamed lower Miocene tuffs of the Santa Barbara coast (for example, the Tranquillon tuff and the Summerland tuff). Collectively, these volcanic units (Tranquillon Volcanics of Dibblee (1950), tuffs in the Lospe Formation, and unnamed lower Miocene tuffs) are distinguished from volcanic rocks of the northern Santa Maria province by lower Hf/Sm, higher La/Nb, and greater light rare earth element enrichment (higher La/Yb and La/Sm). The Obispo Formation volcanic rocks probably were erupted from a source area in the northern part of the Santa Maria province. The source for these rocks is not well established, but paleoflow data and other evidence suggest that an eruptive center was present west (offshore) of the present Obispo outcrop belt. This eruptive center formed welded and nonwelded pyroclastic flow deposits (composed of cusped glass shards, pumice, pyrogenic crystals, and minor lithic grains), some of which were remobilized as eastward-directed submarine sediment gravity flows. Ash clouds from the Obispo eruptive region may also have drifted southward to form a few of the unnamed tuffs of the Santa Barbara coast (for example, tuff samples NB440 and NB399 of Hornafius, 1994; fig. 19 and app. 2).

Volcanic source areas may also have existed in the present southern half of the offshore Santa Maria basin. Lower Miocene strata, including volcanic rocks, thicken across several faults in the offshore region (Crain and others, 1985; McIntosh and others, 1991; Meltzer and Levander, 1991). These faults apparently were growth faults with a normal sense of displacement in a region of extension where volcanic eruptions may have been centered. The volcanic rocks in the southern half of the offshore Santa Maria basin may have accumulated in depocenters that were formed as downdropped blocks bounded by the normal faults.

At least some of the eruptive centers for Santa Maria volcanism may have been localized by zones of crustal extension between rotating crustal blocks as predicted by rotation models of the western Transverse Ranges (Hornafius, 1985; Hornafius and others, 1986; Luyendyk, 1991). When plotted on paleogeographic reconstructions that take into account paleomagnetic rotations, the volcanic eruptive centers and distribution of thick volcanic rocks coincide with crustal gaps that are predicted by the paleomagnetic rotation models.

Volcanic episodes in the Santa Maria province can be related to regional tectonic events. During middle Tertiary time, several segments of the Farallon-Pacific spreading ridge in-

tersected the North American continental margin in the vicinity of the Santa Maria province. As these spreading-ridge segments reached the continental margin, an oblique-slip plate boundary was formed between the Pacific and the North American plates (Atwater, 1970, 1989). The oblique-slip motion resulted in transtension along the preexisting subduction zone (Atwater, 1989; Luyendyk, 1991). During the same time, upper mantle material was juxtaposed beneath the continental margin from the subducted spreading-ridge segments. The volcanic rocks of the Santa Maria province were derived from basaltic magmas of the upper mantle that reached the surface during separate episodes of transtension along the oblique-slip plate boundary (Cole and Basu, 1992, 1995). Early phases of oblique slip resulted in an episode of regional transtension that occurred in central and southern California, during which time the 28-23 Ma Santa Maria volcanic rocks were emplaced (for example, the Morro Rock–Islay Hill complex, the Cambria Felsite, and unnamed volcanic rocks of upper Pine Creek). Subsequent oblique slip resulted in rotations of crustal blocks that included the western Transverse Ranges. Younger Santa Maria volcanic rocks (for example, Tranquillon volcanic units, the Obispo Formation) may have erupted from volcanic centers in zones of extension or transtension between the rotating and nonrotating crustal blocks.

## REFERENCES CITED

- Addicott, W.O., 1972, Provincial middle and late Tertiary molluscan stages, Temblor Range, California: Bakersfield Calif., Pacific Section, Society of Economic Paleontologists and Mineralogists, Proceedings of the Pacific Coast Miocene Biostratigraphic Symposium, p. 1-26.
- Atwater, T.M., 1970, Implications of plate tectonics for the Cenozoic tectonic evolution of western North America: Geological Society of America Bulletin, v. 81, p. 3513-3536.
- 1989, Plate tectonic history of the northeast Pacific and western North America, in Winterer, E.L., Hussong, D.M., and Decker, R.W., eds., The eastern Pacific Ocean and Hawaii: Boulder, Colo., Geological Society of America, The Geology of North America, v. N, p. 21-72.
- Bachman, W.R., and Abbott, P.L., 1988, Lower Paleogene conglomerates in the Salinian block. in Filewicz, M.V., and Squires, R.L., eds., Paleogene stratigraphy, west coast of North America: Los Angeles, Calif., Society of Economic Paleontologists and Mineralogists, Pacific Section, v. 58, p. 135-150.
- Ballance, P.F., Howell, D.G., and Ort, K., 1983, Late Cenozoic wrench tectonics along the Nacimiento, South Cuyama, and La Panza faults, California, indicated by depositional history of the Simmler Formation, in Anderson, D.W., and Rymer, M.J., eds., Tectonics and sedimentation along faults of the San Andreas system: Los Angeles, Calif., Society of Economic Paleontologists and Mineralogists, Pacific Section, p. 1-9.
- Bartow, J.A., 1992, Paleogene and Neogene time scales for southern California: U.S. Geological Survey Open-File Report 92-212, 2 sheets.
- Bougault, H., Joron, J.L., and Treuil, M., 1980, The primordial chondritic nature and large-scale heterogeneities in the mantle: evidence from high and low partition coefficient elements in oceanic basalts: Philosophical Transactions of the Royal Society of London, v. A297, p. 203-213.
- Buckley, S.L., 1986, Geochemistry of the Morro Rock–Islay Hill intrusive complex, San Luis Obispo county, California: M.S. thesis, California State University, Los Angeles.
- Cande, S.C., and Kent, D.V., 1992, A new geomagnetic polarity time scale for the Late Cretaceous and Cenozoic: Journal of Geophysical Research, v. 97, no. B10, p. 13,917-13,951.
- 1995, Revised calibration of the geomagnetic polarity timescale for the Late Cretaceous and Cenozoic: Journal of Geophysical Research, v. 100, no. B4, p. 6,093-6,095.
- Cas, R.A. and Wright, J.V., 1987, Volcanic successions: modern and ancient: a geological approach to processes: London, Allen and Unwin, 528 p.
- Christiansen, R.L., and Lipman, P.W., 1972, Cenozoic volcanism and plate tectonic evolution of the western United States. II: Philosophical Transactions of the Royal Society of London, v. A271, p. 249-284.
- Cole, R.B., and Basu, A.R., 1992, Middle Tertiary volcanism during ridge-trench interactions in western California: Science, v. 258, p. 793-796.
- 1995, Nd-Sr isotopic geochemistry and tectonics of ridge subduction and middle Cenozoic volcanism in western California: Geological Society of America Bulletin, v. 107, p. 167-179.
- Cole, R.B., and Stanley, R.G., 1994, Sedimentology of subaqueous volcanoclastic sediment gravity flows in the Neogene Santa Maria basin, California: Sedimentology, v. 41, p. 37-54.
- Cole, R.B., Stanley, R.G., and Basu, A.R., 1991b, Stratigraphy and origin of lower Miocene volcanic rocks, onshore and offshore Santa Maria province, California [abs.]: Geological Society of America Abstracts With Programs, v. 23, p. A476.
- Cole, R.B., Stanley, R.G., and Johnson, S.Y., 1991a, Origin of tuff deposits in the lower Miocene Lospe Formation, Santa Maria basin, California [abs.]: American Association of Petroleum Geologists Bulletin, v. 75, p. 359-360.
- Crain, W.E., Mero, W.E., and Patterson, D., 1985, Geology of the Point Arguello discovery: American Association of Petroleum Geologists Bulletin, v. 69, no. 4, p. 537-545.
- 1987, Geology of the Point Arguello field, in Ingersoll, R.V., and Ernst, W.G., eds., Cenozoic basin development of coastal California, Rubey Volume 6: Englewood Cliffs, N.J., Prentice-Hall, p. 407-426.
- Crouch, J.K., 1978, Neogene tectonic evolution of the California Continental Borderland and western Transverse Ranges: U.S. Geological Survey Open-File Report 78-606, 23 p.
- Dalrymple, G.B., 1979, Critical tables for conversion of K-Ar ages from old to new constraints: Geology, v. 7, p. 558-560.
- DePaolo, D.J., and Finger, K.L., 1991, High-resolution strontium-isotope stratigraphy and biostratigraphy of the Miocene Monterey Formation, central California: Geological Society of America Bulletin, v. 103, p. 112-124.
- Dibblee, T.W., Jr., 1950, Geology of southwestern Santa Barbara County, California: California Division of Mines Bulletin 150, 95 p.
- 1966, Geology of the central Santa Ynez Mountains, Santa Barbara County, California: California Division of Mines and Geology Bulletin 186, 99 p.

- 1988a, Geologic map of the Santa Rosa Hills and Sacate quadrangles, Santa Barbara County, California: Dibblee Geological Foundation Map DF-17, scale 1:24,000.
- 1988b, Geologic map of the Tranquillon Mountain and Point Arguello quadrangles, Santa Barbara County, California: Dibblee Geological Foundation Map DF-19, scale 1:24,000.
- 1989, Geologic map of the Point Sal and Guadalupe quadrangles, Santa Barbara County, California: Dibblee Geological Foundation Map, scale 1:24,000.
- Dickinson, W.R., and Snyder, W.S., 1979, Geometry of subducted slabs related to the San Andreas transform: *Journal of Geology*, v. 87, p. 609-628.
- Dunham, J.B., and Blake, G.H., 1987, Guide to coastal outcrops of the Monterey Formation of western Santa Barbara County, California: Los Angeles, Calif., Society of Economic Paleontologists and Mineralogists, Pacific Section, 36 p.
- Dunham, J.B., Bromely, B.W., and Rosato, V.J., 1991, Geologic controls on hydrocarbon occurrence within the Santa Maria basin of western California, in Gluskoter, H.J., Rice, D.D., and Taylor, R.B., eds., *Economic geology*, U.S.: Boulder, Colo., Geological Society of America, *The Geology of North America*, v. P-2, p. 431-446.
- Ernst, W.G., and Hall, C.A., 1974, Geology and petrology of the Cambria Felsite, a new Oligocene formation, west-central California Coast Ranges, *Geological Society of America Bulletin*, v. 85, p. 523-532.
- Fischer, T., 1987, Discovery of the Point Arguello oil field from a geophysical perspective: *Geophysics: The Leading Edge of Exploration*, v. 6, no. 10, p. 16-21.
- Fisher, R.V., 1977, Geological guide to subaqueous volcanic rocks in the Nipomo, Pismo Beach and Avila Beach areas: unpublished field guide for the Penrose Conference on the Geology of Subaqueous Volcanic rocks, November 30, 1977.
- Fisher, R.V., and Schmincke, H.-U., 1984, *Pyroclastic rocks*: Berlin, Springer-Verlag, 472 p.
- Fritsche, A.E., and Thomas, G.D., 1990, New early Miocene K-Ar date for basalt in the Hurricane Deck Formation, central Santa Barbara County, California [abs.]: *Geological Society of America Abstracts with Programs*, v. 22, no. 3, p. 23-24.
- Graham, S.A., and Dickinson, W.R., 1978a, Evidence for 115 kilometers of right slip on the San Gregorio-Hosgri fault trend: *Science*, v. 199, p. 179-181.
- 1978b, Apparent offsets of on-land geologic features across the San Gregorio-Hosgri fault trend, in Silver, E.A., and Normark, W.R., eds., *San Gregorio-Hosgri fault zone, California*: California Division of Mines and Geology Special Publication 137, p. 13-23.
- Graham, S.A., and Peabody, C.E., 1981, New evidence for major strike-slip along the San Gregorio-Hosgri fault of the San Andreas transform system [abs.]: *Geological Society of America Abstracts With Programs*, v. 13, no. 7, p. 463.
- Greenhaus, M.R., and Cox, A., 1979, Paleomagnetism of the Morro Rock-Islay Hill complex as evidence for crustal block rotations in central coastal California: *Journal of Geophysical Research*, v. 84, no. B5, p. 2393-2400.
- Hall, C.A., Jr., 1973, Geology of the Arroyo Grande 15-minute quadrangle, San Luis Obispo County, California: California Division of Mines and Geology Map Sheet 24, scale 1:48,000.
- 1974, Geologic map of the Cambria region, San Luis Obispo County, California: U.S. Geological Survey Miscellaneous Field Studies Map MF-599, 2 sheets, scale 1:24,000.
- 1978, Geologic map of Twitchell Dam and parts of Santa Maria and Tepusquet Canyon quadrangles, Santa Barbara County, California: U.S. Geological Survey Miscellaneous Field Studies Map MF-933, 2 sheets, scale 1:24,000.
- 1981a, San Luis Obispo transform fault and middle Miocene rotation of the western Transverse Ranges, California: *Journal of Geophysical Research*, v. 86, no. B2, p. 1015-1031.
- 1981b, Map of geology along the Little Pine fault, parts of the Sisquoc, Foxen Canyon, Zaca Lake, Bald Mountain, Los Olivos, and Figueroa Mountain quadrangles, Santa Barbara County, California: U.S. Geological Survey Miscellaneous Field Studies Map MF-1285, 2 sheets, scale 1:24,000.
- 1982, Pre-Monterey subcrop and structure contour maps, south-central California: U.S. Geological Survey Miscellaneous Investigation Series MF-1384, 6 maps, scale 1:62,500 and accompanying pamphlet, 28 p.
- Hall, C.A., and Corbató, C.E., 1967, Stratigraphy and sedimentology of Mesozoic and Cenozoic rocks, Nipomo quadrangle, southern Coast Ranges, California: *Geological Society of America Bulletin*, v. 78, p. 559-582.
- Hall, C.A., Jr., Ernst, W.G., Prior, S.W., and Wiese, J.H., 1979, Geologic map of the San Luis Obispo-San Simeon region, California: U.S. Geological Survey Miscellaneous Investigation Series Map I-1097, scale 1:48,000.
- Hall, C.A., Jr., and Prior, S.W., 1975, Geologic map of the Cayucos-San Luis Obispo region, San Luis Obispo County, California: U.S. Geological Survey Miscellaneous Field Studies Map MF-686, 2 sheets, scale 1:24,000.
- Hall, C.A., Turner, D.L., and Surdam, R.C., 1966, Potassium-argon age of the Obispo Formation with *Pecten lompocensis* Arnold, southern Coast Ranges, California: *Geological Society of America Bulletin*, v. 77, p. 443-446.
- Hamilton, D.H., 1982, The proto-San Andreas fault and the early history of the Rinconada, Nacimiento, and San Gregorio-Hosgri faults of coastal central California [abs.]: *Eos (American Geophysical Union, Transactions)*, v. 63, no. 45, p. 1194.
- Hopson, C.A., and Frano, C.J., 1977, Igneous history of the Point Sal ophiolite, southern California, in Coleman, R.G., and Irwin, W.P., eds., *North American ophiolites*: Oregon Department of Geology and Mineral Industries Bulletin 95, p. 161-183.
- Hornafius, J.S., 1985, Neogene tectonic rotation of the Santa Ynez Range, western Transverse Ranges, California, suggested by paleomagnetic investigation of the Monterey Formation: *Journal of Geophysical Research*, v. 90, p. 12,503-12,522.
- 1994, Correlation of volcanic ashes in the Monterey Formation between Naples Beach and Gaviota Beach, California, in Hornafius, J.S., ed., *Field Guide to the Monterey Formation Between Santa Barbara and Gaviota, California*: Pacific Section, American Association of Petroleum Geologists, v. GB72, p. 45-58.
- Hornafius, S., Luyendyk, B.P., Terres, R.R., and Kamerling, M.J., 1986, Timing and extent of Neogene tectonic rotation in the western Transverse Ranges, California: *Geological Society of America Bulletin*, v. 97, no. 12, p. 1476-1487.
- Howard, J.L., 1995, Conglomerates of the upper middle Eocene to lower Miocene Sespe Formation along the Santa Ynez fault—implications for the geologic history of the eastern Santa Maria basin area, California: U.S. Geological Survey Bulletin 1995-H, p. H1-H37.

- Ingle, J.C., Jr., 1980, Cenozoic paleobathymetry and depositional history of selected sequences within the southern California continental borderland: Cushman Foundation for Foraminiferal Research Special Publication no. 19, p. 163-195.
- Jennings, C.W., 1958, Geologic map of California, Santa Maria sheet: California Division of Mines and Geology, scale 1:250,000.
- 1959, Geologic map of California, San Luis Obispo sheet: California Division of Mines and Geology, scale 1:250,000.
- Johnson, S.Y., and Stanley, R.G., 1994, Sedimentology of the conglomeratic lower member of the Lospe Formation (lower Miocene), Santa Maria Basin, California: U.S. Geological Survey Bulletin 1995-D, p. D1-D22.
- Kleinpell, R.M., 1938, Miocene stratigraphy of California: Tulsa, Okla., American Association of Petroleum Geologists, 450 p.
- 1980, The Miocene stratigraphy of California revisited: Tulsa, Okla., American Association of Petroleum Geologists Studies in Geology No. 11, p. 1-53.
- Kleinpell, R.M., and Weaver, D.W., 1963, Foraminiferal faunas from the Gaviota and Alegria Formations: Berkeley and Los Angeles, Calif., University of California Publications in Geological Sciences, v. 43, p. 1-77.
- LeBas, M.J., Maitre, R.W., Streckeisen, A., and Zanettin, B., 1986, A chemical classification of volcanic rocks based on the total alkali-silica diagram: *Journal of Petrology*, v. 27, p. 745-750.
- Luyendyk, B.P., 1991, A model for Neogene crustal rotations, transtension, and transpression in southern California: *Geological Society of America Bulletin*, v. 103, p. 1528-1536.
- McCrary, P.A., Ingle, J.C., Jr., Wilson, D.C., and Stanley, R.G., 1995, Neogene geohistory analysis of Santa Maria basin and its relationship to transfer of central California to the Pacific plate: U.S. Geological Survey Bulletin 1995-J, p. J1-J38.
- McCulloch, D.S., 1987, Regional geology and hydrocarbon potential of offshore central California, *in* Scholl, D.W., Grantz, A., and Vedder, J.G., eds., *Geology and resource potential of the continental margin of western North America and adjacent ocean basins: Circum-Pacific Council for Energy and Mineral Resources, Earth Sciences Series*, v. 6, p. 353-401.
- 1989, Evolution of the offshore central California margin, *in* Winterer, E.L., Hussong, D.M., and Decker, R.W., eds., *The eastern Pacific Ocean and Hawaii: Boulder, Colo., Geological Society of America, The Geology of North America*, v. N, p. 439-470.
- McIntosh, K.D., Reed, D.L., and Silver, E.A., 1991, Deep structure and structural inversion along the central California continental margin from EDGE seismic profile RU-3: *Journal of Geophysical Research*, v. 96, no. B4, p. 6459-6473.
- McLean, H., 1994, Geologic map of the Lopez Mountain quadrangle, San Luis Obispo County, California: U.S. Geological Survey Geologic Quadrangle Map GQ-1723, scale 1:24,000.
- Meltzer, A.S., and Levander, A.R., 1991, Deep crustal reflection profiling offshore southern central California: *Journal of Geophysical Research*, v. 96, no. B4, p. 6475-6491.
- Ogle, B.A., 1984, Significant new developments in the Santa Maria/Santa Barbara area, offshore California—the geology and economic potential: *Proceedings of the Southwestern Legal Foundation, Exploration and Economics of the Petroleum Industry: New York, Matthew Bender and Company, Inc.*, v. 22, p. 23-55.
- Pacific Gas and Electric Company, 1988, Map of faults and folds identified during previous investigations and during the long term seismic program, south-central California (plate 3), *in* Final Report of the Diablo Canyon Long Term Seismic Program for the Diablo Canyon Power Plant: U.S. Nuclear Regulatory Commission Docket Nos. 50-275 and 50-323, scale 1:250,000.
- Rigsby, C.A., 1994, Strontium isotope geochronology of the Vaqueros Formation in the western Transverse Ranges, California [abs.]: *American Association of Petroleum Geologists Bulletin*, v. 78, no. 4, p. 674.
- Robyn, E.S., 1979, A description of the Miocene Tranquillon Volcanics and a comparison with the Miocene Obispo tuff [abs.]: *Geological Society of America Abstracts With Program*, v. 11, no. 3, p. 125.
- 1980, A description of the Miocene Tranquillon volcanics and a comparison with the Miocene Obispo tuff: M.A. thesis, Santa Barbara, University of California, 110 p.
- Rollinson, H.R., 1993, Using geochemical data: evaluation, presentation, interpretation: London, Longman Scientific & Technical, 352 p.
- Schneider, J.L., and Fisher, R.V., 1996, Obispo Formation, California: remobilized pyroclastic material: U.S. Geological Survey Bulletin 1995-O, p. O1-O22.
- Severinghaus, J., and Atwater, T.M., 1990, Cenozoic geometry and thermal state of the subducting slabs beneath western North America, *in* Wernicke, B.P., ed., *Basin and Range extensional tectonics near the latitude of Las Vegas, Nevada: Geological Society of America Memoir* 176, p. 1-22.
- Smith, R.L., 1960, Zones and zonal variations in welded ash flows: U.S. Geological Survey Professional Paper 354-F, p. 149-159.
- Snyder, W.S., Dickinson, W.R., and Silberman, M.L., 1976, Tectonic implications of space-time patterns of Cenozoic magmatism in the western United States: *Earth and Planetary Science Letters*, v. 32, p. 91-106.
- Stanley, R.G., 1987, Implications of the northwestwardly younger age of the volcanic rocks of west-central California: alternative interpretations: *Geological Society of America Bulletin*, v. 98, p. 612-614.
- 1988, Late Oligocene-early Miocene volcanism, faulting, and sedimentation in west-central California [abs.]: *American Association of Petroleum Geologists Bulletin*, v. 72, no. 3, p. 396.
- Stanley, R.G., Cotton, M.L., Bukry, D., Filewicz, M.V., Valin, Z.C., and Vork, D.R., 1994, Stratigraphic revelations regarding the Rincon Shale (lower Miocene) in the Santa Barbara coastal area, California [abs.]: *American Association of Petroleum Geologists Bulletin*, v. 78, no. 4, p. 675-676.
- Stanley, R.G., Johnson, S.Y., Cole, R.B., Mason, M.A., Swisher, III, C.C., Cotton Thornton, M.L., Filewicz, M.V., Vork, D.R., Tuttle, M.L., and Obradovich, J.D., 1992a, Origin of the Santa Maria basin, California: U.S. Geological Survey Circular 1074, p. 73.
- Stanley, R.G., Johnson, S.Y., Obradovich, J.D., Tuttle, M.L., Cotton Thornton, M.L., Vork, D.R., Filewicz, M.V., Mason, M.A., and Swisher, C.C., III, 1990, Age and depositional setting of the type Lospe Formation (Lower Miocene), Santa Maria basin, central California: *American Association of Petroleum Geologists Bulletin*, v. 74, p. 770-771.
- Stanley, R.G., Johnson, S.Y., Swisher, C.C., III, Mason, M.A., Obradovich, J.D., Cotton, M.L., Filewicz, M.V., and Vork, D.R., 1996, Age of the Lospe Formation (early Miocene) and origin of the Santa Maria basin, California: U.S. Geological Survey Bulletin 1995-M, p. M1-M37.
- Stanley, R.G., Johnson, S.Y., Tuttle, M.L., Mason, M.A., Swisher, C.C., Cotton-Thornton, M.L., Vork, D.L., Filewicz, M.V., Cole, R.B., and Obradovich, J.D., 1991, Age, correlation, and origin

- of the type Lospe Formation (lower Miocene), Santa Maria basin, central California: *American Association of Petroleum Geologists Bulletin*, v. 75, p. 382.
- Stanley, R.G., Valin, Z.C., and Pawlewicz, M.J., 1992b, Rock-*eval* pyrolysis and vitrinite reflectance results from outcrop samples of the Rincon Shale (lower Miocene) collected at the Tajiguas Landfill, Santa Barbara County, California: U.S. Geological Survey Open-File Report 92-571, 27 p.
- Sun, S.S., and McDonough, W.F., 1989, Chemical and isotopic systematics of oceanic basalts: implications of the earth and mantle evolution: *Earth and Planetary Science Letters*, v. 35, p. 429-448.
- Surdam, R.C., and Hall, C.A., 1984, Diagenesis of the Miocene Obispo Formation, Coast Range, California, *in* Stratigraphic, tectonic, thermal, and diagenetic histories of the Monterey Formation, Pismo and Huasna basin, California: *SEPM Guidebook* no. 2, p. 8-20.
- Tennyson, M.E., Keller, M.A., Filewicz, M.V., and Cotton-Thornton, M.L., 1991, Contrasts in early Miocene subsidence history across Oceanic-West Huasna fault system, northern Santa Maria province, California [abs.]: *American Association of Petroleum Geologists Bulletin*, v. 75, no. 2, p. 383.
- Turner, D.L., 1968, Potassium-argon dates concerning the Tertiary foraminiferal time scale and San Andreas fault displacement: Ph.D. dissertation, Berkeley, University of California, 99 p.
- 1970, Potassium-argon dating of Pacific Coast Miocene foraminiferal stages: *Geological Society of America Special Paper* 124, p. 91-129.
- Turner, D.L., Surdam, R.C., and Hall, C.A., Jr., 1970, The Obispo Formation and associated volcanic rocks in the central California Coast Ranges—K-Ar ages and biochronologic significance [abs.]: *Geological Society of America Abstracts With Programs*, v. 2, p. 155.
- Vedder, J.G., Gower, H.D., Clifton, H.E., and Durham, D.L., 1967, Reconnaissance geologic map of the central San Rafael Mountains and vicinity, Santa Barbara County, California: U.S. Geological Survey Miscellaneous Field Investigations Map I-487, scale 1:48,000.
- Vedder, J.G., McLean, H., and Stanley, R.G., 1994, New 1:24,000-scale geologic maps show stratigraphic and structural relations that require reinterpretation of Cretaceous and Cenozoic tectonic events in the Sierra Madre-San Rafael Mountains area, California [abs.]: *Geological Society of America Abstracts With Programs*, v. 26, no. 2, p. 100-101.
- Vedder, J.G., McLean, H., Stanley, R.G., and Wiley, T.J., 1991, Paleogeographic implications of an erosional remnant of Paleogene rocks southwest of the Sur-Nacimiento fault zone, southern Coast Ranges, California: *Geological Society of America Bulletin*, v. 103, p. 941-952.
- Watson, E.B., 1982, Basalt contamination by continental crust: some experiments and results: *Contributions to Mineralogy and Petrology*, v. 80, p. 73-87.
- Weigand, P.W., 1982, Middle Cenozoic volcanism of the western Transverse Ranges, *in* Fife, D.L., and Minch, J.A., eds., *Geology and mineral wealth of the California Transverse Ranges: Santa Ana, Calif.*, South Coast Geological Society, p. 170-188.
- Wilson, M., 1989, *Igneous petrogenesis*: London, Unwin Hyman, 466 p.
- Wissler, S.G., and Dreyer, F.E., 1943, Correlation of the oil fields of the Santa Maria district, *in* Jenkins, O.P., ed., *Geologic formations and economic development of the oil and gas fields of California*: California Division of Mines Bulletin 118, p. 235-238.
- Woodring, W.P., and Bramlette, M.N., 1950, *Geology and paleontology of the Santa Maria district, California*: U.S. Geological Survey Professional Paper 222, 185 p.

## APPENDIX 1. DATA, INTERPRETATIONS, AND ASSUMPTIONS USED TO CONSTRUCT THE STRATIGRAPHIC CHART FOR MIDDLE TERTIARY VOLCANIC UNITS IN THE SANTA MARIA PROVINCE (FIG. 2).

The age of the boundary between the Miocene and the Oligocene is about 23.8 Ma (Cande and Kent, 1992, p. 13,933). The boundary between the middle Miocene and early Miocene corresponds to the top of chron C5Cn.1n (Cande and Kent, 1992, p. 13,938) which has an age of about 16.014 Ma (Cande and Kent, 1995, p. 6,094). The boundary between the late Oligocene and early Oligocene falls between the base of chron C10n.1n and the top of chron C10n.2n (Cande and Kent, 1992, p. 13,938) which have ages of about 28.512 Ma and 28.578 Ma, respectively (Cande and Kent, 1995, p. 6,094).

In southern California, the boundary between the Luisian and Relizian Stages of Kleinpell (1938, 1980) occurs at about the same stratigraphic level as the boundary between the middle Miocene and early Miocene (Bartow, 1982). The age of the boundary between the Relizian and Saucesian Stages of Kleinpell (1938, 1980) is uncertain but must be younger than 17.4 Ma (Stanley and others, 1996) and may be about 17 Ma (Bartow, 1982). The age of the boundary between the Saucesian and Zemorrian Stages of Kleinpell (1938, 1980) is uncertain but may be slightly younger than the boundary between the Miocene and the Oligocene (Ingle, 1980; Bartow, 1982). New biostratigraphic work suggests that the Zemorrian Stage may not be recognizable in coastal southern California owing to problems with Kleinpell's original definition of the stage (M.L. Cotton, M.V. Filewicz, and D.R. Vork, Unocal Corp., oral and written commun., 1995).

Igneous rocks of the Morro Rock-Islay Hill complex of Ernst and Hall (1974) intrude the Jurassic and Cretaceous Franciscan Complex and have yielded radiometric ages of  $22.7 \pm 0.9$  Ma to  $28.0 \pm 1.0$  Ma (ages from Turner, 1968, and Turner and others, 1970, corrected for changes in decay constants using the method of Dalrymple, 1979; additional ages from Buckley, 1986; see table 1).

In the San Luis Obispo-Cambria area, volcanic rocks of the Obispo Formation have yielded radiometric ages ranging from  $15.7 \pm 0.9$  Ma to  $16.9 \pm 1.2$  Ma (ages from Turner, 1970, corrected for changes in decay constants using the method of Dalrymple, 1979; see table 1). Biostratigraphic data indicate that the Obispo Formation is overlain by Relizian strata variously assigned to the Monterey and Point Sal Formations (Hall and Corbató, 1967, p. 570; Turner, 1970, p. 103; Hall, 1973, 1978; Hall and others, 1979). These biostratigraphic data strongly suggest that the top of the Obispo is of Relizian age and therefore somewhat older than 16.0 Ma, a conclusion that is consistent with the reported estimates of analytical precision of the youngest reported radiometric ages from the Obispo. According to Hall and Corbató (1967, p. 570) and Hall (1973,

p. 3), molluscan fossils from the Obispo suggest an age of Saucesian to Relizian, implying that the base of the Obispo may be older than 17.0 Ma. On our stratigraphic chart (fig. 2), the age of the base of the Obispo is queried and placed at about 18.1 Ma, which is the maximum age allowed by the estimate of analytical precision of the oldest reported radiometric age from the Obispo. The Obispo conformably overlies the Rincon Shale (of Hall and others, 1979) which in this area contains Saucesian benthic foraminifers as well as calcareous nannofossils of early Miocene zones CN1 and (or) CN2 (Tennyson and others, 1991; M.E. Tennyson, oral commun., 1992). The Vaqueros Formation in this area contains molluscan fossils of the "Vaqueros Stage" of Addicott (1972) that have yielded  $^{87}\text{Sr}/^{86}\text{Sr}$  ratios consistent with ages of late Oligocene to early Miocene (Tennyson and others, 1991; M.A. Keller and M.E. Tennyson, oral commun., 1992, 1996). Nonmarine sedimentary rocks in this area (mapped as Lospe Formation by Hall, 1974; Ernst and Hall, 1974; Hall and Prior, 1975; and Hall and others, 1979) have not been directly dated but are of late Oligocene age on the basis of their stratigraphic position between the overlying Vaqueros Formation and the underlying Cambria Felsite of Ernst and Hall (1974). The age of the Cambria Felsite is about 26.5 Ma to about 27 Ma on the basis of unpublished radiometric ages (M.A. Mason and C.C. Swisher, oral commun., 1990; J.D. Obradovich, oral commun., 1994; M.E. Tennyson and M.A. Keller, oral commun., 1994; see table 1).

Near Lopez Mountain, unnamed volcanic rocks (map units Tvt and Tvf of McLean, 1994) apparently overlie Mesozoic sedimentary rocks and are in turn overlain by the Monterey Formation, which in this area contains calcareous nannofossils of middle Miocene zone CN4 and assemblages of benthic foraminifers ranging in age from Saucesian(?) and Relizian to late Mohnian (McLean, 1994). A basaltic interbed in tuff yielded a radiometric age of  $17.0 \pm 0.5$  Ma (map unit Tvt of McLean, 1994; see table 1). These data are consistent with the hypothesis that the unnamed volcanic rocks near Lopez Mountain are about the same age as the Obispo Formation in the nearby San Luis Obispo-Cambria area (fig. 2). In the same general area, but not in contact with the volcanic rocks, are patches of unnamed sandstone and conglomerate to which McLean (1994, map unit Tsc) assigned an age of Miocene and (or) Oligocene.

In the Point Sal area, biostratigraphic data show that the lower part of the Monterey Formation is of Luisian and Relizian age (Woodring and Bramlette, 1950, p. 100) and that the Point Sal Formation is of Relizian and latest Saucesian age (Stanley and others, 1996, p. M12-M13). The boundary between the Monterey and Point Sal Formations must therefore occur within the Relizian Stage, but its precise age is uncertain. The ages of the top and bottom of the Lospe Formation are about 17 and 18(?) Ma, respectively, on the basis of biostratigraphic data and radiometric ages on tuffs (Stanley and others, 1996; see table 1).

On Figueroa Mountain, the Monterey Formation is of Relizian and (or) Luisian age on the basis of biostratigraphic

data (J.G. Vedder, oral commun., 1993, cited by Stanley and others, 1996, p. M27) and therefore may be correlative with parts of the Monterey Formation in the Lopez Mountain and San Luis Obispo-Cambria areas. The age range of the informally-named Catway volcanics is poorly constrained by three radiometric ages that exhibit large reported estimates of analytical precision (table 1). The age of the lower boundary of the volcanic sequence is tentatively placed at 20.3 Ma on the basis of the oldest potassium-argon age reported by Hall (1981, p. 1,017) corrected for changes in decay constants using the method of Dalrymple (1979). The Catway volcanics rest conformably on an unnamed sequence of sandstone and mudstone that contains molluscan fossils of Saucesian and (or) Relizian age (J.G. Vedder, oral commun., 1993, cited by Stanley and others, 1996, p. M27).

Along Santa Rosa Creek, the age of the unnamed basaltic rocks is poorly constrained by a single radiometric age of  $17.4 \pm 1.2$  Ma (from Turner, 1970, corrected for changes in decay constants using the method of Dalrymple, 1979; see table 1). The minimum and maximum ages allowed by this date (16.2-18.6 Ma) were used to depict the age range of the unnamed basaltic rocks on the stratigraphic chart (fig. 2). The unnamed basaltic rocks are overlain by the Monterey Formation, the lower part of which is of Luisian and Relizian age (Dibblee, 1988a). In turn, the unnamed basaltic rocks overlie the Rincon Shale and Vaqueros Formation, which we provisionally correlate with units of the same names in the nearby Santa Barbara coastal area (see discussion below). In the Santa Rosa Creek area, geologic map relations depicted by Dibblee (1988a) indicate that the Vaqueros rests unconformably on marine sedimentary rocks of late and (or) middle Eocene age (Howard, 1995, p. H27).

On Tranquillon Mountain, the Tranquillon Volcanics of Dibblee (1950) have yielded a radiometric age of  $17.80 \pm 0.05$  Ma (Stanley and others, 1996, p. M11; see table 1). The Tranquillon Volcanics are overlain in apparent angular unconformity by the Monterey Formation; the amount of time represented by this unconformity is uncertain but probably not large, because a sample from the lower part of the Monterey yielded early and middle Miocene diatoms and Relizian(?) foraminifers (Dunham and Blake, 1987, p. 31). Thickness trends, available paleocurrents, and similarities in age, petrography, and major and trace element composition indicate that the Tranquillon Volcanics are at least partly correlative with an unnamed tuff at the base of the Monterey Formation along the Santa Barbara coast (Cole and others, 1991a, b; Stanley and others, 1991, 1992a, 1996; Hornafius, 1994); a sample of this tuff from near Naples yielded a radiometric age of  $18.42 \pm 0.06$  Ma (Stanley and others, 1996, p. M11; see table 1). The Tranquillon Volcanics on Tranquillon Mountain rest unconformably on lower Miocene (Saucesian) strata of the Rincon Shale (Stanley and others, 1996, p. M25); the amount of time represented by this unconformity is unknown.

In the Santa Barbara coastal area, the unnamed tuff within the lowest part of the Monterey Formation has long been known

to be of late Saucesian age because the tuff conformably overlies fossiliferous upper Saucesian strata of the Rincon Shale and is conformably overlain by fossiliferous upper Saucesian strata of the Monterey Formation (Dibblee, 1950, p. 34; Kleinpell and Weaver, 1963, p. 11-12; Dibblee, 1966, p. 50; Turner, 1970, p. 105; DePaolo and Finger, 1991; Stanley and others, 1992b, 1994, 1996). As mentioned above, a sample of the unnamed basal Monterey tuff from near Naples yielded a radiometric age of about 18.4 Ma (table 1). Also at Naples, the unnamed tuff occurs below Monterey strata that yielded mean  $^{87}\text{Sr}/^{86}\text{Sr}$  values of  $0.70865 \pm 0.00001$ , which correspond to planktic foraminiferal zone N6 and calcareous nannofossil zone CN2 and falls within the middle of geomagnetic chron C5Dn (DePaolo and Finger, 1991) dated at about 17.3-17.6 Ma (Cande and Kent, 1995). Samples of tuff from the base of the Monterey Formation near Summerland, about 9 km east of Santa Barbara, yielded radiometric ages of  $16.5 \pm 0.6$  Ma and  $17.2 \pm 0.5$  Ma (ages from Turner, 1970, corrected for changes in decay constants using the method of Dalrymple, 1979; see table 1). However, compared to the biostratigraphic and strontium isotopic data from Naples, the younger of these two radiometric ages is too young, even within the reported range of analytical precision, unless the tuff at Summerland is at a higher stratigraphic level than the tuff at Naples. The age of the base of the Rincon Shale in the Santa Barbara coastal area is about 23.3 Ma on the basis of evidence from calcareous nannofossils (Stanley and others, 1994) and calculated rates of rock accumulation (R.G. Stanley, unpublished data). The base of the Vaqueros Formation in the Santa Barbara coastal area is thought to be an unconformity (Howard, 1995, p. H5); strontium isotopic analyses of fossil shells suggest that the age of the lowest part of the Vaqueros is about  $24 \pm 1$  Ma (Rigsby, 1994). According to Howard (1995, p. H27), upper Oligocene strata within the upper part of the Sespe Formation rest unconformably on upper Eocene strata within the lower part of the Sespe, and lower Oligocene strata are absent.

In the offshore Santa Maria basin, unnamed volcanic rocks rest unconformably on Mesozoic and Paleogene strata and are in turn overlain by the Monterey Formation (McCulloch, 1989, p. 446). Little is known about the age of the offshore volcanic rocks, but they are at least partly of early Miocene (Saucesian) age, are overlain by Relizian sedimentary strata, and have been correlated with the onshore Tranquillon Volcanics by Crain and others (1985, p. 540).

**APPENDIX 2.  
COMPILATION OF  
AVAILABLE MAJOR  
ELEMENT AND  
SELECTED TRACE  
ELEMENT DATA FOR  
VOLCANIC ROCKS  
OF THE SANTA  
MARIA AREA**

Volcanic unit and source of data	Sample No	Na <sub>2</sub> O	MgO	Al <sub>2</sub> O <sub>3</sub>	SiO <sub>2</sub>	CaO	K <sub>2</sub> O	TiO <sub>2</sub>	MnO	Fe <sub>2</sub> O <sub>3</sub>	P <sub>2</sub> O <sub>5</sub>	LOI	Total	Th	Nb	La	Ce	Nd	Sm	Yb	Hf	Sc		
<b>Tranquillon Volcanics of Dibblee (1950)</b>																								
Weigand, 1982																								
	TQ-6	3.07	.47	11.08	79.56	58	4.18	.17	.02	1.58	-	1.55	102.26	-	-	-	-	-	-	-	-	-	-	
	TQ-10	2.64	.42	12.56	78.61	39	5.82	.18	.02	1.63	-	.51	102.78	-	-	-	-	-	-	-	-	-	-	-
	TQ-12	2.19	.41	12.78	77.32	38	6.14	.19	.01	1.42	-	1.01	101.85	-	-	-	-	-	-	-	-	-	-	-
	TQ-14	1.54	.42	11.03	83.24	25	6.08	.16	.01	1.06	-	.58	104.37	-	-	-	-	-	-	-	-	-	-	-
	TQ-16	1.61	.44	13.66	73.47	46	5.59	.19	.003	0.53	-	.4	99.95	-	-	-	-	-	-	-	-	-	-	-
	TQ-17	8	.53	12.78	72.89	73	5.96	.15	.01	1.55	-	6.85	102.25	-	-	-	-	-	-	-	-	-	-	-
Robyn, 1980																								
	4101	-	-	-	73.5	15	2.25	-	-	1.9	-	-	-	-	-	-	-	-	-	-	-	-	-	-
	56AA	-	-	-	73.25	10	4.65	-	-	2.55	-	-	-	-	-	-	-	-	-	-	-	-	-	-
	1222	-	-	-	83	05	6.55	-	-	1.95	-	-	-	-	-	-	-	-	-	-	-	-	-	-
	56CC	-	-	-	77	1.38	4.65	-	-	1.95	-	-	-	-	-	-	-	-	-	-	-	-	-	-
	581	-	-	-	77	05	5.4	-	-	2.05	-	-	-	-	-	-	-	-	-	-	-	-	-	-
	4163	-	-	-	77	35	5.8	-	-	1.1	-	-	-	-	-	-	-	-	-	-	-	-	-	-
	4164	-	-	-	83	05	4.9	-	-	0.05	-	-	-	-	-	-	-	-	-	-	-	-	-	-
	416T	-	-	-	79	1	5.25	-	-	0.5	-	-	-	-	-	-	-	-	-	-	-	-	-	-
	4291	-	-	-	77	1.94	3.95	-	-	1.4	-	-	-	-	-	-	-	-	-	-	-	-	-	-
	3194	-	-	-	69	05	6.5	-	-	2.05	-	-	-	-	-	-	-	-	-	-	-	-	-	-
	56FF	-	-	-	79	05	3.7	-	-	1.9	-	-	-	-	-	-	-	-	-	-	-	-	-	-
Cole and Basu, 1995																								
	4	3.11	0.04	11.13	77.1	5	5.06	14	0.1	1.2	0.6	1.38	99.73	14.3	13.5	45.2	101.7	46.3	8.7	5.18	23.4	1.7	-	-
	5	3.09	0.05	11.41	77.28	53	5.34	15	0.1	1.17	0.9	1.27	100.4	14.2	15.8	44.1	85.7	42.5	10.2	5.69	13.7	3.9	-	-
	6	2.57	0.01	11.22	78.32	32	6.25	14	0.1	0.68	0.8	1.04	100.65	14.3	12.9	46.9	99.5	50.7	9.97	4.96	21.4	2.4	-	-
Homafus, 1994																								
	TEA01	2.26	0.09	10.6	79	.26	5.11	.19	-	0.7	0.4	1.31	99.56	14	10	49.5	90	37	7.6	5.81	7	3.4	-	-
	TP03	3.38	0.14	10.9	77.5	47	4.34	.17	-	1.44	0.4	1.31	99.69	16	30	52	110	45	9.52	5.07	6.6	2.2	-	-
	TPMAT	3.81	0.49	12.2	74.3	86	4.31	.24	-	1.84	0.5	1.47	99.57	13.	18	35.1	71	35.8	7.4	3.4	6.3	3.6	-	-
Unnamed basaltic andesite of Santa Rosa Creek																								
Cole and Basu, 1995																								
	10	3.72	3.17	14.58	53.92	6.99	1.27	2.41	20	12.97	45	.01	99.69	3.6	11.9	16.5	42	36.1	6.24	4.08	12.1	31.2	-	-
	11	3.84	2.94	11.41	52.78	4.58	1.28	2.15	18	11.89	48	1.05	99.65	3.59	12.4	17.4	39.5	27.5	7.15	4.55	14.8	26.7	-	-
Weigand, 1982																								
	TQ-18	3.57	3.85	14.31	54.22	6.92	1.1	2.2	21	11.57	-	1.62	96.1	-	-	-	-	-	-	-	-	-	-	-
	TQ-19	3.61	3.27	13.76	53.55	6.67	1.07	2.23	21	10.71	-	2.92	98	-	-	-	-	-	-	-	-	-	-	-
Unnamed lower Miocene tuffs of the Santa Barbara coast																								
Homafus, 1994																								
	NB0 (1t)	2.03	2.84	9.82	68.8	3.32	.69	18	-	.88	1	11.4	100.06	10	16	39.1	78	37.5	7.7	8.6	4.7	3.6	-	-
	NB20 (1t)	66	2.12	13.4	69.2	1.13	3.7	.14	-	1.45	.04	11.2	99.71	16	23	55.9	110	52	9.8	5.8	7.8	2.4	-	-
	TECTT (1t)	70	2.02	10.8	70.7	1.15	5.4	.14	-	1.24	.07	10.9	98.26	12	19	44.9	86.1	40.7	8.8	5	7	2.3	-	-
	NB440 (1t)	2.31	.77	14	66.6	.88	2.37	.19	-	1.88	.02	10.2	99.22	23	14	25.2	53.4	21	4.2	2.7	3.4	3	-	-
	NB151 (2)	2.14	2.58	19.2	53.9	3.2	9.4	.21	-	4.95	.04	15.6	99.88	28	15	66.4	0	55.2	9.6	1	10	2.6	-	-
	NB288 (2)	71	2.59	20.2	52.6	.85	3.1	.27	-	2.39	.02	20.4	100.34	35	15	37.9	79.1	33	6.4	1.7	6.9	4.9	-	-
	NB399 (2)	1.71	1.44	16.3	65.1	1.11	1.35	.23	-	1.62	.03	10.4	99.29	26	12	23.7	51.1	18	2.6	.7	4.2	5.1	-	-
	NB400 (2)	3.47	51	12.8	68.3	.68	2.13	.19	-	.98	.02	10.8	99.88	22	12	45.3	90.9	35.5	6.9	2.9	5.3	2.9	-	-
	TEC1 (2)	2.13	1.96	18	61.3	1.31	.83	.48	-	4.39	.14	9.39	99.93	22.4	20	44.5	89.5	47.6	10.4	3.8	10	6	-	-
Tuffs in the Lospe Formation near Point Sal																								
Cole and Basu, 1995																								
	1	3.81	.97	11.76	74.06	.48	1.76	.17	.01	1.01	.03	6.39	100.45	18.1	9.72	35.6	81.9	32.2	5.98	3	6.58	21.1	-	-
	2	5.07	.51	10.82	76.15	.32	1.23	.11	.01	0.42	.05	4.99	99.69	17.4	10.2	31.1	71.7	33.2	5.21	2.97	6.1	2.3	-	-
	3	1.33	1.65	11.32	68.89	2.37	.8	.13	.01	.6	.07	12.17	99.35	18.9	9.57	36.5	77.2	31.7	6.53	4.09	6.4	2.6	-	-
Cole, unpublished data																								
	1A2	1.95	1.62	10.65	68.6	1.87	1.65	.12	.01	1.33	.03	11.09	99	15.2	-	49	112.2	53.2	9.38	5.49	10.8	2.7	-	-
(INAA method)																								
	1A3	2.55	1.84	11.32	67.59	2.06	1.59	.14	.01	1.44	.05	11.13	99.77	14.8	-	20.8	56.2	27.3	6.47	5.13	9.4	2.8	-	-
	7D2	.93	1.42	9.96	72.5	1.32	1.26	.14	.01	.55	.05	11.61	99.85	21.2	-	40.2	91.8	40.1	6.79	3.79	8.4	3.6	-	-
	8D5	71	1.58	11.52	68.1	3.1	1.2	.14	.01	.76	.04	12.42	99.6	20.5	-	37.4	87.7	40.9	6.64	3.53	6.3	3	-	-
	10D1	1.92	1.45	10.45	71.26	1.74	.7	.12	.01	.27	.06	11.36	99.35	19.7	-	29.3	71.7	27.8	5.07	2.97	6.1	2.5	-	-

Volcanic unit and source of data	Sample No.	Na <sub>2</sub> O	MgO	Al <sub>2</sub> O <sub>3</sub>	SiO <sub>2</sub>	CaO	K <sub>2</sub> O	TiO <sub>2</sub>	MnO	Fe <sub>2</sub> O <sub>3</sub>	P <sub>2</sub> O <sub>5</sub>	LOI	Total	Th	Nb	La	Ce	Nd	Sm	Yb	Hf	Sc	
Sill at Point Sal	LOI3E3	1.01	1.45	10.93	69.71	2.32	1.26	.14	.01	.48	.07	11.67	99.08	20	-	34.7	81.8	34.5	6.01	3.37	6.3	2.8	
	LOI3E3	1.1	1.17	9.56	72.63	1.7	1.22	.13	.01	.5	.07	11.5	99.7	20.6	-	33.8	80.2	36.4	5.7	3.28	8.1	2.7	
	COR1	67	1.14	12.41	65.92	3.17	2.1	.16	.01	.54	.1	13.57	100.1	-	-	-	-	-	-	-	-	-	-
	NB1	616	.1	12.55	72.97	2.26	1.2	.28	.06	.62	.13	6.09	101.45	-	-	-	-	-	-	-	-	-	-
	NB3	5.79	.22	13.45	73.12	1.55	2.3	.28	.03	.41	.13	5.8	101.5	-	-	-	-	-	-	-	-	-	-
	Cole and Basu, 1995 12	3.46	5.36	17.37	47.62	9.25	1.02	1.55	.13	.13	7.91	.26	3.62	99.56	1.56	10.4	9.35	21	14.1	5.5	2.67	7.11	40.1
	Obispo Formation	Cole and Basu, 1995 7	4.15	.8	11.45	66.29	1.06	2.41	.3	.02	2.54	.11	10.21	99.33	9.39	15.6	24.5	54.2	28.9	6.74	3.72	12.8	9.18
		8	2.12	4.71	13.11	55.45	3.97	1.27	.21	.02	2.1	.12	17.25	100.3	14.1	6.99	22.8	49.5	23.6	5.49	3.78	4.84	5.83
		9	2.78	1.24	12.89	68.15	1.19	2.67	.56	.01	1.85	.16	6.3	99.43	17.8	6.12	25.8	47.5	22.1	5.7	4.27	3.71	15.3
		17	3.78	4.14	14.4	48.13	8.75	8.7	3.34	.18	13.6	.46	1.29	98.95	1.97	10.4	12.3	34.8	21	6.19	3.42	7.85	45.2
18		3.84	3.83	13.89	47.68	7.96	7.2	3.21	.12	13.2	.41	1.58	99.25	1.67	12.9	13.9	35.2	25.7	6.11	4.06	8.43	60	
Ernst and Hall, 1974 SLO-56A		0	.6	13.3	68.5	.78	4.97	.35	.01	1.8	-	9.9	100.21	-	-	-	-	-	-	-	-	-	-
SLO-56B		0	.7	13.5	68.5	.7	4.15	.39	.01	1.94	-	10.17	100.06	-	-	-	-	-	-	-	-	-	-
SLO-73A		0	1.06	13.5	67.6	1.84	3.21	.33	.01	1.8	-	11.31	100.66	-	-	-	-	-	-	-	-	-	-
SLO-73B		.63	.37	12.12	69.47	1.47	2.88	.34	-	2.32	-	9.86	99.46	-	-	-	-	-	-	-	-	-	-
SLO-81A		1.87	.11	11.37	67.96	1.3	5.81	.28	-	2.76	-	8.53	99.99	-	-	-	-	-	-	-	-	-	-
Surdam and Hall, 1984 1	SLO-81B	2.19	.21	11.83	68.28	1.11	6.44	.29	-	.74	-	8.65	99.74	-	-	-	-	-	-	-	-	-	-
	2	2.8	1	10.6	76.7	.6	4.2	-	-	-	-	-	-	-	-	-	-	-	-	-	-	-	-
	3	3	2	10.9	72.9	.6	4.1	-	-	-	-	-	-	-	-	-	-	-	-	-	-	-	-
	4	3.4	2	12.8	74	.5	4.3	-	-	-	-	-	-	-	-	-	-	-	-	-	-	-	-
	5	2.2	2	13.6	70.8	1	3.9	-	-	-	-	-	-	-	-	-	-	-	-	-	-	-	-
	6	3.3	7	10.8	74.1	.8	4.5	-	-	-	-	-	-	-	-	-	-	-	-	-	-	-	-
	7	3	4	11.1	72.1	.6	4.4	-	-	-	-	-	-	-	-	-	-	-	-	-	-	-	-
	Cole and Basu, 1995 14	3.47	5.69	16.43	46.7	9.79	7.5	2.33	.12	11.28	.38	2.98	99.92	1.02	10.9	12.3	29.3	21.9	5.67	3.76	5.71	37.8	
	15	3.31	5.78	15.44	47.16	8.12	.82	2.52	.08	10.72	.34	5.47	99.75	.64	10.1	8.46	23.4	14.2	4.29	3.18	5.43	36.2	
	16	3.44	5.83	16.63	46.24	8.68	.64	2.5	.09	11.37	.37	4.98	99.85	1.16	10.6	12.1	29.3	18	5.12	4.16	6.68	44.5	
Weigand, 1982 TE-2	3.63	.5	14.24	48.5	7.1	2.71	.65	.02	2.4	-	4.1	97.76	-	-	-	-	-	-	-	-	-	-	
TE-3	3.53	5.74	16.12	49.3	10.01	.43	1.88	.18	12.29	-	.71	100.19	-	-	-	-	-	-	-	-	-	-	
TE-5	3.99	3.85	14.81	49.34	7.34	.86	1.5	.19	11.89	-	2.47	96.24	-	-	-	-	-	-	-	-	-	-	
TE-6	4.98	4	15.3	47.01	7.28	.6	2.13	.16	10.38	-	4.51	96.35	-	-	-	-	-	-	-	-	-	-	
TE-10	3.16	5.97	16.63	47.7	9.74	.36	1.94	.14	9.81	-	2.76	98.21	-	-	-	-	-	-	-	-	-	-	
Unnamed volcanic rocks of the Lopez Mountain area	Cole and Basu, 1995 13	1.46	14.95	12.4	43.56	5.52	.6	1.09	13	11.56	.2	8.21	98.6	1.14	9.24	6.72	15	9.02	2.44	1.88	3.07	19.1	
	Morro Rock-Islay Hill complex																						
	Ernst and Hall, 1974 SLO-75A	4.12	1.1	16.36	64.07	3.6	2.86	.58	.08	4.15	-	2.95	99.87	-	-	-	-	-	-	-	-	-	-
	SLO-75B	3.88	1.81	16.33	64.5	3.89	2.83	.54	.06	4.5	-	1.47	99.8	-	-	-	-	-	-	-	-	-	-
	SLO-75C	3.32	1.53	15.98	64.35	4.54	3	.46	.06	3.87	-	2.78	99.89	-	-	-	-	-	-	-	-	-	-
	SLO-78B	4.2	.55	16.39	68.5	2.27	3.04	.32	.06	2.6	-	1.46	99.38	-	-	-	-	-	-	-	-	-	-
	SLO-79A	4.08	1.86	16.01	61.4	4.47	2.52	.7	.06	5.95	-	2.38	99.43	-	-	-	-	-	-	-	-	-	-
	SLO-79B	3.96	1.55	16.39	63.2	3.75	2.63	.65	.05	4.95	-	2.23	99.36	-	-	-	-	-	-	-	-	-	-
	SLO-91A	3.92	.24	17.63	66.13	3.9	3	.66	-	1.55	-	1.32	99.75	-	-	-	-	-	-	-	-	-	-
	SLO-91B	4.06	.21	18	65.92	3.86	3.07	.66	-	1.32	-	2.23	99.33	-	-	-	-	-	-	-	-	-	-
SLO-92A	3.22	.9	15.35	64.7	5.66	3.31	.58	-	2.26	-	3.71	99.69	-	-	-	-	-	-	-	-	-	-	
SLO-92B	2.97	.53	17.19	66.74	2.89	2.87	.6	-	1.81	-	4.23	99.83	-	-	-	-	-	-	-	-	-	-	
SLO-93A	3.63	1.38	14.41	65.77	3.47	2.92	.6	-	4.73	-	2.11	99.02	-	-	-	-	-	-	-	-	-	-	
SLO-93B	3.67	1.39	14.46	65.82	3.41	2.98	.6	-	4.63	-	2.43	99.39	-	-	-	-	-	-	-	-	-	-	

Volcanic unit and source of data	Sample No.	Na <sub>2</sub> O	MgO	Al <sub>2</sub> O <sub>3</sub>	SiO <sub>2</sub>	CaO	K <sub>2</sub> O	TiO <sub>2</sub>	MnO	Fe <sub>2</sub> O <sub>3</sub>	P <sub>2</sub> O <sub>5</sub>	LOI	Total	Th	Nb	La	Ce	Nd	Sm	Yb	Hf	Sc
Buckley, 1986	MR1	4.56	1.06	16.11	67.26	3	3.16	.49	.06	3.74	-	1.32	100.76	-	-	-	-	-	-	-	-	-
	MRIAA	3.98	.68	13.93	75.44	1.55	3.75	2	.01	2.26	-	.23	102.03	-	-	-	-	-	-	-	-	-
	MR2-1	7.75	.96	15.23	70.47	2.67	3.18	3.2	.04	2.55	-	.18	103.35	-	-	-	-	-	-	-	-	-
	MR2-2	4.92	.86	14.9	72.12	2.25	3.15	.34	.06	2.58	-	.14	101.32	-	-	-	-	-	-	-	-	-
	MR3-1	4.42	1.16	14.33	75.07	1.5	3.69	2	.02	1.94	-	.27	102.12	-	-	-	-	-	-	-	-	-
	MR3-2	4.39	1.14	15.57	68.28	3.37	3.19	4.4	.06	3.34	-	.66	100.46	-	-	-	-	-	-	-	-	-
	MR5-1	7.81	1.14	16.31	64.55	3.42	2.95	.58	.07	4.2	-	.18	100.17	-	-	-	-	-	-	-	-	-
	MR7-1	4.64	.98	16.61	64.43	2.71	2.98	6.6	.08	4.7	-	1.7	102.35	-	-	-	-	-	-	-	-	-
	MR7-2	4.89	1.24	16.13	63.38	3.93	3.01	6.6	.06	4.34	-	3.01	100.65	-	-	-	-	-	-	-	-	-
	MR8-1	3.9	1.26	16.24	63.42	3.82	2.86	.69	.06	4.89	-	3.62	100.81	-	-	-	-	-	-	-	-	-
	MR9-1	4.54	1.26	16.48	63.26	3.92	2.57	7.5	.08	5.54	-	1.81	100.21	-	-	-	-	-	-	-	-	-
	MR10-2	4.65	1.22	16.51	64.27	3.76	2.74	6.6	.03	4.56	-	2.2	100.6	-	-	-	-	-	-	-	-	-
	MR10-3	4.58	.94	16.54	63.54	2.56	3.27	6.6	.06	4.72	-	1.81	98.68	-	-	-	-	-	-	-	-	-
	MR12	3.86	1.24	16.44	64.56	3.88	2.72	7.1	.02	4.71	-	1.2	99.34	-	-	-	-	-	-	-	-	-
	MR13	3.83	1.06	16.32	63.86	3.12	3.14	7.4	.04	5.66	-	3	100.77	-	-	-	-	-	-	-	-	-
Cole and Basu, 1995	19	4.1	1.11	15.79	67.49	2.72	3.1	.48	.04	3.29	.22	1.36	99.69	15.1	ND	32.9	65.2	28.1	6.3	2.83	6.9	6.1
Cambria Felsite																						
Ernst and Hall, 1974	CAH-5-70	4.25	12	15.46	73.6	76	4.06	1	.02	.67	-	1.01	100.05	-	-	-	-	-	-	-	-	-
	CAH-9-72	3.57	11	13.42	75.22	46	4.88	0.7	-	.75	-	1.49	99.97	-	-	-	-	-	-	-	-	-
	CAH-11-72	1.54	1	14.22	74.16	27	6.33	1	-	1.02	-	2.4	100.14	-	-	-	-	-	-	-	-	-
	CAH-12-72	2.95	26	13.77	73.67	85	5.35	1	-	1.22	-	1.09	99.26	-	-	-	-	-	-	-	-	-
	SLO-69	4.4	.06	16	72.95	.8	4.5	.1	.01	.43	-	.67	99.92	-	-	-	-	-	-	-	-	-
	SLO-70C	1.58	0	16.9	73.5	.35	5.75	.1	.01	.15	-	1.76	100.1	-	-	-	-	-	-	-	-	-
	SLO-71A	3.6	25	17.59	71.5	.69	4.03	1	.01	.49	-	1.82	100.08	-	-	-	-	-	-	-	-	-
	SLO78A	3.24	0.4	18.4	70.68	.36	4.86	.09	.02	.24	-	1.97	99.9	-	-	-	-	-	-	-	-	-
	SLO-86	3.85	.4	12.22	76.23	2.2	4.1	0.8	-	.87	-	1.72	99.69	-	-	-	-	-	-	-	-	-
	SLO-87	3.96	1.3	11.62	71.68	1.2	1.6	1	-	1.28	-	7.96	99.53	-	-	-	-	-	-	-	-	-
	SLO-88	1.83	.06	11.69	78.11	.17	6.11	0.8	-	.27	-	1.14	99.46	-	-	-	-	-	-	-	-	-
Unnamed volcanic rocks of upper Pine Creek																						
Cole and Basu, 1995	37	3.32	5.01	16.79	51.06	8.73	1.42	1.52	.1	8.51	.25	2.33	100.6	12	27.7	28.3	58.5	27.1	5.28	2.16	17.2	26.7
Subsurface volcanic rocks																						
Well P-																						
Hornafius, 1994	0450#1	1.32	2.11	12.3	71.5	1.05	4.79	2.2	-	2.66	.04	3.16	99.15	13	22	34.6	69.4	36.5	7.5	4.7	7.9	3.6

**APPENDIX 3. SUBSURFACE DATA USED TO  
CONSTRUCT LOWER MIOCENE VOLCANIC  
THICKNESS MAP OF FIGURE 15**

Index No.	Well	Total depth (feet)	Lower Miocene volcanic thickness (feet)
1	Getty "Montadoro" 1	6,146	1,270
2	C.C Townsend "Townsend-Gunter" 1	3,286	1,645
3	Pismo Oil "Mello" 1	1,505	>198
4	Holly Oil "Meherin" 1	4,072	670
5	Homestake Prod. "Tar Spring" 1	3,535	926
6	N.B. Hunt 1	10,010	1,500
7	Chevron "Porter" 1	9,690	2,200
8	Gulf "Porter" 1	2,939	850
9	Stansbury Webb "Bosse" 1	2,670	0
10	Union "Vernon Wineman" 2	3,665	1,900
11	Golden Bear Oil "Moretti" 4-1	3,070	0
12	Union "Jesus Maria" 2	1,664	<100
13	Texaco "La Brea" 1	4,519	1,227
14	J.I. Anderson "Elliott" 1	2,455	82
15	Texaco "Miller" 1	5,078	462
16	Texaco "Sorenson" 1	3,004	375
17	Union "Hansen" 1	8,168	4,900
18	Prairie Oil & Gas 1	5,638	204
19	W.H. Taylor "Packard" 1	5,587	193
20	Getty "Leonsis" 1	4,949	890
21	Point Conception COST well (OCS-CAL 78-164)	?	0
22	Rothschild Oil "Sacramento J.M." 2	4,151	270
23	Texaco "Intex-Lagomarsino" 1	4,696	624
24	Anza Pacific "Spanne" 1	6,241	50
25	Amerada Hess "Sudden" 1	1,884	700
26	Gulf "Sudden" 1	2,009	300
27	Gulf "Sudden" 3	2,284	>400
28	Standard "Sudden" 1	2,861	>210
29	Conoco 322-1	9,343	0
30	Mobil 321-1	11,463	0
31	Chevron 318-1	96,43	0
32	Chevron 318-2	8,100	0
33	Chevron 450-3	8,881	0
34	Chevron 316-2	11,416	0
35	Chevron 452-2	7,485	220
36	Chevron 317-1	8,956	0
37	Chevron 446-2	6,733	170
38	Chevron 443-1	6,952	>400
39	Arco 444-1	8,067	10
40	Union 441-2	5,430	0
41	Exxon 440-2	5,837	0
42	Exxon 440-1	5,525	0
43	Arco 437-1	6,609	70

Index No.	Well	Total depth (feet)	Lower Miocene volcanic thickness (feet)
44	Texaco 496-1	6,120	0
45	Pennzoil 427-1	6,156	0
46	Arco 425-1	3,681	>230
47	Exxon 411-1	5,303	480
48	Phillips 406-1	5,755	440
49	Reading & Bates 416-1	5,961	100
50	Sun Exploration 415-2	6,309	160
51	Reading & Bates 415-1	9,916	233
52	Oxy 409-3	9,465	320
53	Oxy 409-6	7,917	0
54	Phillips 408-1	6,895	>210
55	Phillips 402-1	8,687	117
56	Phillips 403-1	6,897	336
57	Getty 395-1	7,746	680
58	Standard-Humble Oceano 1 060-1	8,020	>600
59	Phillips 396-1	7,702	440
60	Phillips 397-2	8,055	>525
61	Phillips 397-1	3,665	300
62	Texaco 394-1	5,475	920
63	Sun 422-1	?	220
64	Phillips 426-1	8,073	0
65	Shell 435-1	6,901	0
66	Getty 424-1	4,010	150
67	Arco 430-1	5,772	0
68	Chevron 450-1	11,950	550
69	Getty 449-1	8,071	0
70	Conoco 320-1	9,234	0



Chapter 5

# Age and Tectonic Inferences from a Condensed(?) Succession of Upper Cretaceous, Paleocene, and Eocene Strata, Big Pine Mountain Area, Santa Barbara County, California

By JOHN G. VEDDER, RICHARD G. STANLEY, HUGH  
McLEAN, MARY LOU COTTON, MARK V. FILEWICZ, and  
DAVID R. VORK

U.S. GEOLOGICAL SURVEY BULLETIN 1995-S

EVOLUTION OF SEDIMENTARY BASINS/ONSHORE OIL AND GAS INVESTIGATIONS—  
SANTA MARIA PROVINCE

Edited by Margaret A. Keller



# Age and Tectonic Inferences from a Condensed(?) Succession of Upper Cretaceous, Paleocene, and Eocene Strata, Big Pine Mountain Area, Santa Barbara County, California

By John G. Vedder<sup>1</sup>, Richard G. Stanley<sup>1</sup>, Hugh McLean<sup>1</sup>, Mary Lou Cotton<sup>2</sup>, Mark V. Filewicz<sup>3</sup>, and David R. Vork<sup>4</sup>

## Abstract

A 350-m-thick mudstone unit near the top of Big Pine Mountain spans the Cretaceous-Tertiary boundary. This mudstone unit is underlain by more than 1,650 m of Upper Cretaceous submarine-fan deposits and overlain by as much as 1,000 m of lower and middle(?) Eocene subsea-fan deposits. Biostratigraphic zonation based upon assemblages of calcareous nannofossils, palynomorphs, and foraminifers indicates that the mudstone unit includes beds of latest Cretaceous, late Paleocene, and early Eocene age spanning an interval of about 22 m.y. Physical stratigraphic evidence for hiatuses is lacking. Paleobathymetric indicators suggest that most of the mudstone was deposited at upper to middle bathyal depths. A tectonically generated barrier to sediment transport—probably a fault-bounded ridge—is the most likely primary cause for the prolonged slow rate of deposition, although eustatic high sea level may have been a secondary control. Presumably, this barrier lay northeast of the present trace of the Sur-Nacimiento fault zone, yet no known vestiges are preserved. Post-middle(?) Eocene, pre-middle Miocene strike-slip tectonism may have shifted the site of the barrier ridge to a position far from its origin, or erosion may have destroyed the ridge before such a shift. Alternatively, post-middle(?) Eocene erosion may have obliterated the ridge after an episode of major displacement along the Sur-Nacimiento fault zone. Uplift of the ridge may be attributable to strike-slip tectonism that resulted from oblique subduction near the end of Cretaceous time.

A 15-km-long belt of mudstone beds along the south side of the Big Pine fault is nearly the same age as the 350-m-thick mudstone sequence on Big Pine Mountain but differs in that it is as much as 800 m thick and contains thin limestone zones of late Paleocene age. This mudstone belt presumably

represents part of the same basin that is manifested by the condensed(?) succession on Big Pine Mountain. Beds within the limestone zones consist mainly of allochemical detritus that was transported downslope from algal-bank deposits and are the same age as the type Sierra Blanca Limestone. Directional features measured at a few places in the mudstone belt suggest sediment transport from opposite sources and imply deposition in a borderland-like basin. Regional distribution of partly coeval deep-water mudstone units, including the Anita Shale of Kelley (1943), indicates that basins containing bathyal, hemipelagic sediments were extensive during late Paleocene and early Eocene time. Deep-water environments, slow deposition rates, and limited short-lived shallow-water conditions may have been controlled by borderland-like topography that developed in response to an episode of widespread strike-slip tectonism.

## INTRODUCTION

### Purpose

Most published geologic maps of the Big Pine Mountain area (figs. 1A, 1B) in eastern Santa Barbara County show Upper Cretaceous strata unconformably overlain by Eocene strata (Gower and others, 1966; Vedder and others, 1967; and Vedder and Brown, 1968; Dibblee, 1973). One exception is a generalized map (Comstock, 1975, fig. 2), which depicts narrow belts of Paleocene strata at Big Pine Mountain and along the south side of the Big Pine fault. In an attempt to reconcile this mapping difference, samples were collected from the upper and lower parts of a mudstone unit that hitherto had produced inconclusive or conflicting biostratigraphic evidence of age. Because these samples yielded microfossil assemblages of Late Cretaceous age from the lower part of the

**Figure 1 (following pages).** A, Location of study area (shaded box) and geographic features mentioned in text; faults shown as heavy lines, dashed where approximately located. B, Generalized distribution of rocks and geologic structures noted in text; approximate locations of stratigraphic columns shown in figure 3 are numbered and areas of geologic maps shown in figures 4 and 6 are outlined.

<sup>1</sup>U.S. Geological Survey, Menlo Park, CA 94025.

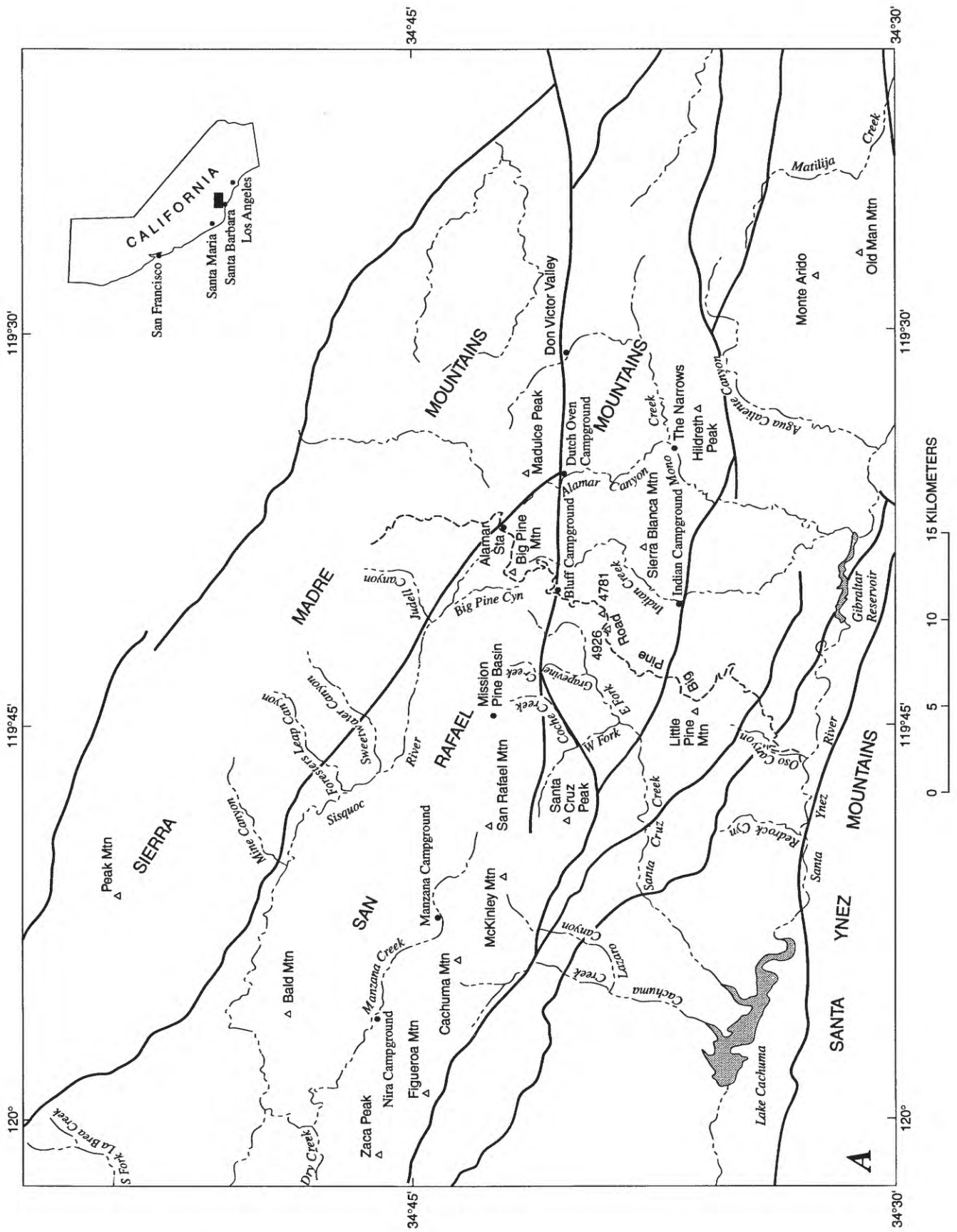
<sup>2</sup>Consultant, 244 Hermosa Drive, Bakersfield, CA 93305.

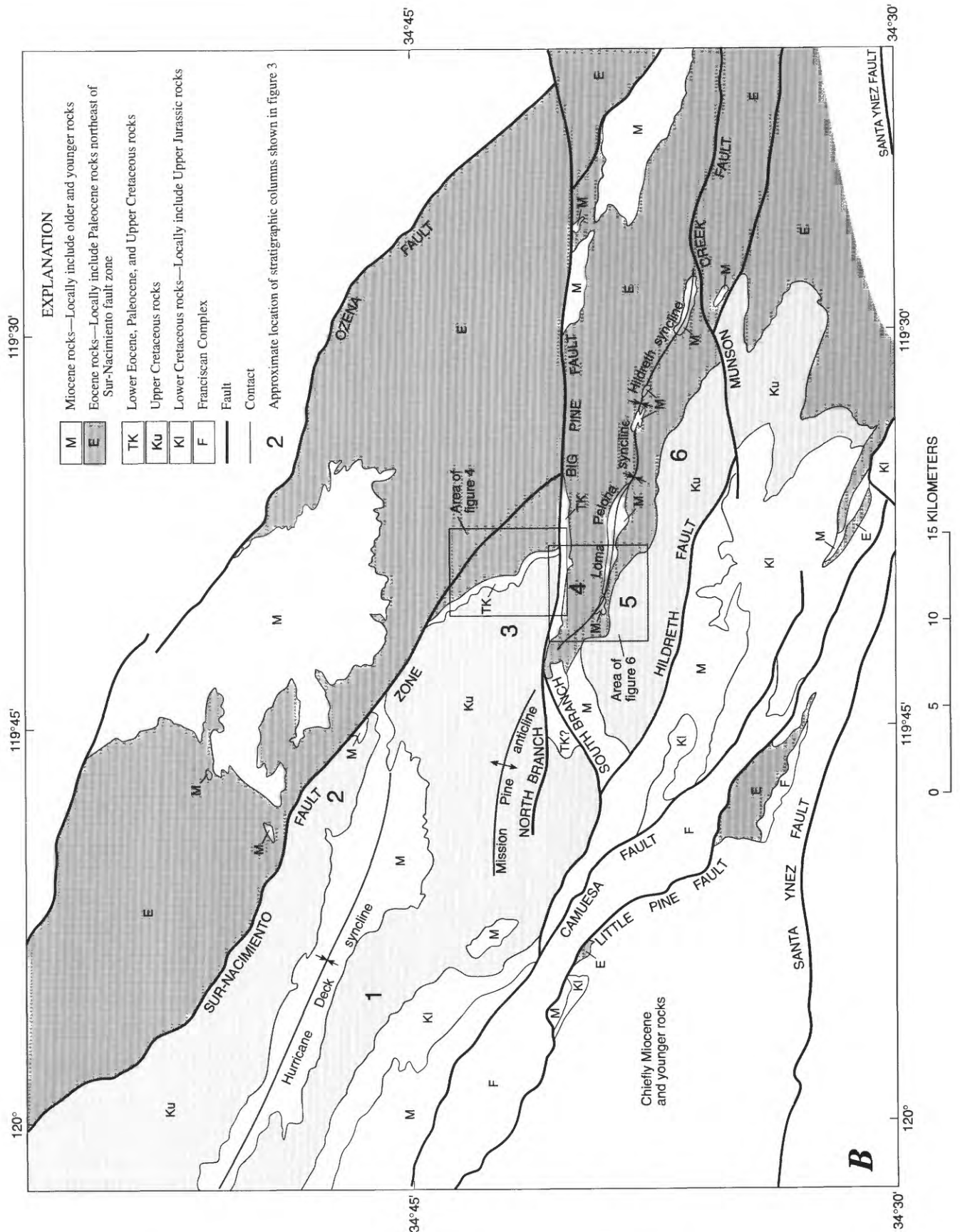
<sup>3</sup>Unocal Frontier Exploration, Far East Group, P.O. Box 4570, Houston, TX 77210.

<sup>4</sup>Unocal Corporation, P.O. Box 4551, Houston, TX 77210.

Approved for publication April 22, 1997

Edited by Sean M. Stone





Age and Tectonic Inferences, Upper Cretaceous, Paleocene, and Eocene Strata, Big Pine Mountain Area, California

mudstone unit and assemblages of late Paleocene and early Eocene age from the upper part, it became evident that the relatively thin succession of mudstone, even if incomplete, represents a very slow rate of deposition. To help resolve the age boundaries and duration of sedimentation, additional samples were collected from throughout the mudstone sequence at Big Pine Mountain.

Mudstone beds that closely resemble those at Big Pine Mountain extend for 15 km along the south side of the Big Pine fault between Coche Creek and Alamar Canyon (figs. 1A, 1B). These mudstone beds were selectively sampled in the vicinity of Bluff Campground to determine whether or not they correlate with the mudstone succession at Big Pine Mountain. Although the biostratigraphic analyses from both units are incomplete and do not explicitly resolve the problems of age and correlation, the preliminary results together with the lithostratigraphic evidence seem to be sufficient to shape some inferences on the effects of tectonism on sedimentation throughout the area. Partly coeval and somewhat similar stratal sequences elsewhere in the Santa Maria-Santa Barbara region are briefly compared in order to clarify age differences and stratigraphic discontinuities.

## Acknowledgments

Some of the biostratigraphic information used in this report was furnished by individuals from several different organizations, especially throughout the reconnaissance phase of the study. During this early work (1965–68), P.J. Smith and R.L. Pierce, U.S. Geological Survey (USGS), and J.W. Ruth, Standard Oil Company of California, provided age assignments for foraminiferal assemblages; and D.L. Jones, USGS, identified the Cretaceous mollusks. More recently collected mollusks were identified (1977–83) by D.L. Jones and J.W. Miller, USGS, and L.R. Saul, Los Angeles County Museum of Natural History. Later (1978–84), calcareous-nannofossil, palynological, and foraminiferal data from supplementary samples were supplied by David Bukry, N.O. Frederiksen, R.E. Arnal, and P.J. Quinterno, USGS. During the last phase of the work (1992–93), W.V. Sliter and K.A. McDougall, USGS, added updated zonations for the foraminiferal assemblages collected before 1984, and David Bukry reported calcareous-nannofossil ages from newly collected samples. A.A. Almgren, consulting geologist and paleontologist, contributed important information on localities and age assignments from his own studies. W.P. Elder, USGS, revised some of the molluscan taxonomy and age ranges for the Late Cretaceous mollusks.

Permission by the U.S. Forest Service to use their cabin at Bluff Campground facilitated the fieldwork, and their continuing support is much appreciated. Information contributed by S.C. Comstock, Mobil Oil Corp., and D.G. Howell, USGS, was helpful in interpreting depositional environments. Comments and suggestions by J.A. Bartow, USGS, and W.V. Sliter

on a preliminary version of the manuscript helped to improve the final report.

## Previously Published Work

Fairbanks (1894) was the first to recognize the general structural and stratigraphic elements of the San Rafael Mountains on the basis of traverses he made east and northwest of Big Pine Mountain. Nelson (1925) and Keenan (1932) mapped and described parts of the large expanse of Cretaceous and Tertiary strata south of the Big Pine fault. Reed and Hollister (1936, pl. VI–A through pl. VII–B) photographed outcrops along the newly constructed Big Pine Road and apparently made the first published reference to the presence of Cretaceous beds at Big Pine Mountain. Dibblee (1966) mapped unnamed Upper Cretaceous sandstone and shale units west of Big Pine Mountain between Cachuma Mountain and Mission Pine Basin, as well as in the lower Indian Creek-Agua Caliente Canyon area. Gower and others (1966) and Vedder and others (1967) mapped the San Rafael Primitive Area (now San Rafael Wilderness) and recorded the presence of Upper Cretaceous and Eocene fossils in the vicinity of Big Pine Mountain. Mapping east of Big Pine Mountain by Vedder and others (1973) revealed details of Upper Cretaceous and Eocene stratigraphy in the upper Mono Creek area. Comstock (1975) was the first to present evidence for the occurrence of Paleocene fossils in the Big Pine Mountain area. On the basis of preliminary biostratigraphic data, Vedder and others (1991) mentioned the mudstone beds at Big Pine Mountain and briefly noted that the sequence ranges in age from Late Cretaceous to early Eocene. In a regional study of Paleogene limestone, Whidden and others (1995a) concluded that the Sierra Blanca Limestone represents both Paleocene and Eocene shallow-water deposition on locally uplifted and tilted Cretaceous forearc strata.

## GEOLOGIC SETTING

### Regional Stratigraphy

Exposed strata in the vicinity of Big Pine Mountain constitute the upper part of a thick late Mesozoic and early Cenozoic sedimentary cover on regionally extensive rocks that were designated the Stanley Mountain terrane (fig. 2) by Blake and others (1982). This terrane is characterized by accreted Middle and Late Jurassic oceanic-arc ophiolite and positionally overlying Late Jurassic and Early Cretaceous forearc-basin accumulations, which generally consist of thin basal tuffaceous chert and succeeding thick, terrigenous flyschlike deposits (Howell and others, 1987; Robertson, 1989). Late Cretaceous and Paleogene sedimentation was largely on submarine fans that developed during the unroofing of mid-Cretaceous granitoid plutons in neighboring continental terranes

to the east (Page, 1970; Howell and others, 1977; Lee-Wong and Howell, 1977; Vedder and others, 1983). Regional tectonic events that influenced these late-stage forearc depositional systems included oblique subduction, terrane accretion, and likely strike-slip deformation (Page and Engebretson, 1984; Nilsen, 1987).

In the central San Rafael Mountains north of the Big Pine fault (fig. 1B), unnamed Upper Cretaceous strata, chiefly sandstone, mudstone, and conglomerate turbidites, are more than 3,400 m thick (fig. 3, cols. 1, 2, and 3) and represent a remnant of a widespread submarine-fan system (Howell and others, 1977; Vedder and others, 1983). Farther southeast, in the lower Mono Creek-Agua Caliente Canyon area south of the Munson Creek fault, a correlative sequence may be more than 5,000 m thick and is overlain by Paleogene marine strata nearly 3,000 m thick (Page and others, 1951; Dibblee, 1966; Vedder and others, 1973, 1983; MacKinnon, 1978).

A distinctive white limestone generally less than 70 m thick (fig. 3, col. 5) forms a narrow belt along the south limb of the Loma Pelona syncline and extends from East Fork Santa Cruz Creek southeastward to a point about 3 km west of the confluence of Alamar Canyon and Mono Creek (figs. 1A, 1B). Named the Sierra Blanca Limestone by Nelson (1925), this limestone consists largely of calcareous detritus derived by downslope transport from algal bank deposits (Keenan, 1932; Walker, 1950; Johnson, 1968; Comstock, 1975, 1976; Sliter and others, 1994; Whidden and others, 1995a). New bios-

stratigraphic evidence indicates that the age of the Sierra Blanca Limestone in the area of the type section (Vedder, 1972) is late Paleocene on the basis of planktonic foraminifers (W.V. Sliter, written commun., 1993) rather than early Eocene. In the vicinity of its type locality at Indian Creek, the Sierra Blanca lies unconformably on Upper Cretaceous beds and is overlain by lower and middle Eocene strata that commonly are assigned to the Juncal Formation. Northeast of Sierra Blanca Mountain these Eocene strata consist largely of sandstone and mudstone turbidites nearly 1,000 m thick. In the southeastern San Rafael Mountains east of Agua Caliente Canyon, the Juncal Formation is as much as 1,600 m thick (Thompson, 1988).

Middle and upper Eocene marine strata, as well as the unconformably overlying upper Eocene(?) to lower Miocene(?) redbeds, are present east and southeast of the study area. Miocene marine strata, including a basal transgressive sandstone and overlying deep-marine shale, are unconformable on all of the older rocks throughout the region (Dibblee, 1966; Dickinson and Lowe, 1966; Vedder and others, 1967, 1973; Fritsche and Shmitka, 1978).

## Regional Structure

The northwest-trending Sur-Nacimiento fault zone (fig. 1B) presumably is the surface expression of the boundary between the Stanley Mountain and Salinia terranes and is the primary structural feature in the Sierra Madre-San Rafael Mountains area. This fault zone truncates the Eocene strata that flank the northeastern side of Big Pine Mountain. Although the history, nature of movement, and amount of offset along the Sur-Nacimiento fault zone are poorly understood, major events along it have been episodic (Vedder and Brown, 1968; Page, 1970; Dibblee, 1976; Yaldezian and others, 1983; Vedder and others, 1983, 1991; Dickinson, 1983). The east-trending Big Pine fault, which truncates the Upper Cretaceous and Paleogene strata along the south side of Big Pine Mountain, is a strike-slip fault, along which there has been about 14 km of post-Oligocene left-lateral separation (Hill and Dibblee, 1953; Crowell, 1962; Carman, 1964; Vedder and others, 1973). Its early history is unknown, although Carman (1964) speculated that the fault may have been active near the end of the Oligocene, and Stewart and Crowell (1992) pointed out that dip slip occurred along the eastern part during Oligocene-early Miocene time.

Primary folds that deform rocks in the study area include the post-middle Miocene Hurricane Deck syncline and the post-early Eocene Mission Pine anticline, which is truncated along its south limb by the Big Pine fault. The Loma Pelona syncline is a complex post-middle Miocene structure that trends eastward to join the Hildreth syncline north of the Hildreth and Munson Creek faults (fig. 1B). All of these folds are asymmetric, show slight to moderate southward vergence, and are oblique to the major faults (Vedder and others, 1967,

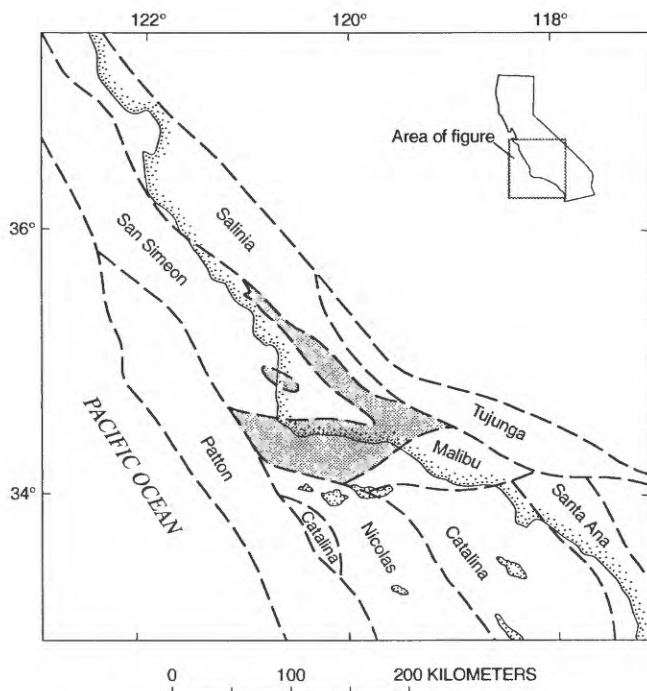
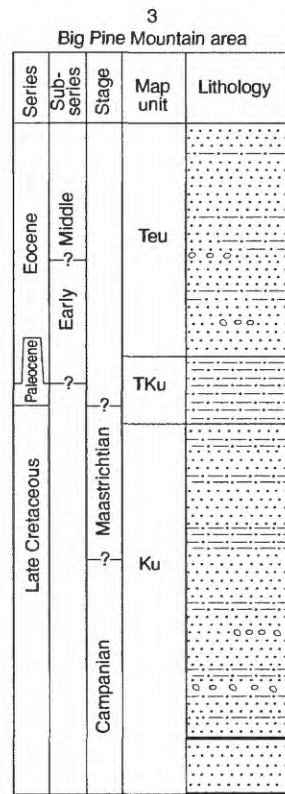
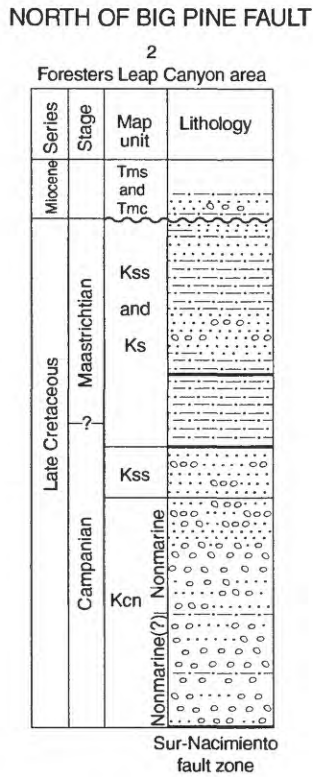
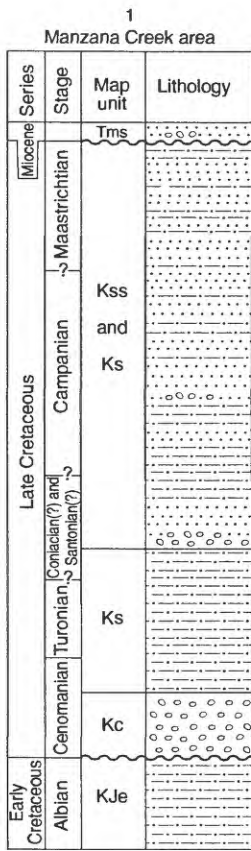
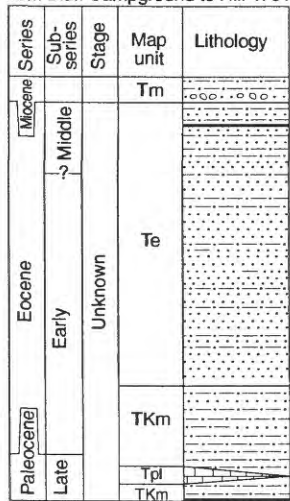


**Figure 2.** Tectonostratigraphic terranes of part of southwestern California. Modified from Blake and others (1982). Shaded area shows extent of Stanley Mountain terrane; stipple pattern depicts coastline.

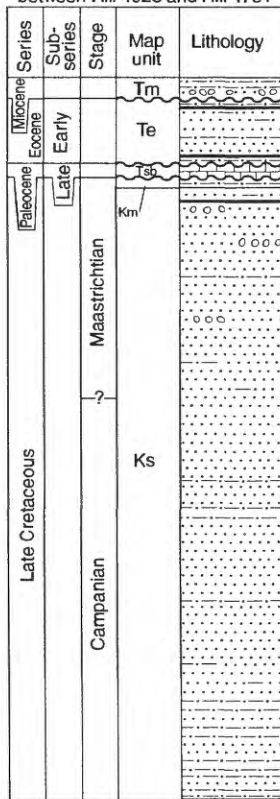


4  
Big Pine Road corridor southward from Bluff Campground to Hill 4781

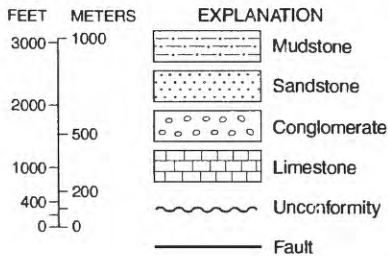
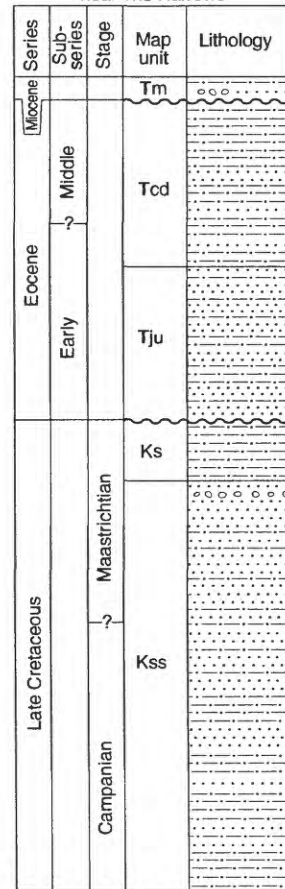


SOUTH OF BIG PINE FAULT

5  
Indian Campground on Indian Creek northward to Big Pine Road between Hill 4926 and Hill 4781



6  
Mono Creek north of Hildreth fault near The Narrows



structure sections *B–B'* and *C–C'*; Vedder and others, 1973, structure sections *A–A'* and *C–C'*).

Paleomagnetic evidence for tectonic rotation is lacking for structural blocks in the central San Rafael Mountains. It is likely, however, that late Cenozoic rotations farther south and east (Luyendyk, 1991; Whidden and others, 1995b) affected parts of the study area. If future work demonstrates such rotations, sediment-transport directions described herein must be revised accordingly.

## STRATIGRAPHIC RELATIONS AT BIG PINE MOUNTAIN

The 350-m-thick condensed(?) succession of Upper Cretaceous to lower Eocene mudstone near the top of Big Pine Mountain records a prolonged episode of greatly diminished coarse-clastic sedimentation, even though the preserved rocks may not represent continuous deposition (figs. 4, 5). This relatively thin sequence of mudstone beds overlies regionally extensive Upper Cretaceous strata that are more than 3,000 m thick and underlies a limited tract of lower and middle(?) Eocene strata at least 1,000 m thick north of the Big Pine fault (fig. 3). Brief descriptions of the underlying and overlying thick stratal units together with details of the relatively thin mudstone unit provide a frame of reference for comparison with similar coeval rock units south of the Big Pine fault.

Bates and Jackson (1987) defined a condensed succession as “a relatively thin but uninterrupted stratigraphic succession of considerable time duration, in which the deposits accumulated very slowly; it is generally represented by a time-equivalent thick succession elsewhere in the same sedimentary basin or region.” The word “condensed” is queried herein because the continuity of the described succession is uncertain.

### Subjacent Upper Cretaceous Strata

West of Big Pine Mountain and north of the Big Pine fault, a 1,650-m-thick sequence of interbedded Upper Cretaceous sandstone, mudstone, and subordinate conglomerate forms the high-standing ridge that links Big Pine Mountain and San Rafael Mountain (fig. 1A; fig. 3, col. 3). These lenticular submarine-fan strata continue northwestward from the San Rafael Mountain-McKinley Mountain area to the north side of Manzanita Creek and from there, extend across the

**Figure 3.** Generalized composite stratigraphic columns of Upper Cretaceous and Paleogene sedimentary rocks at selected sites in Sierra Madre and San Rafael Mountains. Approximate locations of columns shown on figure 1B. Map-unit symbols on columns 3–5 refer to map units on figures 4 and 6; those on columns 1 and 2 refer to rock units mapped and described by Vedder and others (1967); and those on column 6 refer to rock units mapped and described by Vedder and others (1973).

Sisquoc River into the Sierra Madre Mountains southwest of the Sur-Nacimiento fault zone (fig. 1A). Nonmarine and shallow-marine conglomerate and sandstone beds are intertongued with the submarine-fan deposits along the southwestern flank of the Sierra Madre (fig. 3, col. 2), where they form a narrow, 32-km-long, fault-disrupted belt between South Fork La Brea Creek and Sweetwater Canyon (Vedder and others, 1967, 1977).

Upper Cretaceous beds that are stratigraphically below the thick succession exposed between Big Pine Mountain and the San Rafael Mountain-McKinley Mountain area are present along the south side of Manzanita Creek between Manzanita Camp and Dry Creek, where they consist of an additional 1,150 m of submarine-fan deposits (fig. 3, col. 1). The entire Upper Cretaceous submarine-fan system from Big Pine Mountain to Dry Creek is composed largely of mid-fan and inner fan-channel deposits in which sediment transport generally varied from northwestward to southwestward (Comstock, 1975, 1976; Howell and others, 1977). Exceptions are in the McKinley Mountain and upper Coche Creek areas, where Comstock (1976) noted northward transport directions based upon a limited number of observations. The near-shore deposits in the Sisquoc River-La Brea Creek belt show sediment-transport directions that range from westward to southward (Vedder and others, 1977). In combination, these transport directions, if not tectonically rotated, imply a sediment source that lay northeast of the Sur-Nacimiento fault zone. The exact location of this source, however, has not been identified.

Although the thick sequence of Upper Cretaceous strata north of the Big Pine fault is sparsely fossiliferous, age-diagnostic foraminifers and mollusks are present in sufficient numbers and at enough places to permit a generalized biostratigraphic zonation. Several taxa of ammonites representative of the Cenomanian and Turonian Stages have been reported from the lower part of the sequence along a 2-km stretch of Manzanita Creek near Nira Campground (Vedder and others, 1967; Vedder and Elder, unpub. data, 1994). Fossils are rare in stratigraphically higher beds along the south limb of Hurricane Deck syncline north of Manzanita Creek, but those found suggest the presence of the Campanian and (or) Maastrichtian Stages. North of Hurricane Deck syncline, mollusks, including ammonites, from sites along the Sisquoc River between Mine and Sweetwater Canyons are indicative of the upper Campanian and (or) lower Maastrichtian Stages (Vedder and others, 1967, 1977). Structural complications and covering Miocene rocks, however, hamper direct correlation of Upper Cretaceous strata along the Sisquoc River with those on the south limb of Hurricane Deck syncline.

In areas northwest and west of Big Pine Mountain, most sites sampled for foraminifers yielded sparse assemblages diagnostic only of a Cretaceous, undifferentiated, age. One exception, a sample from the ridge about 3.5 km east of San Rafael Mountain (Vedder and others, 1967, M13), contains an assemblage of benthic foraminifers that is assigned to the

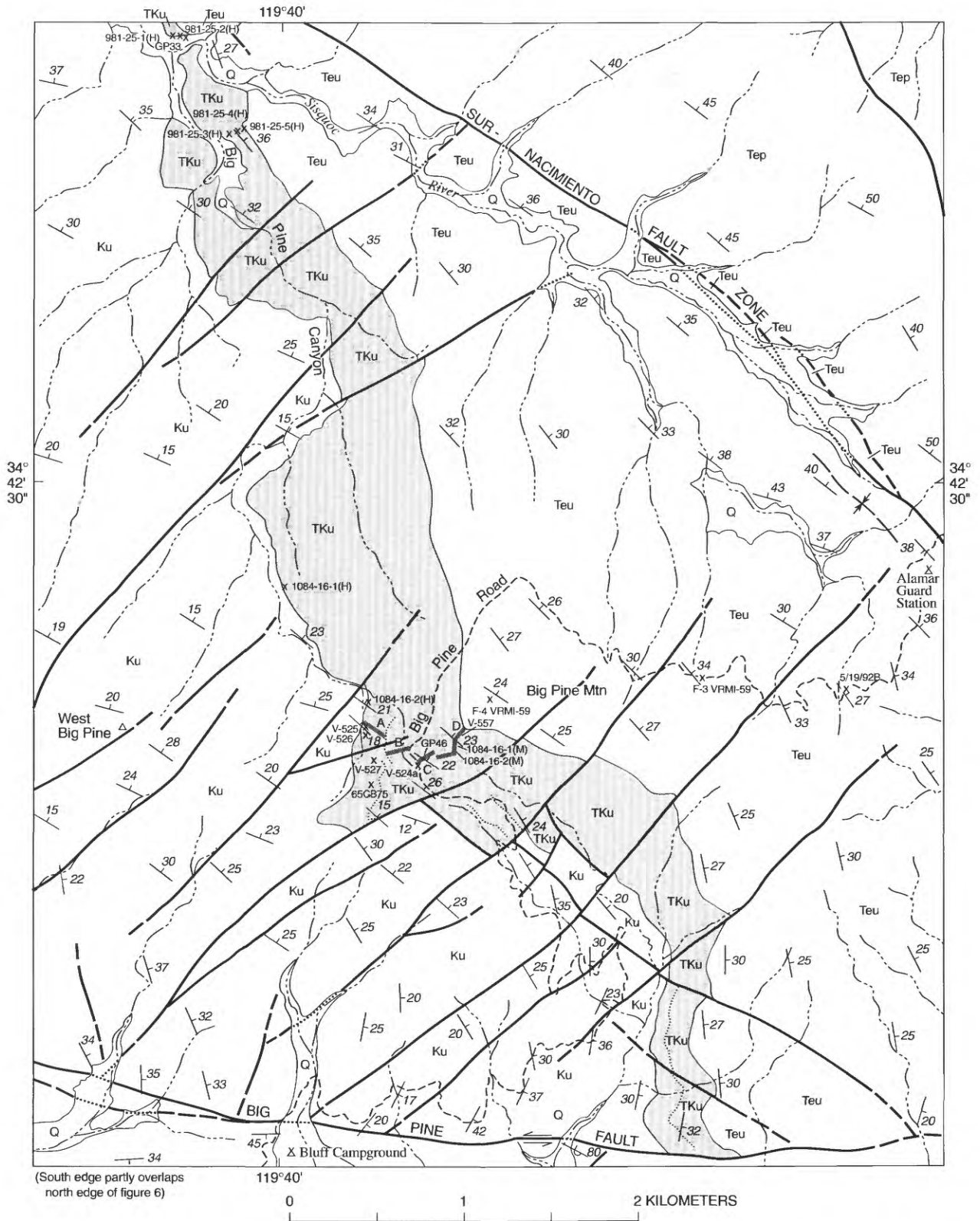


**Figure 4.** Generalized geologic map of Big Pine Mountain area. Location shown on figure 1B. Shaded area indicates distribution of condensed(?) succession (TKu). Modified from Vedder and others (1967) and J.G. Vedder, Hugh McLean, and R.G. Stanley (unpub. mapping, 1990–93).

## EXPLANATION

CENOZOIC	Q	Surficial deposits (Quaternary)
	Tep	Sedimentary rocks (Eocene and Paleocene?)—Chiefly sandstone, northeast of Sur-Nacimiento fault zone
MESOZOIC	Teu	Sedimentary rocks (middle and lower Eocene)—Chiefly sandstone, southwest of Sur-Nacimiento fault zone
	TKu	Sedimentary rocks (lower Eocene, Paleocene, and Upper Cretaceous)—Condensed(?) succession, chiefly mudstone
	Ku	Sedimentary rocks (Upper Cretaceous)—Chiefly interbedded sandstone and mudstone
—		Contact—Includes well defined, poorly defined, and inferred
=		Fault—Dotted where concealed; dashed where uncertain. Arrows indicate direction of movement
⊥		Syncline—Approximately located
— 20		Strike and dip of beds Inclined—Representative of numerous readings, both measured and estimated
— 80		Overtuned
B		Line of measured section—Includes sample sites V-689 to V-692 and V-628 to V-651 on figure 5 and table 1
.....		Sandstone lentil—Shown in unit TKu between Big Pine Mountain and Big Pine fault; mapping incomplete
x V-527		Fossil locality—Shown on figure 5 or noted in table 1 or in text

upper Campanian or lower Maastrichtian (R.L. Pierce, written commun., 1967). Calcareous nannofossils are exceptionally rare and poorly preserved, and samples generally are barren; one site about 1.0 km northeast of Nira Campground produced several taxa that range from Coniacian to Maastrichtian. Palynomorphs from a sample locality about 1.5 km south of Big Pine Mountain (fig. 4, V-556) have a likely range of Santonian to Danian (N.O. Frederiksen, written commun., 1985); the same locality contains poorly preserved Late Cretaceous calcareous nannofossils (David Bukry, written commun., 1992).

Despite the absence of well-founded evidence for the occurrence of the Coniacian and Santonian Stages in the central San Rafael Mountains north of the Big Pine fault, it seems reasonable to expect that these stages are represented in the thick Upper Cretaceous stratal successions north of Manzana Creek and along the Sisquoc River.

## Condensed(?) Succession

### Stratigraphy

The mudstone sequence that is the primary target of this study extends from near the confluence of Big Pine Canyon and the Sisquoc River southeastward across the western and southern flanks of Big Pine Mountain (fig. 4). At its northern end, the

unit is truncated by the Sur-Nacimiento fault zone at the mouth of Judell Canyon; at its southern end, it is cut by the Big Pine fault 2.0 km east of Bluff Campground. Thinning in both directions from Big Pine Mountain is suggested by the mapped relations. However, placement of the lower contact is uncertain along the western side of Big Pine Canyon, and dips may be steeper than indicated in the southernmost exposures near the Big Pine fault. Consequently, the thinning may only be apparent. Most of the northeast-trending faults that cut the mudstone have vertical displacements of less than 15 m. Incomplete exposures and deeply weathered zones in parts of the section measured at Big Pine Mountain (figs. 4, 5) hindered collection of equally spaced samples suitable for biostratigraphic analysis. Stratigraphic intervals between the samples taken are approximate because bedding inclinations cannot be accurately determined in the highly fractured, indistinctly layered mudstone.

The base of the measured section (fig. 5) is marked by an abrupt sandstone-mudstone contact. Very coarse to coarse-grained sandstone beds directly beneath the contact are laterally persistent, thick-bedded, normally graded turbidites; these resemble lithofacies B submarine-fan deposits described by Ricci-Lucchi (1975). The upper surface of the uppermost sandstone is imprinted with numerous crossing trails and burrows, most of which are horizontal, meandering and straight back-filled feeding traces about 1 to 2 cm wide (?*Planolites*). Although the lowermost part of the overlying mudstone sequence consists of a 2- to 3-m-thick zone of silty and sandy mudstone with thin interbeds of normally graded fine- and medium-grained sandstone (lithofacies D and E beds of Ricci-Lucchi, 1975), silty mudstone characteristic of lithofacies G (Ricci-Lucchi, 1975) is the dominant rock type throughout the remainder of the condensed(?) succession. Cursory microscopic examination reveals that most samples are composed of poorly sorted micaceous clayey siltstone and silty claystone and that beds in the lower part tend to be siltier and more micaceous. Rare, irregular grains of glauconite are present about 150 m above the base. Bedding is indistinct, and fracture varies from splintery or hackly to conchoidal. Fresh exposures are dark gray to olive gray; weathered ones, brownish gray to light-olive gray. Zones of randomly scattered ellipsoidal calcareous concretions are conspicuous in the lower and middle parts of the measured section. Sand-filled burrows are common in the lower part, and very small, tubular, clay-rich traces (?*Helminthoida* sp.) give the mudstone a mottled appearance in many beds throughout the entire section. Common plant fragments and sparse fish remains are disseminated as dark particles in much of the mudstone.

Benthic foraminifers suggest that the lower 270 m of the measured section was deposited at bathyal depths in a basin environment and that the uppermost 50 m was deposited at upper to middle bathyal depths in slope and (or) basin environments. Beds near the top of the mudstone sequence in Big Pine Canyon include benthic species that range into lower bathyal depths (table 1).

About 70 m above the base of the measured section, a ledge-forming sandstone lentil less than 1 m thick interrupts

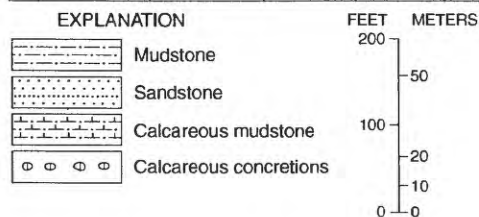
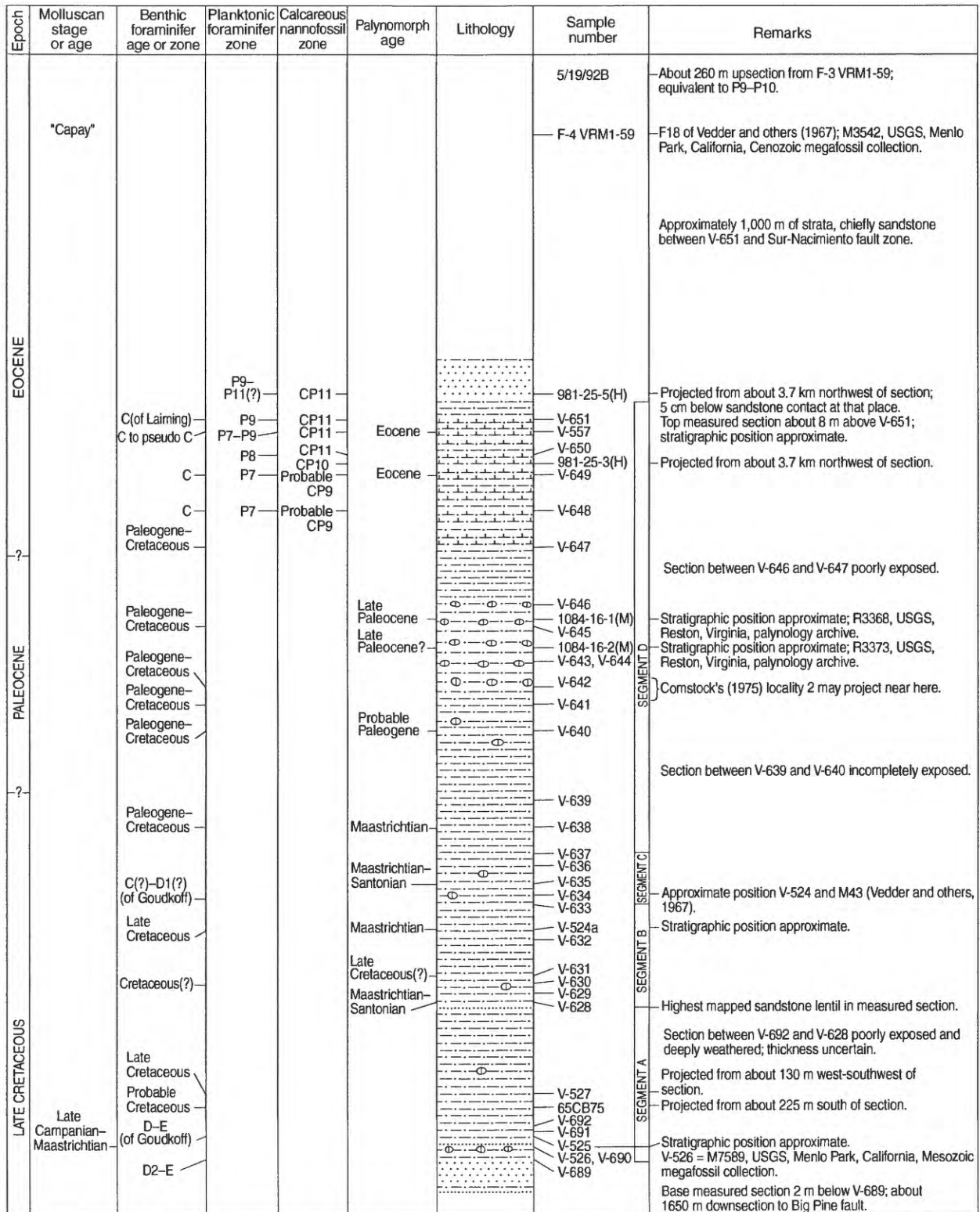


**Figure 5.** Measured section of condensed(?) succession of Upper Cretaceous, Paleocene, and lower Eocene mudstone (map unit TKu, fig. 4) at Big Pine Mountain. Zonation and age assignments are explained in table 1; molluscan data from W.P. Elder and J.G. Vedder (unpub. data, 1991). Segments A-D refer to divisions of measured section shown on figure 4.

**Table 1.** Age-diagnostic taxa, zonation, and paleobathymetry of microfossils from Big Pine Mountain area

[Localities shown on figures 4 and (or) 5. Arranged stratigraphically from top to bottom. Assignments by M.L. Cotton, M.V. Filewicz, and D.R. Vork unless noted as follows: R.L.P., R.L. Pierce; J.W.R., J.W. Ruth; R.E.A., R.E. Arnal; D.B., David Bukry; N.O.F., N.O. Frederiksen; P.J.S., P.J. Smith; P.J.Q., P.J. Quintero; K.M., K.A. McDougall. Zonation schemes used: dinoflagellates, Williams and Bujak (1985); calcareous nannofossils, Okada and Bukry (1980); planktonic foraminifers, Blow (1969, as emended by Toumarkine and Luterbacher, 1985); benthic foraminifers, Goudkoff (1945), Laiming (1939, as emended by Almgren and others, 1988). Age boundaries from Haq and others (1987). Paleobathymetry based upon classifications by Hedgpeth (1957) and Ingle (1975)]

Field No.	Age-diagnostic and associated taxa	Age or zone	Paleobathymetry	Remarks
981-25-5(H)	Calcareous nannofossils: <i>Coccolithus crassus</i> , <i>Zygrabliuthus bijugatus</i> , <i>Discoaster barbadiensis</i> , <i>D. lodoensis</i> , <i>Discoasteroides kuepperi</i> , <i>Helicosphaera seminulum</i> , <i>Pontosphaera plana</i> Benthic foraminifers: assemblage  Planktonic foraminifers: assemblage	CP11 ( <i>Discoaster lodoensis</i> Zone) (D.B.) Probable Laiming pseudo-C (R.E.A., K.M.) P9 to P11 (R.E.A.)		Sample collected 5 cm below contact with overlying sandstone unit about 3.7 km northwest of measured section at Big Pine Mountain.
981-25-4(H)	Calcareous nannofossils: <i>Coccolithus grandis</i> , <i>C. crassus</i> , <i>Discoasteroides kuepperi</i> , <i>Sphenolithus radians</i> , <i>Zygrabliuthus bijugatus</i> Benthic foraminifers: assemblage  Planktonic foraminifers: assemblage	CP11 ( <i>Discoaster lodoensis</i> Zone) (D.B.) Probable Laiming C to pseudo-C (R.E.A., K.M.) P8 to P10 (K.M.)	≥ 2,000 m (K.M.)	Approximately 10 m below 981-25-5(H).
981-25-2(H)	Calcareous nannofossils: <i>Chiasmolithus grandis</i> , <i>Coccolithus crassus</i> , <i>C. magnicrassus</i> , <i>Discoaster lodoensis</i> , <i>Discoasteroides kuepperi</i>  Benthic foraminifers: assemblage  Planktonic foraminifers: assemblage	CP11 ( <i>Discoaster lodoensis</i> Zone) (D.B.) Probable Laiming C to pseudo-C (R.E.A., K.M.) P8 (K.M.)	≥ 2,000 m (K.M.)	Sample collected from upper part of the mudstone unit about 4.2 km northwest of measured section. Presumably a few meters above stratigraphic position of 981-25-3(H).
981-25-3(H)	Calcareous nannofossils: <i>Zygrabliuthus bijugatus</i> , <i>Tribrachiatus orthostylus</i> Benthic foraminifers: assemblage  Planktonic foraminifers: assemblage	CP10 (D.B.) Probable Laiming C to pseudo-C (R.E.A., K.M.) P8 to P9 (K.M.)	≥ 2,000 m (K.M.)	Approximately 10 m below 981-25-4(H). <i>Tibrachiatus orthostylus</i> is sparse and possibly redeposited; <i>Coccolithus crassus</i> is absent.
GP33	Benthic and planktonic foraminifers: assemblage	Eocene (P.J.S.)		Relative stratigraphic position uncertain, probably close to 981-25-2(H).
981-25-1(H)	Calcareous nannofossils: <i>Coccolithus crassus</i> , <i>Discoaster lodoensis</i> , <i>Braarudosphaera</i> sp., <i>Micrantholithus</i> sp., <i>Pontosphaera</i> sp., <i>Zygrabliuthus</i> sp. Benthic foraminifers: assemblage  Planktonic foraminifers: assemblage	CP11 ( <i>Discoaster lodoensis</i> Zone) Laiming C(?) to pseudo-C(?) (R.E.A., K.M.) P8 to P9 (K.M.)	≥ 2,000 m (K.M.)	Approximately 10 m below 981-25-2(H).
V-651	Calcareous nannofossils: <i>Sphenolithus radians</i> , <i>Zygrabliuthus bijugatus</i> , <i>Discoaster lodoensis</i> , <i>Helicosphaera lophota</i> , <i>Coccolithus crassus</i> , <i>Rhabdosphaera mortionum</i> , <i>R. tenuis</i> , <i>Helicosphaera seminulum</i> , <i>Discoaster binodosus</i> Benthic foraminifers: <i>Bulimina macilentia</i> , <i>B. callahani</i> , <i>Anomalina dorri aragonensis</i> , <i>Marginulina asperuliformis</i> Planktonic foraminifers: <i>Globorotalia bullbrooki</i> , <i>G. griffinae</i> , <i>G. caucasica</i>	CP11 Laiming C to pseudo-C P9	Upper to middle bathyal	
V-557	Calcareous nannofossils: <i>Coccolithus crassus</i> , <i>Discoaster lodoensis</i> , <i>Discoasteroides kuepperi</i> Benthic foraminifers: assemblage  Planktonic foraminifers: assemblage	CP11 ( <i>Discoaster lodoensis</i> Zone) Probable Laiming C to pseudo-C (R.E.A., K.M.) P7 to P9 (K.M.)	Middle(?) bathyal (P.J.Q.)	Includes Eocene dinoflagellates (N.O.F.) and trace fossil ? <i>Helminthoidea</i> sp.

**Table 1.** Age-diagnostic taxa, zonation, and paleobathymetry of microfossils from Big Pine Mountain area—Continued

Field No.	Age-diagnostic and associated taxa	Age or zone	Paleobathymetry	Remarks
V-650	Calcareous nannofossils: <i>Sphenolithus radians</i> , <i>Zygrabliothus bijugatus</i> , <i>Discoaster lodoensis</i> , <i>Helicosphaera lophota</i> , <i>Coccolithus crassus</i> , <i>Tribraehiatius orthostylus</i> Benthic foraminifers: <i>Bulimina macilenta</i> , <i>B. callahani</i> , <i>Anomalina dorri aragonensis</i> , <i>Marginulina asperuliformis</i> Planktonic foraminifers: <i>Globorotalia caucasica</i> , <i>G. broedermanni</i> , <i>G. subbotinae</i> , <i>G. aragonensis</i> , <i>G. soldadoensis</i>	CP11 Laiming C P8	Upper to middle bathyal	
V-649	Palynomorphs: <i>Wetzeliella articulata</i> Calcareous nannofossils: <i>Tribraehiatius orthostylus</i> , <i>Sphenolithus radians</i> , <i>S. anarrhopus</i> , <i>Chiasmolithus grandis</i> , <i>Discoaster mirus</i> , <i>D. minimus</i> , <i>D. barbadiensis</i> , <i>Rhabdosphaera crebra</i> , <i>Toweius</i> sp. Benthic foraminifers: <i>Bulimina macilenta</i> , <i>B. callahani</i> , <i>Anomalina dorri aragonensis</i> Planktonic foraminifers: <i>Globorotalia subbotinae</i> , <i>G. aragonensis</i> , <i>G. soldadoensis</i>	Eocene Probable CP9 Laiming C P7	Upper to middle bathyal	<i>Discoaster diastypus</i> absent.
V-648	Calcareous nannofossils: <i>Tribraehiatius orthostylus</i> , <i>Sphenolithus radians</i> , <i>Chiasmolithus grandis</i> , <i>Lophodolithus nascens</i> , <i>Transversopontis pulcher</i> , <i>Coccolithus cribellum</i> , <i>Toweius</i> sp., <i>Markalius</i> sp. Benthic foraminifers: <i>Bulimina macilenta</i> , <i>B. callahani</i> , <i>Anomalina dorri aragonensis</i> Planktonic foraminifers: <i>Globorotalia subbotinae</i> , <i>G. aragonensis</i> , <i>G. soldadoensis</i>	Probable CP9 Laiming C P7	Upper to middle bathyal	Rare specimens of <i>Micula staurophora</i> reworked from Upper Cretaceous strata; <i>Discoaster diastypus</i> absent.
V-647	Palynomorphs: assemblage (not zoned) Calcareous nannofossils: barren Benthic foraminifers: <i>Recurvoides</i> spp., <i>Silicosigmoilina</i> sp., <i>Saccamina</i> sp.	Cretaceous to Paleogene	Bathyal	
V-646	(Report pending)			
1084-16-1(M)	Palynomorphs: <i>Alangiopollis cribellata</i> type, <i>Betulaepollinites</i> sp., <i>Paraanipollinites confusus</i> , probable <i>Ulmipollinites tricostatus</i>	Late Paleocene (N.O.F.)		Assigned to R3368, USGS, Reston, Va., palynology archive.
V-645	Palynomorphs: assemblage not zoned Benthic foraminifers: <i>Recurvoides</i> spp., <i>Silicosigmoilina</i> sp., <i>Saccamina</i> sp.	Cretaceous to Paleogene	Bathyal	
1084-16-2(M)	Palynomorphs: "Much the same flora as in R3368," Field number 1084-16-1(M)	Probable late Paleocene (N.O.F.)		Assigned to R3373, USGS, Reston, Va., palynology archive.
V-644	Calcareous nannofossils: barren			
V-643	do.			
V-642	Benthic foraminifers: (same as in V-645)	Cretaceous to Paleogene	Bathyal	
V-641	Palynomorphs: <i>Areoligera</i> sp. Benthic foraminifers: (same as in V-645)	Late Cretaceous to Paleogene Cretaceous to Paleogene	Bathyal	
V-640	Palynomorphs: ? <i>Cyclonepheum</i> sp., <i>Glaphyrocysta</i> sp. Benthic foraminifers: (same as in V-645)	Probable Paleogene Cretaceous to Paleogene	Bathyal	Comstock's (1975) locality 2 (late Paleocene) may project stratigraphically between here and V-642.
V-639	(Report pending)			
V-638	Palynomorphs: <i>Isabelidium cretaceum</i> , <i>Dinogymnium acuminatum</i> Benthic foraminifers: (same as in V-645)	Maastrichtian Cretaceous to Paleogene	Bathyal	Rare specimens of both taxa.

**Table 1.** Age-diagnostic taxa, zonation, and paleobathymetry of microfossils from Big Pine Mountain area—Continued

Field No.	Age-diagnostic and associated taxa	Age or zone	Paleobathymetry	Remarks
V-637	(Report pending)			
V-636	(Report pending)			
V-635	Palynomorphs: <i>Dinogymnium acuminatum</i>	Santonian to Maastrichtian		
GP46, V-524, V-634	Benthic foraminifers: <i>Cribrostomoides cretacea</i> , <i>Silicosigmoilina californica</i> , <i>Dorothia bulletta</i> , <i>Trochammina</i> sp. cf. <i>T. ribstonensis</i> , <i>Bathysiphon</i> sp., <i>Gaudryina</i> sp. cf. <i>G. filiformis</i> , <i>Cibicides</i> sp. cf. <i>C. coonensis</i> (R.L.P., GP46)	Late(?) Cretaceous, possibly Goudkoff C and (or) D1 (R.L.P.); Late Cretaceous (R.E.A., V-524)		GP46 = M43 of Vedder and others (1967). All three samples from approximately same site.
V-633	Palynomorphs: <i>Proteacidites thalmani</i>	Late Cretaceous to Paleogene		Rare specimens.
V-524a	Palynomorphs: <i>Isabelidium cretaceum</i> , <i>Dinogymnium acuminatum</i> Benthic foraminifers: assemblage not zoned (R.E.A.)	Maastrichtian Late Cretaceous (R.E.A.)	Bathyal	Common specimens of <i>I. cretaceum</i> .
V-632	(Report pending)			
V-631	Palynomorphs: <i>Proteacidites thalmani</i> Benthic foraminifers: <i>Recurvoides</i> spp., <i>Silicosigmoilina</i> sp., <i>Saccammina</i> sp.	Possible Late(?) Cretaceous Cretaceous to Paleogene	Bathyal	Common specimens of <i>P. thalmani</i> . Abundance of <i>Recurvoides</i> spp. suggests Cretaceous rather than Paleogene age.
V-630	Benthic foraminifers: (same as in V-631)	do.	do.	Do.
V-629	do.	do.	do.	Do.
V-628	Palynomorphs: <i>Dinogymnium acuminatum</i> Benthic foraminifers: (same as in V-631)	Santonian to Maastrichtian Cretaceous to Paleogene	do.	Do.
V-527	Benthic foraminifers: assemblage (not zoned)	Late Cretaceous (R.E.A.)		Stratigraphic position uncertain. Collected about 130 m WSW of V-628.
65CB75	do.	Probable Cretaceous (J.W.R.)		Stratigraphic position uncertain. Collected about 225 m S of V-628.
V-692	(Report pending)			
V-691	(Report pending)			
V-525	Benthic and planktonic foraminifers: assemblage (not zoned)	Late Campanian or Maastrichtian Goudkoff D2 to E (R.E.A.)		Contains calcareous benthic, planktonic, and arenaceous foraminifera (R.E.A.).
V-690	(Report pending)			Approximately same stratigraphic position as megafossil locality V-526 <i>Pachydiscus ootacodensis?</i> (M7589, USGS, Menlo Park, Calif., Mesozoic megafossil collection).

**Table 1.** Age-diagnostic taxa, zonation, and paleobathymetry of microfossils from Big Pine Mountain area—Continued

Field No.	Age-diagnostic and associated taxa	Age or zone	Paleobathymetry	Remarks
V-689	Benthic foraminifers: <i>Eponides</i> sp. cf. <i>E. bandyi</i> , <i>Gyroidina quadrata</i> , <i>Gaudryina navarroensis crassiformis</i> , <i>Bulimina spinata</i>	Goudkoff D2 to E	Bathyal	
1084-16-1(H)	Palynomorphs: <i>Proteacidites</i> spp. and assemblage	Santonian to Danian (N.O.F.)		Stratigraphic position uncertain; within 10 m of base. About 175 m north of measured section. Assigned to R3370, USGS, Reston, Va., palynology archive.

the mudstone sequence. This lentil consists of medium- to coarse-grained micaceous quartzofeldspathic sandstone in which bedding is normally graded, indistinct, or absent. Other lenticular sandstone beds are present in the mudstone along Big Pine Road less than 1 km southeast of the measured section, where they are as much as 5 m thick. All of these lenticular sandstone beds are interpreted to be channel-fill deposits. Farther southeast near the Big Pine fault, a zone of sandstone beds within the mudstone unit is estimated to be about 15 m thick.

Although covered by colluvium and landslides at Big Pine Mountain, the upper contact of the condensed(?) succession is sharply defined along the sheer eastern wall of lower Big Pine Canyon near its juncture with the Sisquoc River. On the cliff face, mudstone beds (lithofacies G) are depositionally overlain without discordance by resistant sandstone beds (lithofacies C and B of Ricci-Lucchi, 1975) that constitute the basal part of the superjacent sequence. Where examined, the contact is characterized by flame structures, small load casts, and an absence of large-scale erosional features.

### Zonation and Age

Paleontologic evidence indicates that the condensed(?) succession includes strata that range in age from Late Cretaceous through most of the early Eocene. The assigned ages are based upon zonations that are derived chiefly from assemblages of calcareous nannofossils, palynomorphs, and foraminifers supplemented by rare mollusks in the lower part. Biostratigraphic subdivision of the microfossil assemblages is based upon the following schemes:

Calcareous nannofossils: CP zones, Okada and Bukry (1980);

Palynomorphs: age or stage, Williams and Bujak (1985);

Planktonic foraminifers: P zones, Blow (1969), as emended by Toumarkine and Luterbacher (1985); and

Benthic foraminifers: H-C zones, Goudkoff (1945), as emended by Almgren (1986) for Upper Cretaceous assemblages; E-A zones, Laiming (1939), as emended by Almgren and others (1988) for Paleogene assemblages.

Ages of geochronologic units and boundary ages of chronostratigraphic units follow the usage of Haq and others

(1987) with the exception of the early Eocene-middle Eocene boundary, which, in California, is more easily defined by the CP11/CP12a indicators. Preliminary results from the biostratigraphic analyses are summarized in tabular form (table 1), and the zones represented are shown on the stratigraphic column (fig. 5).

Fossils from the lowermost 30 m of the measured section (fig. 5) include foraminifers and mollusks indicative of the Campanian and (or) Maastrichtian Stages (table 1, V-689, V-525, and V-526). Identifiable calcareous nannofossils and palynomorphs are absent in samples from the same 30-m-thick interval. Above an overlying deeply weathered, partly covered interval about 40 m thick, palynomorph assemblages that range from Santonian to Maastrichtian occur through 80 m of section; two of these assemblages (V-524a, V-638) are restricted to the Maastrichtian Stage. Foraminifers from the same 80-m-thick interval are long-ranging agglutinated taxa that were assigned either a Cretaceous age or a Cretaceous to Paleogene age. The Paleocene foraminiferal assemblage listed by Comstock (1975, locality 2; 1976, locality BP-4m) from a single site on Big Pine Mountain, when projected into the measured section, falls at least 60 m above the 80-m-thick interval (near V-642). Thus, the Cretaceous-Tertiary boundary may lie between 160 m and 200 m from the base (between V-638 and V-641). Late Paleocene palynomorphs are present in samples about 238 m and 250 m above the base (1084-16-2(M), 1084-16-1(M)). The lowest stratigraphic occurrence of early Eocene taxa is in a sample from approximately 300 m above the base (V-648), in which Zone CP9 calcareous nannofossils and Zone P7 planktonic foraminifers occur together. Younger early Eocene assemblages represent Zones CP10 and CP11 and Zones P8 and P9 in the uppermost 30 m of section (V-650 to V-651). A sample (981-25-5(H)) from 5 cm below the upper contact in Big Pine Canyon contains microfossils indicating Zone CP11 and Zone P9(?)–P13(?).

If the duration of sedimentation is interpreted to have lasted from the end of early Maastrichtian through Zone CP11, as suggested by the preliminary biostratigraphic data in table 1, the time interval represented by the condensed(?) succession may have been 21.5 m.y. (Haq and others, 1987, time scale). Because there is no definitive fossil evidence for the presence or absence of the uppermost Maastrichtian Stage and all of the Danian Stage in the sequence, deposition may or may not have been continu-

ous. If deposition was interrupted by an hiatus or erosion, a physical record of such an event is not apparent, and the sample suite is not biostratigraphically complete enough to be conclusive. If, indeed, the absence of uppermost Maastrichtian and Danian beds can be verified, approximately 8 m.y. of time are unaccounted for in the depositional record. Alternatively, these chronostratigraphic units may be present but are not recognizable biostratigraphically for several reasons, among which are the following:

- 1) Benthic foraminifers from open-ocean, deep-water forearc settings tend to have longer stratigraphic ranges than those from shallower water restricted environments (Almgren and others, 1988);
- 2) Exceptionally slow sedimentation rates and macro-benthic predation reduces microfaunal preservation (R.G. Douglas and D.S. Gorsline, written commun., 1993);
- 3) Diagenetic dissolution selectively destroys extremely small, age-diagnostic foraminifers;
- 4) Post-depositional deep weathering dissolves most calcareous foraminifers and nanofossils; and
- 5) Insufficient sampling and widely spaced sampling intervals hinder precise zonation.

In summary, nearly 22 m.y. of Late Cretaceous and early Tertiary time may have elapsed during deposition of the mudstone in the measured section at Big Pine Mountain; yet the position of the Cretaceous-Tertiary boundary in this section has not been established on either biostratigraphic or lithostratigraphic discontinuities. Evidence for the presence or absence of the Danian Stage is equivocal, and a definite Paleocene-Eocene boundary cannot be determined from the samples examined. Despite the lack of documentation for positioning these two boundaries and the Danian Stage in the measured section, the duration of time represented by the condensed(?) succession seems incontestable, even though unrecognized hiatuses may break the apparent continuity of deposition. Because stratal sequences that show uninterrupted sedimentation across the Cretaceous-Tertiary boundary have not been identified with certainty elsewhere in southern California, the assertion that deposition was continuous at Big Pine Mountain is likely to be challenged.

### Superjacent Lower and Middle(?) Eocene Strata

The cliff-forming unit that overlies the condensed(?) succession is composed mainly of submarine-fan sandstone (lithofacies B). In the area between the top of Big Pine Mountain and the topographic saddle north of the former site of Alamar Guard Station (fig. 4), at least 1,000 m of strata are included in this sandstone unit; 3 to 4 km farther southeast, the unit may be 1,200 m or more thick. Along its entire northeastern margin, this sandstone unit is truncated by the Sur-Nacimiento fault zone.

The sandstone in this unit is quartzofeldspathic, poorly sorted, and largely medium to very coarse grained. Thin, non-persistent zones of granules and small pebbles are interspersed

in some beds, and pebble-cobble conglomerate (lithofacies A of Ricci-Lucchi, 1975) is interbedded at a few places. Bedding in the sandstone generally is thick to massive and locally is normally graded. Some beds display dish structure; others commonly are bioturbated. Relatively thin zones of mudstone and thin-bedded sandstone characteristic of lithofacies D and (or) E are sporadically present throughout the dominantly sandstone unit. Siltstone and very fine to fine-grained sandstone partings commonly delineate bedding.

Sediment-transport directions within this unit have been measured only along Big Pine Road, and the influence of post-depositional tectonic rotation is unknown. Bidirectional paleocurrent features, chiefly parting lineations, indicate either northeastward or southwestward flow. Rare groove and flute casts, together with fairly common, preferentially oriented flame structures suggest southward and westward flow directions. A sediment source northeast of the Sur-Nacimiento fault zone is inferred.

Biostratigraphic data from this unit are sparse. A small assemblage of poorly preserved mollusks collected about 120 m above the base of this unit at Big Pine Mountain suggests an age of early Eocene ("Capay" Stage). A larger assemblage of mollusks from granule-pebble conglomerate about 335 m above the base (fig. 5) may be early or middle Eocene in age ("Capay" or "Domengine" Stage). Although these assemblages were provisionally assigned a middle Eocene age by Vedder and others (1967, localities F18, F19), revisions of the West Coast Eocene stages (Squires, 1988) require the change to older Eocene ages. Comstock (1975, 1976) reported early Eocene foraminifers from a locality (8, BP 3m) 2.0 km east-southeast of Big Pine Mountain. If projected along strike, his locality apparently falls stratigraphically slightly below the higher of the two mollusk localities. Foraminifers from a 15-cm-thick mudstone zone (5/19/92B) about 260 m stratigraphically above the upper mollusk locality include benthic species that range from early into middle Eocene (equivalent to Zone P9-P10) and that suggest a depth of 2,000 m or more (K.A. McDougall, written commun., 1993).

### Conclusions

The condensed(?) succession of mudstone at Big Pine Mountain is indicative of very slow, possibly continuous, deep-sea hemipelagic sedimentation. The lower contact represents an abrupt shutdown of rapid, coarse-clastic sedimentation, and the upper contact indicates a sudden renewal of relatively high rates of coarse-clastic deposition. Although slow deposition rates occurred in other Paleogene formations in the southern Coast Ranges, such as the Lodo Formation and Anita Shale of Kelley (1943), no other mudstone unit in this region is known to have endured as long or to have spanned the Cretaceous-Tertiary boundary. Other formations in the region may incorporate both upper Maastrichtian and Danian beds (Saul, 1983, 1986), but these rock units consist largely of relatively rapidly deposited sandstone and conglomerate.

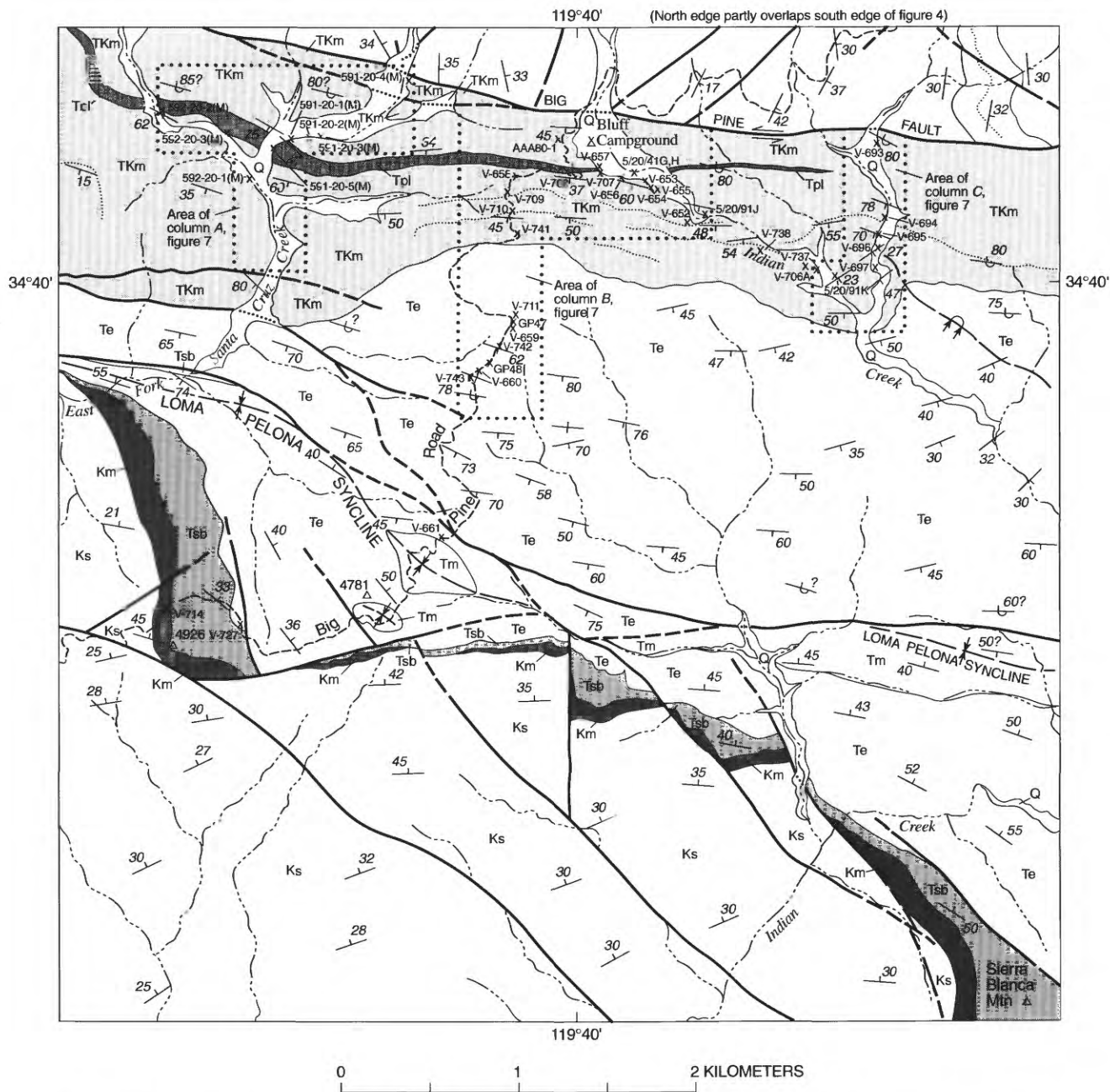


**Figure 6.** Generalized geologic map of area south of Big Pine fault. Location shown on figure 1B. Patterns indicate distribution of limestone units and adjacent Cretaceous to Eocene strata. Modified from Vedder and others (1967) and J.G. Vedder, R.D. Brown, Jr., T.W. Dibblee, Jr., Hugh McLean, and R.G. Stanley (unpub. mapping, 1965–93).

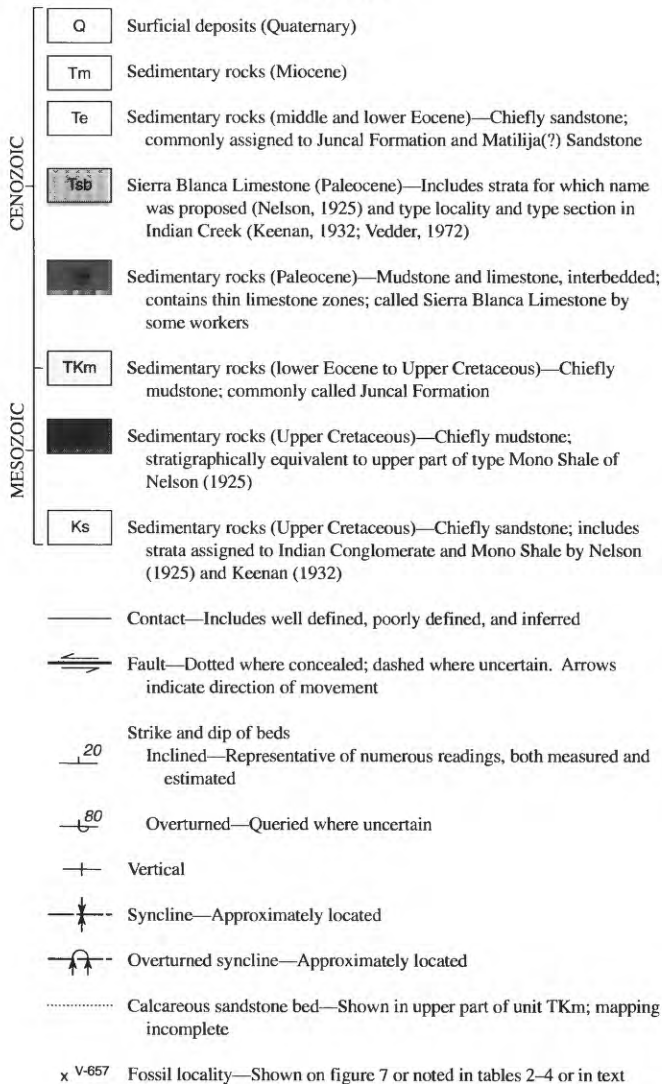
## CORRELATIVE SEQUENCES SOUTH OF BIG PINE FAULT

### Grapevine Creek–Bluff Campground–Alamar Canyon Area

South of Big Pine Mountain and flanking the south side of the Big Pine fault is a 12-km-long belt of strata, chiefly mudstone, that extends eastward along the north limb of Loma Pelona syncline from the vicinity of Grapevine Creek to

Alamar Canyon (figs. 1A and 6). Beds within this belt, the base of which is not exposed, contain microfossils that are Late Cretaceous, late Paleocene, and early Eocene in age (tables 2–4). As much as 800 m of strata are exposed in the segment of this belt that extends westward from Bluff Campground to East Fork Santa Cruz Creek. Discontinuous, thin zones of bioclastic limestone that were assigned to the Sierra Blanca Limestone by Gower and others (1966), Vedder and others (1967), and Comstock (1975, 1976) are present in the middle part (fig. 7A, B). In contrast to the

EXPLANATION



type area of the Sierra Blanca on the south limb of Loma Pelona syncline, there is no evidence for an unconformity at the base of the limestone zones (fig. 8). Where examined in the Bluff Campground area, the limestone commonly exhibits normally graded bedding, Bouma sequences, sharp erosional bases, and gradational tops; these features suggest turbidity-current deposition. The enclosing mudstone beds contain upper to middle and middle to lower bathyal assemblages of benthic foraminifers. Farther west, in the Grapevine Creek-East Fork Santa Cruz Creek area (fig. 7A), bioclastic limestone breccia probably represents downslope-transported algal-bank rubble (Vedder and others, 1994) rather than in situ bank deposits as interpreted by Comstock (1975, 1976). Stratigraphically above the limestone zones, beds of reddish and greenish foraminifer mudstone are locally present (fig. 7B, C). These variegated mudstone beds are similar to the “Poppin

shale” of local usage in the Anita Shale of Kelley (1943). Non-persistent, largely calcareous sandstone turbidites 1 to 10 m thick are interspersed in the mudstone upsection from the limestone zones (fig. 6). In the upper Indian Creek area, some of these calcareous quartzofeldspathic sandstone beds were mapped as Sierra Blanca Limestone by earlier workers. The mudstone belt is overlain gradationally by more than 1,000 m of lower and middle Eocene strata, chiefly sandstone (fig. 6; fig. 7B), in which southward to westward sediment transport is suggested by measurements along Big Pine Road.

The stratigraphically lowest sample (V-693) from the mudstone belt was collected close to the trace of the Big Pine fault in a tributary of Indian Creek about 1.5 km east of Bluff Campground and contains calcareous nannofossils that range from Santonian into Maastrichtian (fig. 7C, table 4). Zones CP5 into CP10 and CP11(?) and Zones P6 into P8-P9 are represented in samples from higher in the sequence (fig. 7; tables 2-4). The limestone zones near Bluff Campground are bracketed by mudstone beds that are assigned to Zones CP7 and CP8. Foraminifers from the Sierra Blanca Limestone at Big Pine Road (fig. 6) are assigned to Zone P4 or older and represent an open-marine, slope(?) setting (W.V. Sliter, written commun., 1993). Calcareous nannofossils from poorly exposed reddish and greenish mudstone beds directly overlying the Sierra Blanca where it crosses Big Pine Road (V-727, fig. 6) are assigned to Zone CP10 (David Bukry, written commun., 1993), and Zone CP8 and CP9 beds are absent.

The easternmost outcrops of the mudstone belt that parallels the south side of the Big Pine fault extend across Alamar Canyon and are truncated by the fault in a tributary about 1.0 km east of Dutch Oven Campground (fig. 1A) (Vedder and others, 1973, unit Ks?). Comstock (1975, 1976) reported late Paleocene foraminifers from two sites east of the area shown on figure 6. Algal limestone beds apparently are absent in Alamar Canyon.

**Coche Creek Area**

Mudstone beds exposed along a 4-km stretch of Coche Creek between the North and South Branches of the Big Pine fault (figs. 1A, 1B) are similar to and probably correlative with those in the mudstone belt that extends between Grapevine Creek and Alamar Canyon. Samples collected from the banks of Coche Creek contain deep-water (≥2,000 m) foraminifer assemblages that probably are early Tertiary in age (K.A. McDougall, written commun, 1993). Comstock (1975, 1976) reported late Paleocene foraminifers from a tributary to Coche Creek adjacent to the trace of the Big Pine fault. Algal limestone beds are not known to be present in this mudstone sequence.

Beds within the mudstone belt that parallels the south side of the Big Pine fault are coeval with those in the con-

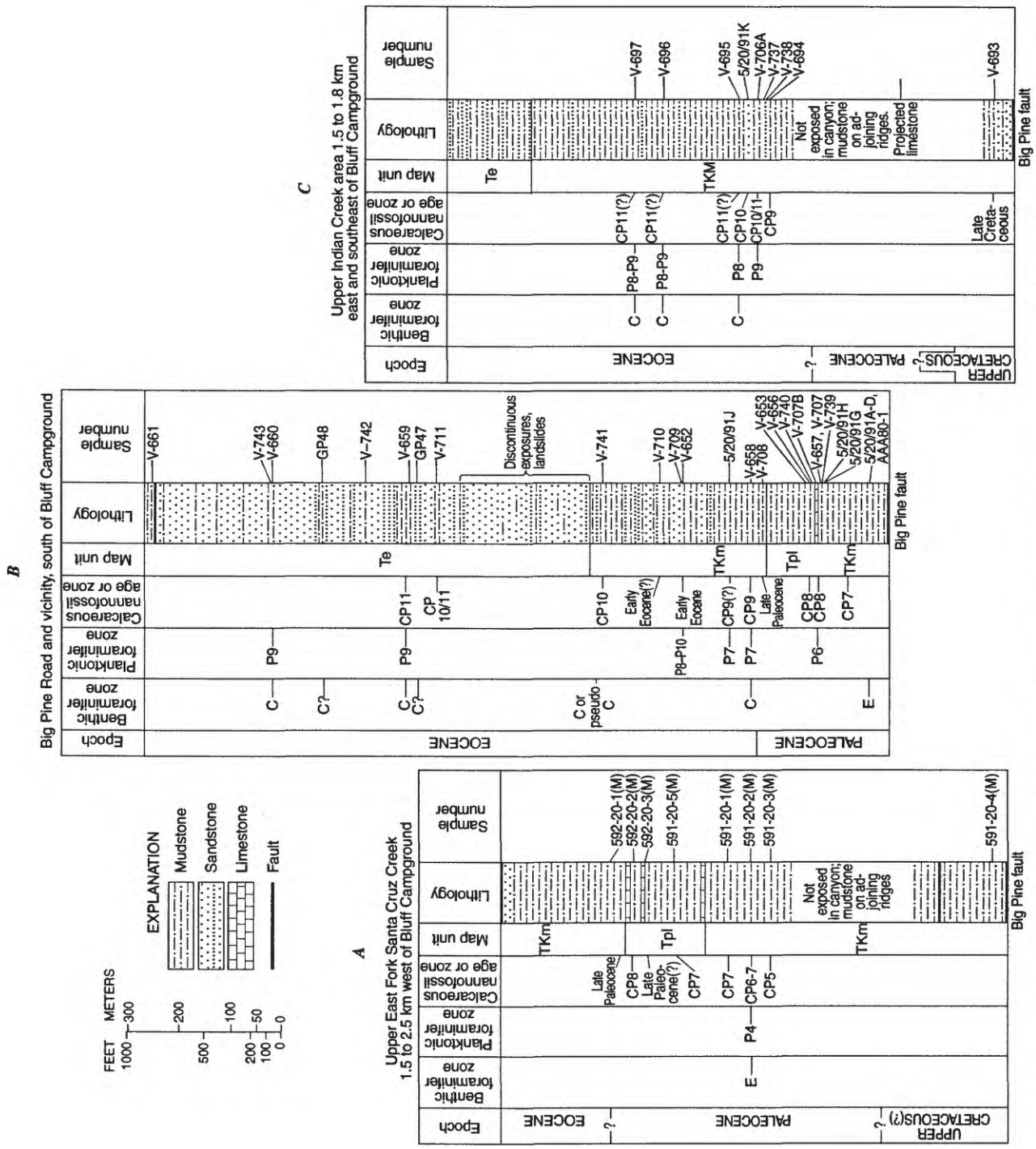


Figure 7. Generalized composite stratigraphic columns of Upper Cretaceous and Paleogene rocks south of Big Pine fault (map units TKm, Tpl, and lower part of Te, fig. 6). Approximate locations of columns are shown on figure 6. Zonation and age assignments are explained in tables 2-4.

Table 2. Age-diagnostic taxa, zonation, and paleobathymetry of microfossils from upper East Fork Santa Cruz Creek

[Localities shown on figures 6 and (or) 7A. Arranged stratigraphically from top to bottom. See table 1 for sources of data]

Field No.	Age-diagnostic and associated taxa	Age or zone	Paleobathymetry	Remarks
592-20-1(M)	Calcareous nannofossils: <i>Coccolithus pelagicus</i> , <i>Neochiastozygus junctus</i> Benthic foraminifers: large assemblage (>45 taxa) (K.M.)	Late Paleocene (D.B.) Late Paleocene (K.M.)	Upper bathyal (K.M.)	Sample contains abundant calcareous debris. Includes planktonic taxa (K.M.).
592-20-2(M)	Calcareous nannofossils: <i>Discoaster falcatus</i> , <i>D. multiradiatus</i> , <i>Ellipsolithus macellus</i> , <i>Fasciculithus typaniformis</i> , <i>Neochiastozygus distentus</i> , <i>Zygrablithus bijugatus</i> Benthic foraminifers: large assemblage (>75 taxa) (K.M.)	CP8 (D.B.) Late Paleocene (K.M.)	≥2,000 m	Abundant flora. Includes displaced upper bathyal and neritic indicators.
592-20-3(M)	Calcareous nannofossils: <i>Coccolithus pelagicus</i> , <i>Fasciculithus typaniformis</i> (?), <i>Zygrablithus sigmoides</i> (?) Benthic foraminifers: large assemblage (>75 taxa) (K.M.)	Late Paleocene(?) (D.B.) Late Paleocene (K.M.)	≥2,000 m	Contains reworked specimens of Cretaceous <i>Micula decussata</i> . Includes displaced upper bathyal and neritic indicators.
591-20-5(M)	Calcareous nannofossils: <i>Toweius</i> sp., <i>Coccolithus pelagicus</i> , <i>Fasciculithus typaniformis</i> , <i>Discoaster nobilis</i> , <i>D. delicatus</i> Benthic foraminifers: (Report pending)	CP7		Specimens rare and poorly preserved.
591-20-1(M)	Calcareous nannofossils: <i>Toweius</i> sp., <i>Coccolithus pelagicus</i> , <i>Fasciculithus typaniformis</i> , <i>Discoaster nobilis</i> , <i>D. delicatus</i> , <i>D. mohleri</i> , <i>Chiasmolithus consuetus</i> Benthic foraminifers: (Report pending)	CP7		Specimens rare and poorly preserved.
591-20-2(M)	Calcareous nannofossils: <i>Coccolithus pelagicus</i> , <i>Fasciculithus typaniformis</i> , <i>Chiasmolithus consuetus</i> , <i>Zygodiscus</i> sp., <i>Ericsonia robusta</i> , <i>Heliolithus reideli</i> , <i>Neochiastozygus chiastus</i> , <i>Prinsius bisulcus</i> Benthic foraminifers: <i>Bulimina arkadelphia</i> , <i>B. macilenta</i> , <i>Dorothia oxycona</i> , <i>Silicosigmoilina californica</i> Planktonic foraminifers: <i>Globorotalia psuedomenardii</i> , <i>Globigerina triloculinoides</i>	CP6-CP7 Laiming E P4	Middle to lower bathyal	Specimens rare and poorly preserved.
591-20-3(M)	Calcareous nannofossils: <i>Coccolithus pelagicus</i> , <i>Toweius</i> sp., <i>Fasciculithus typaniformis</i> , <i>Heliolithus kleinpelli</i> , <i>Chiasmolithus consuetus</i> , <i>C. bidens</i> , <i>Zygrablithus</i> sp., <i>Scapholithus fossilis</i> Benthic foraminifers: (Report pending)	CP5		Specimens rare and poorly preserved.

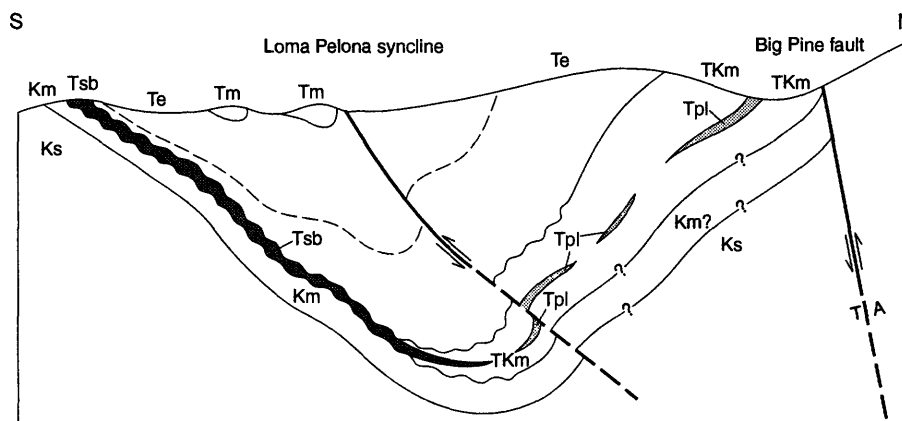


Figure 8. Schematic cross section, Loma Pelona syncline, vicinity of Big Pine Road. See figure 6 for symbol explanation. Units Tsb and Tpl represent Sierra Blanca Limestone and coeval limestone lenses. Dashed line in unit Te represents highest stratigraphic occurrence of beds similar to "Poppin shale" of local usage. T, toward; A, away. Small faults not shown.

Table 3. Age-diagnostic taxa, zonation, and paleobathymetry of microfossils from Big Pine Road south of Bluff Campground

[Localities shown on figures 6 and (or) 7B. Arranged stratigraphically from top to bottom. See table 1 for sources of data]

Field No.	Age-diagnostic and associated taxa	Age or zone	Paleobathymetry	Remarks
V-661	Calcareous nannofossils: <i>Sphenolithus radians</i> , <i>Chiasmolithus grandis</i> , <i>Coccolithus crassus</i> , <i>Discoaster lodoensis</i> , <i>Helicosphaera lophota</i> , <i>Rhabdosphaera tenuis</i> , <i>Discolithina distincta</i> , <i>Chipfragmolithus acanthodes</i> , <i>Reticulofenestra samudorovi</i> , <i>Neochiastozygus distentus</i> Benthic foraminifers: <i>Bulimina macilenta</i> , <i>B. callahani</i> , <i>Anomalina dorri aragonensis</i> Planktonic foraminifers: <i>Globorotalia caucasica</i> , <i>G. spinulosa</i> , <i>Globigerina inaequispira</i>	Probable CP12a  Laiming C to pseudo-C P9	Upper to middle bathyal	Specimens frequent, poorly preserved. Subzone tentative in absence of <i>Discoaster sublodoensis</i> . Stratigraphic position uncertain.
V-743	Calcareous nannofossils: <i>Coccolithus crassus</i> , <i>Helicosphaera lophota</i> (D.B.) Benthic foraminifers: <i>Karrerella conversa</i> , <i>Silicosigmoilina californica</i> , <i>Cibicidoides subspiratus</i> , <i>Pullenia eocenica</i> (K.M.)	CP11 (D.B.)  Early to middle Eocene (K.M.)	Lower bathyal	Benthic assemblage coeval with P9 (K.M.)
V-660	Benthic foraminifers: <i>Bulimina macilenta</i> , <i>B. callahani</i> , <i>Anomalina dorri aragonensis</i> Planktonic foraminifers: <i>Globorotalia caucasica</i> , <i>G. spinulosa</i> , <i>Globigerina inaequispira</i>	Laiming C to pseudo-C P9	Upper to middle bathyal	
GP48	Benthic foraminifers: <i>Vaginulinopsis asperuliformis</i> , <i>Nodosaria latejugata</i> , <i>Rhabdammina eocenica</i> , <i>Tritaxilina colei</i> , <i>Haplophragmoides eggeri</i> , <i>Verneulina triangulata</i> , <i>Plectofrondicularia kerni</i> , <i>Parrella culter midwayana</i> (R.L.P.) Planktonic foraminifers: <i>Globigerina yeguaensis</i> , <i>Globorotalia aragonensis</i> , <i>G. spinoinflata</i> (R.L.P.)	Early or early middle Eocene (R.L.P.)  P9 to P11		M51 of Vedder and others (1967). Benthic assemblage equivalent to P8 to early P9 (K.M.)
V-742	Calcareous nannofossils: <i>Coccolithus crassus</i> , <i>Discoaster lodoensis</i> , <i>Discoasteroides kuepperi</i> , <i>Helicosphaera lophota</i> , <i>Toweius magnicrassus</i> (D.B.) Benthic foraminifers: large assemblage (>30 taxa) (K.M.)	CP11 (D.B.)  Early to middle Eocene (K.M.)	≥2,000 m (K.M.)	Benthic assemblage coeval with P8 to P9 (K.M.)
V-659	Calcareous nannofossils: <i>Toweius</i> sp., <i>Chiasmolithus crassus</i> , <i>Discoasteroides kuepperi</i> , <i>Tribrachiatius orthostylus</i> , <i>Sphenolithus radians</i> , <i>S. anarrhopus</i> , <i>Zygrabliothus bijugatus</i> , <i>Discoaster lodoensis</i> , <i>D. barbadiensis</i> , <i>D. diastypus</i> , <i>Helicosphaera seminulum</i> Benthic foraminifers: <i>Bulimina macilenta</i> , <i>B. callahani</i> , <i>Anomalina dorri aragonensis</i> Planktonic foraminifers: <i>Globorotalia caucasica</i> , <i>G. spinulosa</i> , <i>Globigerina inaequispira</i>	CP11  Laiming C to pseudo-C P9	Upper to middle bathyal	
GP47	Benthic foraminifers: <i>Martinottiella</i> sp. cf. <i>M. petrosa</i> , <i>Rhabdammina eocenica</i> , <i>Haplophragmoides eggeri</i> , <i>Eggerella</i> sp., <i>Dorothia principiensis</i> , <i>Tritaxalina colei</i> , <i>Clavulinoides californicus</i> , <i>Allomorphina conica</i> , <i>Plectofrondicularia kerni</i> , <i>Amphimorphina ignota</i> , <i>Cibicidoides</i> sp. cf. <i>C. venezuelanus</i> , <i>Cibicides martinezensis</i> , <i>C. pachecoensis</i> , <i>Asterigina crassaformis umbilicatula</i> , <i>Trifarina advena californica</i> , <i>Hastigerina micra</i> , <i>Dentalina basiplanata</i> , <i>Lenticulina theta</i> , <i>Pleurostomella</i> sp. cf. <i>P. alternans</i> Planktonic foraminifers: <i>Globigerina</i> cf. <i>G. yeguaensis</i> , <i>Globorotalia aragonensis</i> , <i>G. spinuloinflata</i> (R.L.P.)	Laiming C  P9 to P11		M47 of Vedder and others (1967). Benthic assemblage equivalent to P8 to early P9 (K.M.)
V-711	Calcareous nannofossils: <i>Zygrabliothus bijugatus</i> , <i>Chiasmolithus grandis</i> , <i>C. magnicrassus</i> , <i>Discoaster lodoensis</i> , <i>Discoasteroides kuepperi</i> , <i>Helicosphaera seminulum</i> , <i>Lophodolithus reniformis</i> , <i>Sphenolithus radians</i> , <i>Tribrachiatius orthostylus</i> (D.B.) Benthic foraminifers: large assemblage (>75 taxa) (K.M.)	CP10/CP11 (D.B.)  Early Eocene (K.M.)	≥2,000 m (K.M.)	Specimens common.  Includes abundant planktonic taxa. Benthic assemblage equivalent to P9 (K.M.)
V-741	Calcareous nannofossils: <i>Zygrabliothus bijugatus</i> , <i>Toweius magnicrassus</i> , <i>Tribrachiatius orthostylus</i> (D.B.) Benthic foraminifers: <i>Bulimina macilenta</i> , <i>Cibicidoides venezuelana</i> , <i>Spiroplectammia richardi</i> (K.M.)	CP10 (D.B.)	Middle to lower bathyal	Benthic assemblage coeval with P7 to P14 (K.M.)

Table 3. Age-diagnostic taxa, zonation, and paleobathymetry of microfossils from Big Pine Road south of Bluff Campground—Continued

Field No.	Age-diagnostic and associated taxa	Age or zone	Paleobathymetry	Remarks
V-710	Calcareous nannofossils: <i>Tribracliatulus orthostylus</i> (large and small) (D.B.) Benthic foraminifers: unidentifiable (K.M.)	Early Eocene(?) (D.B.)		Very sparse flora. Casts and molds only (K.M.).
V-709	Calcareous nannofossils: <i>Chiasmolithus grandis</i> , <i>Coccolithus formosus</i> , <i>Discoaster salisburgensis</i> , <i>Sphenolithus radians</i> , <i>Tribracliatulus orthostylus</i> , <i>Zygrabliothus bijugatus</i> , <i>Braarudosphaera bigelowii</i> (D.B.) Benthic foraminifers: large assemblage (>50 taxa) (K.M.)	Early Eocene (D.B.) Early to middle Eocene, probable early (K.M.)	2,000 to 4,000 m (K.M.)	Abundant flora. Includes displaced neritic indicators. Benthic assemblage equivalent to P8 to P10 (K.M.).
V-652	Benthic foraminifers: <i>Anomalina garzaensis</i> , <i>Buliminella grata</i> Planktonic foraminifers: <i>Globigerina eocaena</i> , <i>G. linaperta</i>	Eocene do.	Upper to middle bathyal	Approximately the same stratigraphic position as V-709.
5/20/91J	Calcareous nannofossils: <i>Zygrabliothus bijugatus</i> , <i>Sphenolithus radians</i> , <i>Tribracliatulus orthostylus</i> , <i>Discoasteroides kuepperi</i> , <i>Toweius</i> sp., <i>Discoaster barbadiensis</i> , <i>D. minimus</i> , <i>D. falcatus</i> , <i>Transversopontis pulcher</i> , <i>Lophodolitus mascens</i> , <i>Ellipsolithus macellus</i> Benthic foraminifers: (Report pending)	CP9		Contains reworked specimens of Late Cretaceous <i>Micula staurophora</i> .
V-658	Calcareous nannofossils: <i>Tribracliatulus orthostylus</i> , <i>Sphenolithus radians</i> , <i>S. anarrhopus</i> , <i>Chiasmolithus grandis</i> , <i>Toweius</i> sp., <i>Discoaster delicatus</i> , <i>D. medius</i> , <i>Ellipsolithus macellus</i> , <i>Ericsonia subpertusa</i> , <i>Neochiastozygus chiastus</i> Benthic foraminifers: <i>Bulimina macilenta</i> , <i>B. callahani</i> , <i>Anomalina dorri aragonensis</i> Planktonic foraminifers: <i>Globorotalia formosa formosa</i> , <i>G. formosa gracilis</i> , <i>G. subbotinae</i>	Probable CP9 Laiming C P7	Upper to middle bathyal	Species frequent to rare, poorly preserved. CP9 tentative in the absence of <i>Discoaster diastypus</i> .
V-708	Calcareous nannofossils: <i>Neochiastozygus junctus</i> , <i>Coccolithus pelagicus</i> , <i>Chiasmolithus californicus?</i> , <i>Micrantholithus aequalis</i> Benthic foraminifers: <i>Anomalinoidea welleri</i> , <i>Bulimina midwayensis</i> , <i>B. callahani</i> , <i>Cibicoides dayi</i> , <i>C. hypalis</i> , <i>Osangularia velascoensis</i> , <i>Alabamina wilcoxensis</i> (K.M.)	Late Paleocene (D.B.) Late Paleocene (K.M.)	Upper middle bathyal (K.M.)	Sparse, poorly preserved flora. Limestone debris in mudstone turbidite 3 m upsection. Includes displaced neritic indicators. Benthic assemblage equivalent to P5 to P6a (K.M.).
V-653	Calcareous nannofossils: <i>Toweius</i> sp., <i>Discoaster multiradiatus</i> , <i>Ellipsolithus macellus</i> , <i>Fasciculithus tympaniformis</i> , <i>Zygrabliothus bijugatus</i> Benthic foraminifers: <i>Anomalina garzaensis</i> , <i>Buliminella grata</i> Planktonic foraminifers: <i>Globigerina eocaena</i> , <i>G. linaperta</i>	CP8 Eocene do.	Upper to middle bathyal	Contains reworked specimens of Late Cretaceous <i>Micula staurophora</i> .
V-654	Benthic foraminifers: assemblage; age-diagnostic taxa absent		Bathyal	
V-655	do.		Bathyal	
V-656	Benthic foraminifers: <i>Anomalina garzaensis</i> , <i>A. dorri aragonensis</i> , <i>Bulimina corrugata</i> Planktonic foraminifers: <i>Globorotalia quetra</i>	Laiming C to pseudo-C P6 to P9	Upper to middle bathyal	Sampled beds may have been displaced by landslide.
V-740	Calcareous nannofossils: <i>Discoaster multiradiatus</i> , <i>Fasciculithus schaubii</i> , <i>Neochiastozygus distentus</i> Benthic foraminifers: assemblage of >20 taxa, difficult to identify (K.M.)	CP8 (D.B.) Late Paleocene (K.M.)	Middle bathyal	Specimens poorly preserved. Assemblage coeval with P4 to P6 (K.M.).
V-707B	Calcareous nannofossils: <i>Coccolithus pelagicus</i> , <i>Fasciculithus tympaniformis?</i> Benthic foraminifers: <i>Anomalinoidea rubiginosus</i> , <i>Bulimina callahani</i> (K.M.)	Late Paleocene(?) (D.B.) Late Paleocene (K.M.)	Upper middle bathyal (K.M.)	Very sparse specimens, abundant calcareous debris. About 50 cm upsection from limestone lens. Includes displaced neritic indicators (K.M.).

Table 3. Age-diagnostic taxa, zonation, and paleobathymetry of microfossils from Big Pine Road south of Bluff Campground—Continued

Field No.	Age-diagnostic and associated taxa	Age or zone	Paleobathymetry	Remarks
V-707	Calcareous nannofossils: <i>Coccolithus pelagicus</i> , <i>Discoaster nobilis</i> , <i>Heliolithus</i> sp., <i>Fasciculithus</i> sp. cf. <i>F. involutus</i>	Late Paleocene (D.B.)		Abundant calcareous debris. Specimens sparse and poorly preserved. One reworked specimen of Cretaceous <i>Micula decussata</i> . About 40 cm downsection from limestone lens 10 cm thick.
	Benthic foraminifers: <i>Anomalinoidea welleri</i> , <i>Bulimina cacumenta</i> , <i>B. callahani</i> , <i>B. midwayensis</i> , <i>Cibicidoides dayi</i> , <i>Osangularia velascoensis</i> , <i>Alabamina wilcoxensis</i> (K.M.)	Late Paleocene (K.M.)	Upper middle bathyal (K.M.)	Includes many displaced upper bathyal and neritic indicators (K.M.).
V-657	Calcareous nannofossils: <i>Toweius</i> sp., <i>Discoaster multiradiatus</i> , <i>Ellipsolithus macellus</i> , <i>Fasciculithus tympaniformis</i> , <i>F. involutus</i> , <i>F. schaubi</i> , <i>Helicolithus kleinPELLI</i> , <i>Zygodiscus plectopons</i>	CP8		
	Benthic foraminifers: <i>Anomalina garzaensis</i> , <i>A. dorri aragonensis</i> , <i>Bulimina corrugata</i>	Laiming C	Upper to middle bathyal	
	Planktonic foraminifers: <i>Globorotalia aequa</i>	P6		
V-739	Benthic foraminifers: assemblage of >20 identifiable taxa (K.M.)	Late Paleocene (K.M.)	Middle bathyal	Specimens poorly preserved. Assemblage coeval with P4 to P6 (K.M.).
5/20/91H	Calcareous nannofossils: <i>Toweius</i> sp., <i>Coccolithus pelagicus</i> , <i>Fasciculithus tympaniformis</i> , <i>Discoaster nobilis</i> , <i>D. delicatus</i> , <i>D. mohleri</i> , <i>Chiasmolithus consuetus</i>	CP7		Specimens rare, poorly preserved.
5/20/91G	Calcareous nannofossils: <i>Toweius</i> sp., <i>Coccolithus pelagicus</i> , <i>Fasciculithus tympaniformis</i> , <i>Discoaster nobilis</i> , <i>D. delicatus</i>	CP7		Specimens rare, poorly preserved. Contains reworked specimens of Late Cretaceous <i>Micula staurophora</i> .
AAA80-1	Benthic foraminifers: <i>Bathysiphon</i> sp. cf. <i>B. vitta</i> , <i>B. varians</i> , <i>Trochammina</i> sp. cf. <i>T. boehmi</i> , <i>Silicosigmoilina californica</i> , <i>Spiroplectammina gryzbowskii</i>	Laiming E(?)		Sample collected and analyzed by A.A. Almgren.

densed(?) succession at Big Pine Mountain. This belt differs only in that it locally contains thin zones of limestone and variegated mudstone and is more than twice as thick, even though the lower part is truncated by the Big Pine fault.

## PARTLY CORRELATIVE SEQUENCES, SOUTHEASTERN SAN RAFAEL MOUNTAINS

### Upper Mono Creek—Upper Agua Caliente Canyon Area

About 12 km southeast of Big Pine Mountain on the south limb of Loma Pelona syncline near the juncture of Alamar Canyon and Mono Creek, lower Eocene mudstone at the base of the Juncal Formation rests without discordance on unnamed Upper Cretaceous mudstone and thin-bedded sandstone (Vedder and others, 1973), and the Sierra Blanca Limestone is absent (fig. 3, col. 6). In the bed of Mono Creek about 1.0 km east-northeast of The Narrows, the base of the Juncal is marked by a 0- to 10-cm-thick layer of poorly sorted, very fine to very coarse grained sandstone that includes abundant subangular pebbles of mudstone and rare rounded pebbles of limestone. A 10-m-thick sequence

of reddish and greenish silty claystone beds directly above the base contains Zone CP11 calcareous nannofossils, together with Zone P8 to lower P9 and pseudo-C Zone foraminifers (Bukry and others, 1977; R.L. Pierce, written commun., 1968; K.A. McDougall, written commun., 1993). Early to middle Eocene nannofossil and foraminiferal assemblages are present in the overlying 475 m of interbedded sandstone and mudstone in the Juncal Formation along this segment of Mono Creek.

The thin belt of reddish and greenish silty claystone in the lower part of the Juncal Formation is traceable for more than 10 km from the southeastern side of Sierra Blanca Mountain, where it overlies the Sierra Blanca Limestone, to the Munson Creek fault in Agua Caliente Canyon (figs. 1A, B). The limestone, however, lenses out about 3 km southeast of Sierra Blanca Mountain, and Paleocene mudstone beds similar to those along the south side of the Big Pine fault are not known to be present between Alamar Canyon and Agua Caliente Canyon. A foraminiferal assemblage from about 75 m below the base of the Juncal northeast of The Narrows in Mono Creek is assigned to Zones upper E to lower D-2 (late Campanian to early Maastrichtian) (R.L. Pierce, written commun., 1968; W.V. Sliter, written commun., 1992). Although there is no measurable discordance across the contact, a 15- to 20-m.y.

Table 4. Age-diagnostic taxa, zonation, and paleobathymetry of microfossils from upper Indian Creek and vicinity

[Localities shown in figures 6 and (or) 7C. Arranged stratigraphically from top to bottom. See table 1 for sources of data]

Field No.	Age-diagnostic and associated taxa	Age or zone	Paleobathymetry	Remarks
V-697	Calcareous nannofossils: <i>Discoaster lodoensis</i> , <i>Coccolithus crassus</i> , <i>C. pelagicus</i> , <i>C. formosus</i> , <i>C. gammaton</i> , <i>Chiasmolithus grandis</i> , <i>Zygrhablithus bijugatus</i> , <i>Sphenolithus radians</i> , <i>Discoaster kuepperi</i>	Probable CP11		Specimens rare, poorly preserved. Zone assignment questionable owing to uncertainty of first occurrence of <i>C. crassus</i> .
	Benthic foraminifers: <i>Anomalina dorri</i> , <i>Asterigina crassaformis</i> , <i>Marginulina asperuliformis</i>	Laiming C	Upper to middle bathyal	Sample from reddish and greenish mudstone zone similar to "Poppin shale" of local usage.
	Planktonic foraminifers: <i>Globorotalia aragonensis</i> , <i>G. caucasica</i> , <i>G. broedermanni</i> , <i>G. quetra</i>	P8 to P9		
V-696	Calcareous nannofossils: <i>Discoaster lodoensis</i> , <i>Coccolithus crassus</i> , <i>C. pelagicus</i> , <i>C. formosus</i> , <i>C. grammation</i> , <i>Chiasmolithus grandis</i> , <i>Zygrhablithus bijugatus</i> , <i>Sphenolithus radians</i> , <i>Discoaster kuepperi</i>	Probable CP11		Specimens rare, poorly preserved. Zone assignment questionable owing to uncertainty of first occurrence of <i>C. crassus</i> .
	Benthic foraminifers: <i>Anomalina dorri</i> , <i>Asterigina crassaformis</i> , <i>Marginulina asperuliformis</i>	Laiming C	Upper to middle bathyal	Sample from reddish and greenish mudstone zone similar to "Poppin shale" of local usage.
	Planktonic foraminifers: <i>Globorotalia aragonensis</i> , <i>G. caucasica</i> , <i>G. broedermanni</i> , <i>G. quetra</i>	P8 to P9		
V-695	Calcareous nannofossils: <i>Discoaster lodoensis</i> , <i>Coccolithus crassus</i> , <i>C. pelagicus</i> , <i>C. formosus</i> , <i>C. grammation</i> , <i>Chiasmolithus grandis</i> , <i>Zygrhablithus bijugatus</i> , <i>Sphenolithus radians</i> , <i>Discoaster kuepperi</i>	Probable CP11		
	Benthic foraminifers: <i>Anomalina dorri</i> , <i>Asterigina crassaformis</i> , <i>Marginulina asperuliformis</i>	Laiming C	Upper to middle bathyal	
	Planktonic foraminifers: <i>Globorotalia caucasica</i> , <i>G. aragonensis</i> , <i>G. subbotinae</i>	P8		Co-occurrence of <i>G. subbotinae</i> and <i>G. caucasica</i> suggests assignment to P8 rather than P8 to P9 as in V-696 and V-697.
5/20/91K	Calcareous nannofossils: <i>Coccolithus pelagicus</i> , <i>C. eopelagicus</i> , <i>C. formosus</i> , <i>C. grandis</i> , <i>Tribraehiatus orthostylus</i> , <i>Discoaster lodoensis</i> , <i>Zygrhablithus bijugatus</i> , <i>Sphenolithus radians</i> , <i>Rhabdosphaera rudis</i>	CP10		Specimens frequent, poorly preserved. Stratigraphic position uncertain.
	Benthic foraminifers: <i>Asterigerina crassaformis</i> , <i>Vulvulina curta</i>	Laiming C	Upper to middle bathyal	
	Planktonic foraminifers: <i>Globorotalia</i> sp. cf. <i>G. subbotinae</i> , <i>G. aragonensis</i>	P8		
V-706A	Calcareous nannofossils: <i>Chiasmolithus grandis</i> , <i>Coccolithus magnicrassus</i> , <i>Discoasteroides kuepperi</i> , <i>Tribraehiatus orthostylus</i>	CP10/CP11 (D.B.)		Specimens abundant, overgrown.
	Benthic foraminifers: large assemblage (>70 taxa) (K.M.)	Early Eocene (K.M.)	Lower bathyal (K.M.)	Includes planktonic taxa. Benthic assemblage equivalent to early P9 (K.M.).
V-737	Calcareous nannofossils: <i>Chiasmolithus grandis</i> , <i>Discoaster barbadiensis</i> , <i>Rhabdosphaera perlonga</i> , <i>Tribraehiatus orthostylus</i> (D.B.)	Early Eocene (D.B.)		
	Benthic foraminifers: large assemblage (>60 taxa) (K.M.)	Early Eocene (K.M.)	≥2,000 m (K.M.)	Includes abundant planktonic foraminifers. Benthic assemblage equivalent to P8 to P9 (K.M.).
V-738	Calcareous nannofossils: <i>Chiasmolithus grandis</i> , <i>Discoaster lodoensis</i> , <i>Cophodolitus nascens</i> (D.B.)	CP10 to CP12 (D.B.)		Poor flora.
	Benthic foraminifers: large assemblage (>45 taxa) (K.M.)	Late early Eocene (K.M.)	Lower bathyal (K.M.)	Includes abundant planktonic foraminifers. Benthic assemblage equivalent to early P9 (K.M.). Relative stratigraphic position uncertain.
V-694	Calcareous nannofossils: <i>Zygrhablithus bijugatus</i> , <i>Sphenolithus radians</i> , <i>Tribraehiatus orthostylus</i> , <i>Discoaster kuepperi</i> , <i>D. barbadiensis</i> , <i>Toweius</i> sp.	CP9		Specimens frequent, poorly preserved.
V-693	Calcareous nannofossils: <i>Micula staurophora</i>	Coniacian to Maastrichtian		Specimens rare, poorly preserved; includes unidentifiable placolith fragments.

interval of nondeposition and (or) erosion is indicated by the biostratigraphic evidence; and the lowermost part of the Juncal in Mono Creek north of the Hildreth and Munson Creek faults correlates with only the uppermost part of the condensed(?) succession at Big Pine Mountain.

### **Lower Mono Creek–Santa Ynez River Area**

About 20 to 25 km south of Big Pine Mountain near the Santa Ynez River, Campanian and older strata are disconformably overlain by shale and sandstone of the Juncal Formation, and here the Sierra Blanca Limestone has limited distribution (Page and others, 1951; Dibblee, 1966). According to Thompson (1988), the lowermost shale beds in the Juncal east of lower Agua Caliente Canyon contain Zone CP11 calcareous nannofossils and Zone P8 planktonic foraminifers, which suggest that a 20-m.y. hiatus separates the Campanian strata and the base of the Juncal Formation in that area, and beds coeval with most of the condensed(?) succession are absent. Moreover, Thompson (1988) reported redeposited Late Cretaceous and late Paleocene calcareous nannofossils in his study area, which suggests that strata of these ages were being eroded nearby during deposition of the Juncal.

Near the confluence of Mono Creek and the Santa Ynez River, the Sierra Blanca Limestone unconformably overlies Upper Jurassic to Lower Cretaceous strata; about 2.5 to 3.5 km to the southeast near the mouth of Agua Caliente Canyon, the limestone is unconformable on Upper Cretaceous strata. The Sierra Blanca Limestone in these two areas is early Eocene in age (Sliter and others, 1994; Whidden and others, 1995a).

## **PARTLY CORRELATIVE SEQUENCES, SOUTHWESTERN SAN RAFAEL MOUNTAINS**

### **Redrock Canyon–Oso Canyon area**

In the Redrock–Oso Canyon area about 20 km southwest of Big Pine Mountain (fig. 1A), lower Eocene strata on the south side of the Little Pine fault unconformably overlie the Franciscan Complex and were mapped as the Sierra Blanca Limestone and Juncal Formation by Dibblee (1966). Although biostratigraphic data from these units are incomplete, preliminary results suggest an age range of early to middle Eocene. Schussler (1981) reported long-ranging Zone P4 to P10 foraminifers from glauconitic mudstone in the fore-slope-talus limestone facies and Zone P9 and P10 assemblages from the lower part of the Juncal. Samples of limestone collected by K.J. Whidden in Oso Canyon contain Zone P7 to P8 and P9 to P10 planktonic foraminifers (W.V. Sliter, written commun., 1993; Whidden and others, 1995a). Accordingly, this sequence includes

beds that are the same age as the uppermost part of the condensed(?) succession at Big Pine Mountain.

### **Lazaro Canyon–Cachuma Creek area**

About 22 km west-southwest of Big Pine Mountain, Franciscan Complex rocks are depositionally overlain by a small tract of lower Eocene strata along the ridge that separates Lazaro Canyon and Cachuma Creek (figs. 1A, 1B). These strata were mapped as the Meganos Formation by Nelson (1925), who found orbitoid foraminifers, echinoids, and mollusks in limestone at the base. The same beds were mapped as Sierra Blanca Limestone and Juncal Formation by both Dibblee (1966) and Hall (1981), who showed them in a fault-bounded block within the Little Pine fault zone. Vedder and others (1991) reported orbitoid foraminifers from the limestone and early or middle Eocene planktonic foraminifers from mudstone beds estimated to be about 45 to 75 m upsection from the limestone. The age of these mudstone beds is here revised to latest early and earliest middle Eocene on the basis of recently collected samples that contain Zone CP11 or CP12a and CP12a to CP12b calcareous nannofossils. Thus, the highest sampled mudstone beds near Lazaro Canyon are slightly younger than the uppermost beds in the condensed(?) sequence at Big Pine Mountain and are partly correlative with beds that may be as much as 1,800 m upsection from the Paleocene limestone zones in the Bluff Campground area south of the Big Pine fault.

## **COMPARABLE SEQUENCES IN ADJACENT AREAS**

### **Upper Pine Creek Area**

Near upper Pine Creek about 30 km north-northeast of Santa Maria (fig. 1A inset), a limited exposure of lower Eocene mudstone on the southwest side of the Sur-Nacimiento fault zone apparently is unconformable on Upper Cretaceous beds (Vedder and others, 1991). Samples from the mudstone, which is less than 25 m thick, contain Zone CP9 calcareous nannofossils, Zone P6 to P8 planktonic foraminifers, and Zone C to D bathyal benthic foraminifers. The presence of these zones indicates a direct correlation of this mudstone unit with strata in the upper part (fig. 5 and table 1, V-648 and V-649, Zones CP9, P7, C) of the condensed(?) succession at Big Pine Mountain.

### **Western Santa Ynez Mountains**

Much of the Anita Shale of Kelley (1943) in the western Santa Ynez Mountains and adjacent offshore areas has lithogenetic and biostratigraphic aspects that are similar

to those of the condensed(?) succession at Big Pine Mountain. Descriptions by several workers (Kelley, 1943; Dibblee, 1950; Weaver, 1965; and Gibson, 1976) indicate that the Anita in its type area is about 300 m thick and consists largely of gray clayey mudstone and siltstone beds, some of which are tinted red and green. Limestone nodules, glauconitic zones, and thin sandstone beds are subordinate constituents that are only locally present. According to A.A. Almgren (written commun., 1993), limestone beds about 15 cm thick are present in the lower part in the type area. Biostratigraphic review and emendation of earlier work by Almgren and others (1988) showed that the Anita Shale includes benthic foraminifer Zones E, D, C, and pseudo-C and calcareous nannofossil Zones CP6 to CP13 and therefore ranges in age from late Paleocene into middle Eocene. Slow sedimentation rates in lower bathyal depths dominated the overall depositional environment (Almgren and others, 1988). About 15 km northeast of the type area, a 20-m thick limestone unconformably underlies the Anita and is assigned a late Paleocene age (Gibson, 1976; Whidden and others, 1995a).

Although microfossil assemblages in the Anita Shale are more diverse and better preserved than those in the condensed(?) succession, an unqualified correlation can be made between the lower part of the Anita and the upper part of the condensed(?) succession. Similarly, the belt of mudstone that borders the south side of the Big Pine fault closely matches the Anita, both biostratigraphically and lithologically.

## ORIGIN OF THE CONDENSED(?) SUCCESSION AT BIG PINE MOUNTAIN

Diminished sedimentation that characterizes condensed sequences commonly is attributed to the effects of eustatically controlled high-standing sea level or to deposition in mid-ocean environments. Less commonly, slow sedimentation is ascribed to blockage or diversion of the influx of terrestrial material. To explain the origin of the condensed(?) succession at Big Pine Mountain, several means of shutting off coarse clastic sedimentation need to be considered. Leading causes for condensed successions in general include the following:

- 1) Eustatic high stand of sea level,
- 2) Formation of tectonically generated barriers,
- 3) Planation or subsidence of the source terrane,
- 4) Diversion of sediment by changes in coastal morphology, or
- 5) Combinations of the above.

Global eustatic sea level curves show a generally high stand punctuated by short-term fluctuations during late Campanian through early Eocene time (Haq and others, 1987). The same curves indicate that the long-term oscillations during the same time interval were relatively subdued and that several major condensed sequences developed worldwide. The

origin of the sequence at Big Pine Mountain, however, may be attributable to causes other than protracted high sea level or stacking of sediment-starved units. Among such causes, likely contributors may have been barriers to sedimentation, diminishment of sediment sources, and redirected sediment-dispersal patterns. Despite the fact that evidence is incomplete for the size and configuration of Upper Cretaceous to lower Eocene basins in the San Rafael Mountains region, paleobathymetric data (table 1) imply that deposition in the basins took place mainly at mid-bathyal depths. Uncertainties about timing of tectonic events and undetermined completeness of the sedimentary record hinder confident interpretation of the history of the condensed(?) succession. Particularly frustrating for making such interpretations are the gaps in the biochronologic record, which may or may not signify episodes of nondeposition, erosion, or biota impoverishment.

## Precursory Events

On a regional scale, sediment dispersal that preceded deposition of the condensed(?) succession at Big Pine Mountain generally was westward and southward in a very large forearc submarine-fan system (Howell and others, 1977; Vedder and others, 1983), chiefly in bathyal environments. A noteworthy exception to the widespread, deep-water conditions are the paralic facies manifested in the narrow, 32-km-long belt that parallels the southwest side of the Sur-Nacimiento fault zone between South Fork La Brea Creek and Sweetwater Canyon (Vedder and others, 1977; 1983). Clast compositions in both the deep- and shallow-water environments suggest derivation from partly unroofed mid-Cretaceous batholithic rocks in the western Cordillera (Lee-Wong and Howell, 1977; Vedder and others, 1983). The relatively rapid rate of deposition of these submarine-fan and paralic strata contrasts sharply with the ensuing slow rate indicated by the condensed(?) succession at Big Pine Mountain (fig. 9) and the mudstone belt along the south side of the Big Pine fault.

Tectonic events that controlled these Late Cretaceous depositional systems are obscure. Suturing of the Stanley Mountain and Salinia Terranes presumably was underway or complete by early Maastrichtian time (Vedder and others, 1983; Howell and others, 1987). Local structures that may have been associated with such an event, however, have not been identified. Indeed, even the kinds of structures that may have developed as a result of this suturing are uncertain since the orientation of the travel paths of these terranes and the distances traveled are debatable. Because there is no evidence for a regional fold-and-thrust belt, orthogonal approach and collision are doubtful. Low-oblique or subparallel travel paths and development of transpressional and (or) transtensional structures upon conjunction are in better accord with dextral-oblique plate convergence and accompanying strike-slip tectonics that were operative near the end of Cretaceous time (Page and Engebretson, 1984; Stewart and Crowell, 1992).

## Contributory Factors

The prolonged period of diminished sedimentation at Big Pine Mountain may have resulted from a single event or a combination of events. Likely causative circumstances include uplift of an intervening submarine barrier ridge in concert with planation or subsidence of the source terrane. Ancillary factors may have involved long-term sediment diversion by changes in the submarine-fan dispersal system without a barrier ridge or tectonic extension and consequent formation of borderland-like topography. Although global sea level was relatively high between 75 and 52 Ma, this long-term high stand may have had little additional influence on the suddenly reduced influx of sediment during that time. Processes accompanying terrane accretion, plate-motion change, and subduc-

tion-angle variation may have contributed to the aforementioned causes, but discussion of the effects of plate reorientation and terrane conjoinment are beyond the scope of this paper.

Evidence is lacking not only for the size and shape of the supposed barrier ridge but also its geographic position. Any such site to the north or northeast presumably was translocated by post-middle(?) Eocene strike-slip movement on the Sur-Nacimiento fault zone. However, the history, direction, and amount of slip along this fault zone are uncertain.

Late Paleocene uplift just before and during deposition of the Sierra Blanca Limestone in the Grapevine Creek-upper Indian Creek area is indicated by northward downslope transport of allochemical detritus derived from algal-bank deposits that lay directly to the south but are now completely eroded. An unconformity at the base of lower Eocene limestone near

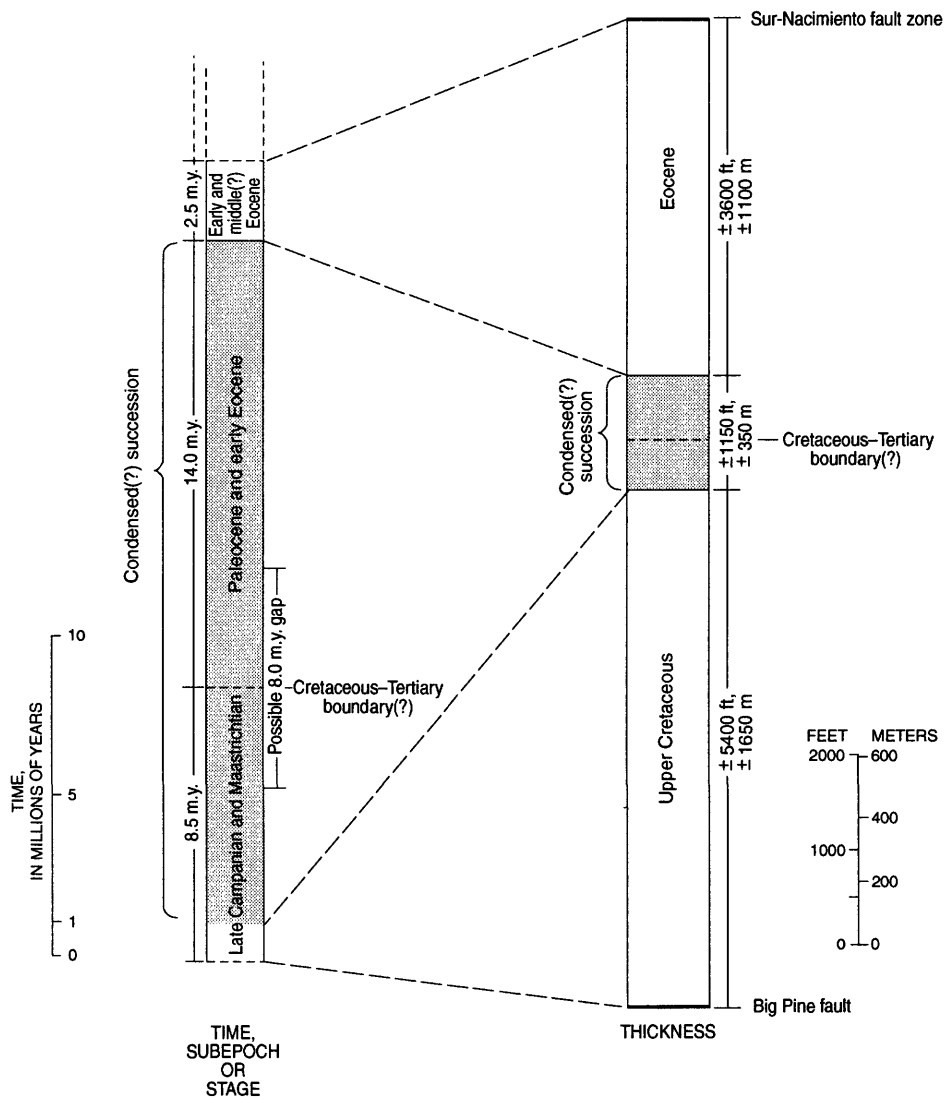


**Figure 9.** Diagram comparing time of deposition and thickness of strata in vicinity of Big Pine Mountain. Shaded segments represent the condensed(?) succession of mudstone (map unit TKu, fig. 4; fig. 5).

the Santa Ynez River east of Gibraltar Reservoir substantiates a later phase of local uplift (Johnson, 1968; Schroeter, 1972, Comstock, 1976; Whidden and others, 1995a). Additional evidence for local uplift is the presence of abundant Franciscan detritus in the lower Eocene limestone in the Redrock Canyon-Oso Canyon area (Schussler, 1981) and Lazaro Canyon-Cachuma Creek area (Vedder and others, 1983), where the limestone was deposited directly on the Franciscan Complex. Because these uplift events began after initial development of the condensed(?) succession at Big Pine Mountain, they may have had little effect on reduced sedimentation there. Reed and Hollister's (1936) San Rafael uplift, a hypothetical Paleogene structural high to the west and south, may have affected depositional patterns in late early and middle Eocene time (Thompson, 1988), but this feature may not have culminated until Oligocene time (Vedder and others, 1991). Late Cretaceous, Paleocene, and Eocene events together with their effects and evidence for them are summarized in figure 10.

In the San Rafael Mountains, Late Cretaceous and early Paleogene shorelines, insular platforms, and submarine ridges are represented only by small remnants or are not preserved. Consequently, a borderland-like configuration of basins and ridges cannot be fully ascertained. Highly generalized, regional paleogeographic reconstructions (Howell, 1975; Nilsen and Clarke, 1975; Nilsen, 1987), however, indicate that Paleocene and Eocene borderland features were present. Although fault-bounded ridges of this age have not been identified, precursors of the Little Pine and Camuesa faults (fig. 1B) may have created such a ridge. It is significant that pre-middle Eocene folding occurred in areas north of the Santa Ynez fault (Page and others, 1951). Such local upwarping and downwarping rather than faulting would better explain a basin-and-ridge setting and would be comparable to the larger anticlinal welts that form the Santa Rosa-Cortes Ridge west of Santa Cruz and San Nicolas Basins on the modern southern California borderland. Moreover, oblique subduction, regional wrenching, and disassembly of the Late Cretaceous forearc basin (Vedder and others, 1983; Nilsen, 1987) were conducive to development of borderland-like morphology. Barriers to sedimentation are commonplace on the modern borderland (Gorsline, 1990). A similar setting (fig. 11), therefore, is considered plausible for the depositional environments in the San Rafael Mountains region during latest Cretaceous and earliest Tertiary time.

### Subsequent Events

The lower and middle(?) Eocene submarine-fan deposits that overlie the condensed(?) succession at Big Pine Mountain signify renewed rapid sedimentation (fig. 10). The largely coarse-clastic sequence that lies north and east of Big Pine Mountain is truncated by the Sur-Nacimiento and Big Pine fault zones, which converge to restrict the lateral extent and vertical succession of these strata. As a result, interpretations

of depositional environments within this tract are hampered by incomplete distributional and stratigraphic data. If not tectonically rotated, the few directional features examined suggest westward and southward paleocurrent flow. Because the age of the upper part of this fault-truncated sequence is not known, duration of sedimentation is questionable (fig. 9). At least the lower 600 m of the 1,200-m-thick section was deposited in late early and early middle(?) Eocene time, and the entire sequence may represent a span of time as short as 5.0 m.y. Even though waning tectonism and regional lowering of relief may have begun early in the Eocene (Howell and others, 1987), the sandstone unit that lies north and east of Big Pine Mountain presumably was derived from a relict high-standing area northeast of the Sur-Nacimiento fault zone. According to Haq and others (1987), eustatic sea level dropped abruptly between 49.5 Ma and 49.0 Ma. This event may have been partly responsible for the renewed episode of rapid sedimentation, but the global occurrence of such a low stand has been challenged by Miall (1993).

South of the Big Pine fault, subsea-fan deposits are present in the lower part of a regionally extensive remnant of an Eocene forearc basin (Nilsen and Clarke, 1975; Howell, 1975; Thompson, 1988). Within this basin remnant, lower and middle Eocene strata are preserved eastward from East Fork Santa Cruz Creek to Mono Creek and beyond. These strata consist mainly of sandstone and subordinate interbedded mudstone that conformably overlie the Upper Cretaceous to lower Eocene mudstone belt that lies along the south side of the fault. Throughout the southeastern San Rafael Mountains, the largely coarse-clastic lower and middle Eocene beds are customarily assigned to the Juncal Formation (Page and others, 1951; Dibblee, 1966; Vedder, 1972; Vedder and others, 1973).

Post-Oligocene rotations of small crustal blocks in the western Transverse Ranges (Hornafius and others, 1986; Luyendyk, 1991) also may have occurred in the parts of the San Rafael Mountains in which the condensed(?) succession and mudstone belt are present. Recently acquired paleomagnetic data from an area north of the Santa Ynez fault just east of figures 1A and 1B suggest a clockwise rotation of 70° to 90° (Whidden and others, 1993, 1995b). Because the extent, direction, and amount of late Cenozoic rotations are incompletely known, the original orientation of sediment flow in older strata is uncertain. As measured now, regional sediment-transport directions during the Eocene were largely southwestward and westward (Howell, 1975; Nilsen, 1987). Locally, however, transport may have been northward (Comstock, 1975, fig. 7; J.G. Vedder, Hugh McLean, and R.G. Stanley, unpub. data, 1984, 1992–93). Although based upon a limited number of measurements, chiefly in sandstone turbidites, this local northward transport is supportive evidence for the presence of short-lived, actively eroding submarine ridges or banks farther south. Biostratigraphic analyses of samples from outcrops along Big Pine Road on the north limb of Loma Pelona syncline (figs. 6, 7B) suggest that the approximately 1,500-m-thick chiefly sandstone sequence there has a short age range

Time (Ma)		Event	Effects and evidence	Record at Big Pine Mountain	
				Lithostratigraphy	Biostratigraphy
Eocene	Middle	Continuing regional uplift and erosion of granitoid plutons north and east of study area.	Prevailing bathyal deposition of predominantly coarse-clastic submarine-fan sequences northeast of Big Pine Mountain and along trough of Loma Pelona syncline. Sandstone quartzofeldspathic.		
	52.0	Renewed regional uplift and erosion of granitoid plutons north and east of study area. Widespread uplift to south and west (incipient San Rafael uplift?).	Abrupt change from slow bathyal-abyssal sedimentation to accelerated rates in submarine-fan complex. Sharp contact between mudstone sequence and quartzofeldspathic sandstone/conglomerate sequence at Big Pine Mountain. Similar, less abrupt change from mudstone to sandstone along north limb of Loma Pelona syncline.  Unconformity at base of "Poppin shale" of local usage on south limb of Loma Pelona syncline; continuous deposition on north limb. Unconformity at base of Juncal Formation throughout southeastern San Rafael Mountains. Franciscan detritus in Eocene limestone south and west of study area.		
	Early				
Paleocene	57.8	Dwindling growth of submarine barrier ridge north or east of study area. Local sea floor upwarps south of Loma Pelona syncline.	Prevailing slow, deep-water deposition of hemipelagic mudstone at Big Pine Mountain. Unconformity at base of Sierra Blanca Limestone on south limb of Loma Pelona syncline; continuous deposition of hemipelagic mudstone and interbedded limestone on north limb. Algal-bank development on structural highs south of Loma Pelona syncline accompanied by northward downslope transport of algal detritus. Evolving borderland-like sea floor morphology.		
	62.3				
	Early	Culmination of growth of submarine barrier ridge accompanied by curtailment of sedimentation to the south and west.	Very slow sedimentation rates or hiatus(?). Biostratigraphic record absent. Lithostratigraphic evidence suggests continued hemipelagic deposition in sediment-starved basin at Big Pine Mountain.		?
Late Cretaceous	66.4	Incipient uplift of fault-bounded(?) submarine ridge between eroding plutons and northern part of study area to form growing barrier to sedimentation.	Diminishing sediment supply. Sharp contact between sandstone turbidites and massive mudstone at Big Pine Mountain.	?	
	Ca. 75.0	Continuing uplift and erosional unroofing of granitoid plutons north and east of study area. Persisting regional forearc basin remaining from Cenomanian-Campanian precursor.	Rapid bathyal sedimentation in regional coalescing submarine-fan system. Widespread deposition of quartzofeldspathic sandstone and granitoid/siliceous metavolcanic pebble-boulder conglomerate.		?

**Figure 10.** Chronology of events and geologic evidence for Late Cretaceous, Paleocene, and Eocene tectonism in San Rafael Mountains. Estimated ages of boundaries from Berggren and others (1985). Named topographic and structural features used only as geographic reference points and should not be construed as being present at time designated. If future work demonstrates late Cenozoic tectonic rotations, sediment transport directions must be revised accordingly.

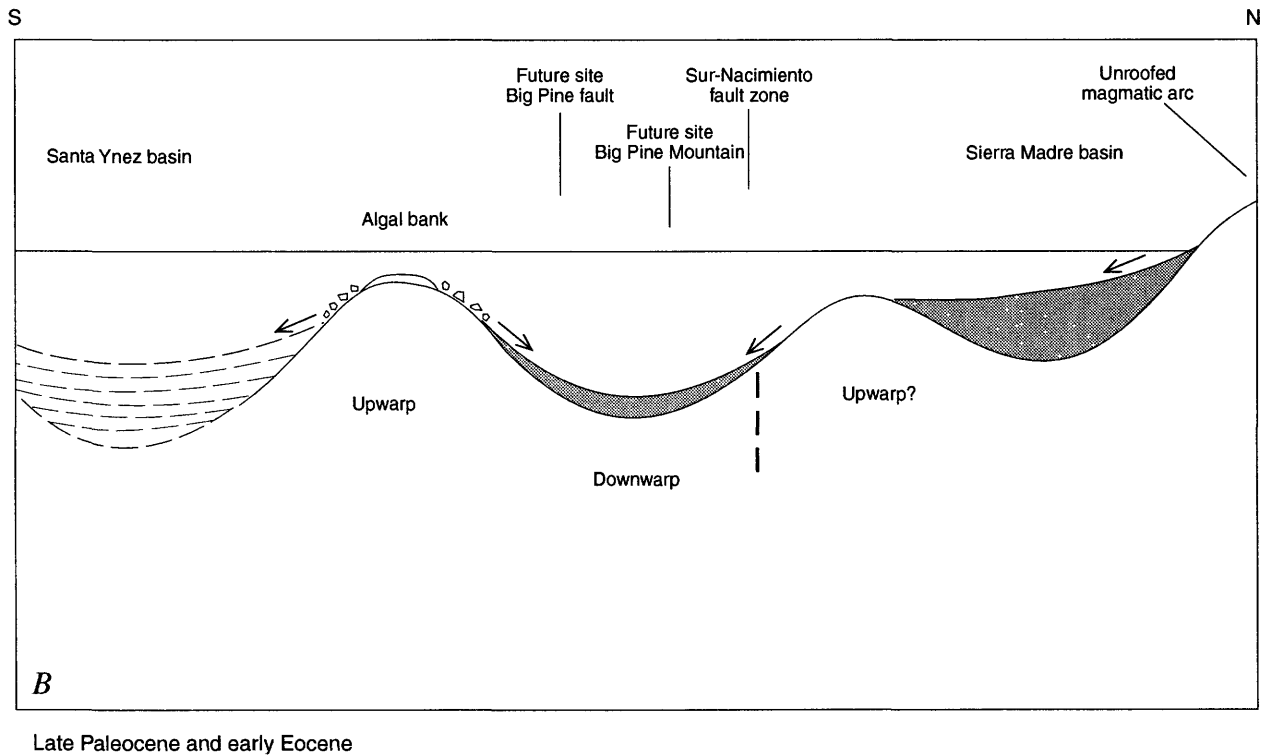
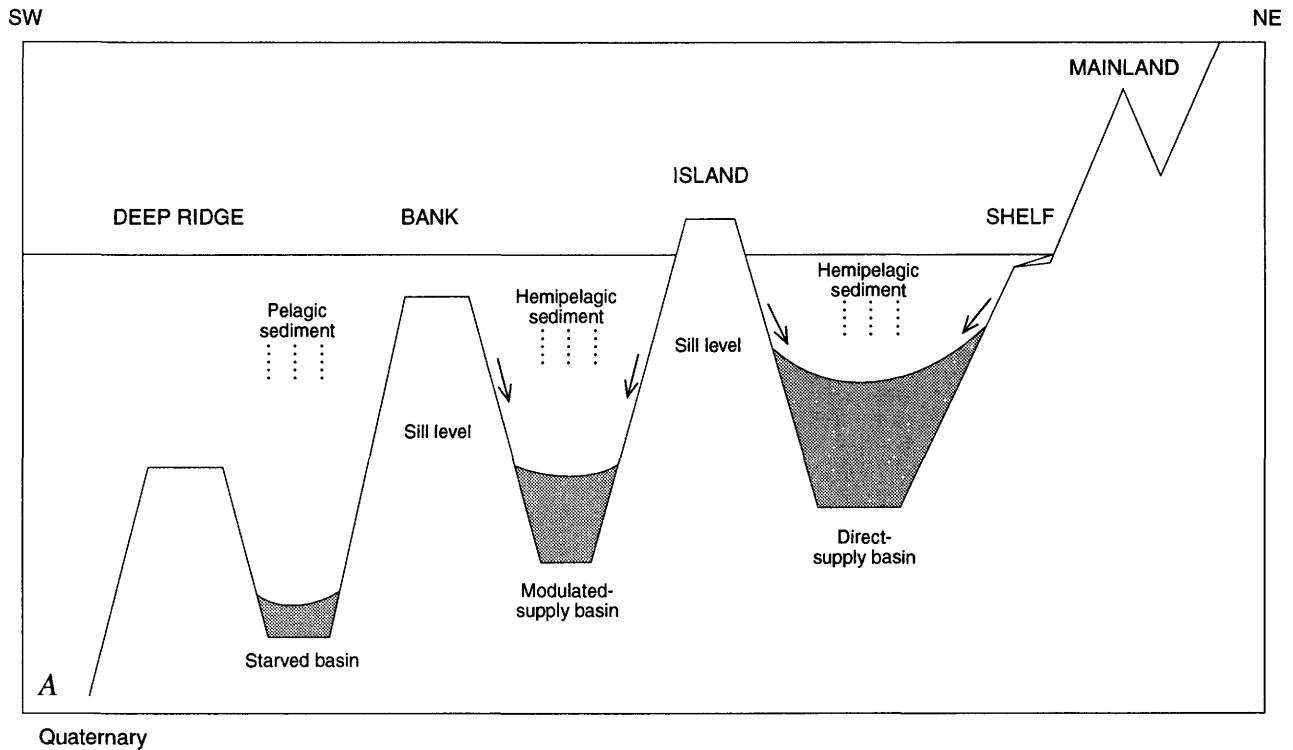


**Figure 11.** Schematic diagrams of tectonic barriers to sedimentation. *A*, Quaternary, California Continental Borderland (modified from Gorsline, 1990); *B*, Paleocene and early Eocene borderland, San Rafael Mountains area.

within the late early to earliest middle Eocene (CP10/11 into CP12a) (table 2), perhaps as short as 3.0 m.y.

## CONCLUSIONS

Available biostratigraphic data indicate that the 350-m-thick mudstone unit near the crest of Big Pine Mountain possibly is a condensed succession that ranges in age from latest Cretaceous (late Campanian or Maastrichtian) into earliest Tertiary (early Eocene). Elapsed time of accumulation may have been as long as 22 m.y. Even though the position of time boundaries within the succession are poorly constrained and the presence or absence of the Danian Stage has not been determined, physical evidence for stratigraphic discontinuities are not apparent. Pre-late Paleocene and early Eocene erosional events in neighboring areas, however, cannot be disregarded; for these events may have influenced depositional continuity in the mudstone succession at Big Pine Mountain. Ostensibly, the exceptionally long duration of sedimentation in bathyal depths suggests that this possible condensed succession resulted from the tectonic development of a barrier ridge (or system of ridges) rather than from a long-term stand of eustatic high sea level. Perplexing uncertainties about the origin, site, and fate of such a barrier remain. Strike-slip tectonism accompanying oblique subduction and terrane accretion near the end of the Cretaceous, when the Stanley Mountain terrane presumably was juxtaposed against the Salinia terrane, may have been partly responsible for inception of the barrier. Barring large amounts of late Cenozoic tectonic rotation, southwestward sediment-transport directions in the enclosing strata imply that the intervening ridge lay to the northeast. Movement along the ancestral Sur-Nacimiento fault near the end of the early Eocene may have translocated the barrier so that it no longer effectively blocked rapid sedimentation.

The belt of mudstone that flanks the south side of the Big Pine fault is the same age as the condensed(?) succession at Big Pine Mountain. Despite the presence of limestone lenses, greater thickness, and indication of local northward sediment transport, the mudstone belt south of the fault is believed to be a lateral equivalent of the condensed(?) succession on Big Pine Mountain but represents a shallower facies on the flank of the same sediment-starved basin. Restoration of about 14 km of left-lateral strike slip along the Big Pine fault would place the direct counterpart of the condensed(?) succession east of upper Mono Creek, where the mudstone beds presumably are concealed beneath middle Eocene and younger strata. Because at least two different high-standing areas were contributing detritus to the basin south of the present site of the fault during the late Paleocene and early to middle Eocene, a borderland-like paleogeographic setting seems to be a reasonable inference. If the late Paleocene to middle Eocene Anita Shale in the western Santa Ynez Mountains is considered to be a separate basin entity, and if the San Rafael high began to develop at the same time, borderland topography in the Santa

Maria-Santa Barbara region was more extensive and complex in early Paleogene time than heretofore supposed.

## REFERENCES CITED

- Almgren, A.A., 1986, Benthic foraminiferal zonation and correlations of Upper Cretaceous strata of the Great Valley of California—a modification, *in* Abbott, P.L., ed., *Cretaceous stratigraphy, western North America: Society of Economic Paleontologists and Mineralogists, Pacific Section*, p. 137–152.
- Almgren, A.A., Filewicz, M.V., and Heitman, H.L., 1988, Lower Tertiary foraminiferal and calcareous nannofossil zonation of California: an overview and recommendation, *in* Filewicz, M.V., and Squires, R.L., eds., *Paleogene stratigraphy, West Coast Paleogene symposium: Society of Economic Paleontologists and Mineralogists, Pacific Section*, v. 58, p. 83–105.
- Bates, R.L., and Jackson, J.A., eds., 1987, *Glossary of Geology* (3d ed.): Falls Church, Va., American Geological Institute, 749 p.
- Berggren, W.A., Kent, D.V., Flynn, J.J., and Van Couvering, J.A., 1985, *Cenozoic geochronology: Geological Society of America Bulletin*, v. 96, no. 11, p. 1407–1418.
- Blake, M.C., Jr., Howell, D.G., and Jones, D.L., 1982, Preliminary tectonostratigraphic terrane map of California: U.S. Geological Survey Open-File Report 82–593, 10 p., scale 1:500,000, 3 map sheets.
- Blow, W.H., 1969, Late middle Eocene to Recent planktonic foraminiferal biostratigraphy, *in* Brönnimann, R., and Renz, H.H., eds., *Proceedings of the International Conference on Planktonic Microfossils*, 1st, Geneva, 1967, v. 1: Leiden, E.J. Brill, p. 199–421.
- Bukry, David, Brabb, E.E., and Vedder, J.G., 1977, Correlation of Tertiary nannoplankton assemblages from the Coast and Peninsular Ranges of California, *in* *Memoria Segundo Congreso Latinoamericano de Geologia, Caracas, Venezuela, November 11–16, 1973: Venezuela Boletín de Geologia Publicacion Especial*, no. 7, v. 3, p. 1461–1483.
- Carman, M.F., 1964, *Geology of the Lockwood Valley area, Kern and Ventura Counties, California: California Division of Mines and Geology Special Report 81*, 62 p.
- Comstock, S.C., 1975, Upper Cretaceous and Paleocene stratigraphy along the western Big Pine fault, Santa Barbara County, California, *in* Weaver, D.W., Hornaday, G.R., and Tipton, Ann, eds., *Paleogene symposium and selected technical papers, Conference on Future Energy Horizons of the Pacific Coast, Long Beach, Calif., April 1975: American Association of Petroleum Geologists—Society of Economic Paleontologists and Mineralogists—Society of Exploration Geophysicists, Pacific Sections*, p. 155–168.
- , 1976, *Stratigraphy and structure along the western Big Pine fault, Santa Barbara County, California: Santa Barbara, University of California, M.S. thesis*, 102 p.
- Crowell, J.C., 1962, Displacement along the San Andreas fault, California: *Geological Society of America Special Paper 71*, 61 p.
- Dibblee, T.W., Jr., 1950, *Geology of southwestern Santa Barbara County, California: California Division of Mines Bulletin 150*, 95 p.
- , 1966, *Geology of the Central Santa Ynez Mountains, Santa Barbara County, California: California Division of Mines and Geology Bulletin 186*, 99 p.

- 1973, Regional geologic map of San Andreas and related faults in Carrizo Plain, Temblor, Caliente, and La Panza Ranges and vicinity, California: U.S. Geological Survey Miscellaneous Geologic Investigations Map I-757, scale 1:125,000.
- 1976, The Rinconada and related faults in the southern Coast Ranges, California, and their tectonic significance: U.S. Geological Survey Professional Paper 981, 55 p.
- Dickinson, W.R., 1983, Cretaceous sinistral slip along Nacimiento fault in coastal California: American Association of Petroleum Geologists Bulletin, v. 67, no. 4, p. 624–645.
- Dickinson, W.R., and Lowe, D.R., 1966, Stratigraphic relations of phosphate- and gypsum-bearing upper Miocene strata, upper Sespe Creek, Ventura County, California: American Association of Petroleum Geologists Bulletin, v. 50, no. 11, p. 2464–2481.
- Fairbanks, H.W., 1894, Geology of the northern Ventura, Santa Barbara, San Luis Obispo, Monterey and San Benito Counties: Report of the State Mineralogist, 12th, California, 36 p.
- Fritsche, A.E., and Shmitka, R.O., 1978, Introduction to a field trip along upper Sespe Creek, Ventura County, California, with comments on Tertiary stratigraphy of the area, in Fritsche, A.E., ed., Depositional environments of Tertiary rocks along Sespe Creek, Ventura County, California: Society of Economic Paleontologists and Mineralogists, Pacific Section, Pacific Coast Paleogeography Field Guide 3, p. 1–5.
- Gibson, J.M., 1976, Distribution of planktonic foraminifera and calcareous nannoplankton, Late Cretaceous and early Paleogene, Santa Ynez Mountains, California: Journal of Foraminiferal Research, v. 6, no. 2, p. 87–106.
- Gorsline, D.S., 1990, Controls on deep-marine sedimentation, in Brown, G.C., Gorsline, D.S., and Schweller, W.J., eds., Deep-marine sedimentation: depositional models and case histories in hydrocarbon exploration and development: SEPM (Society for Sedimentary Geology), Pacific Section, p. 23–51.
- Goudkoff, P.P., 1945, Stratigraphic relations of Upper Cretaceous in the Great Valley, California: American Association of Petroleum Geologists Bulletin, v. 29, no. 7, p. 956–1007.
- Gower, H.D., and others, 1966, Mineral resources of the San Rafael Primitive Area, California: U.S. Geological Survey Bulletin 1230-A, 28 p.
- Hall, C.A., Jr., 1981, Map of geology along the Little Pine fault, parts of the Sisquoc, Foxen Canyon, Zaca Lake, Bald Mountain, Los Olivos, and Figueroa Mountain quadrangles, Santa Barbara County, California: U.S. Geological Survey Miscellaneous Field Studies Map MF-1285, scale 1:24,000.
- Haq, B.U., Hardenbol, J., and Vail, P.R., 1987, Chronology of fluctuating sea levels since the Triassic: Science, v. 235, p. 1156–1167.
- Hedgpeth, J.W., 1957, Classification of marine environments, in Hedgpeth, J.W., ed., Treatise on marine ecology and paleoecology: Geological Society of America Memoir 67, v. 1, p. 17–27.
- Hill, M.L., and Dibblee, T.W., Jr., 1953, San Andreas, Garlock, and Big Pine faults, California—a study of the character, history, and tectonic significance of their displacements: Geological Society of America Bulletin, v. 64, no. 4, p. 443–458.
- Hornafius, J.S., Luyendyk, B.P., Terres, R.R., and Kamerling, M.J., 1986, Timing and extent of Neogene tectonic rotation in the western Transverse Ranges, California: Geological Society of America Bulletin, v. 97, no. 12, p. 1476–1487.
- Howell, D.G., 1975, Middle Eocene paleogeography of southern California, in Weaver, D.W., Hornaday, G.R., and Tipton, Ann, eds., Paleogene symposium and selected technical papers, Conference on Future Energy Horizons of the Pacific Coast, Long Beach, Calif., April 1975: American Association of Petroleum Geologists—Society of Economic Paleontologists and Mineralogists—Society of Exploration Geophysicists, Pacific Sections, p. 272–293.
- Howell, D.G., Champion, D.E., and Vedder, J.G., 1987, Terrane accretion, crustal kinematics, and basin evolution, southern California, in Ingersoll, R.V., and Ernst, W.G., eds., Cenozoic basin development of coastal California, Rubey Volume 6: Englewood Cliffs, N.J., Prentice-Hall, p. 242–258.
- Howell, D.G., Vedder, J.G., McLean, Hugh, Joyce, J.M., Clarke, S.H., Jr., and Smith, Greg, 1977, Review of Cretaceous geology, Salinian and Nacimiento blocks, Coast Ranges of California, in Howell, D.G., Vedder, J.G., and McDougall, K.A., eds., Cretaceous geology of the California Coast Ranges, west of the San Andreas fault: Society of Economic Paleontologists and Mineralogists, Pacific Section, Pacific Coast Paleogeography Field Guide 2, p. 1–46.
- Ingle, J.C., Jr., 1975, Paleocologic indicators and trace fossils, in Dickinson, W.R., ed., Current concepts of depositional systems with applications for petroleum geology: Bakersfield, Calif., San Joaquin Geological Society Short Course Lecture Syllabus, p. 8–1 to 11–12.
- Johnson, C.J., 1968, Petrography and paleoecology of the Sierra Blanca Limestone, California: Riverside, University of California, M.S. thesis, 42 p.
- Keenan, M.F., 1932, The Eocene Sierra Blanca limestone at the type locality in Santa Barbara County, California: Transactions of the San Diego Society of Natural History, v. 7, no. 8, p. 57–84.
- Kelley, F.R., 1943, Eocene stratigraphy in western Santa Ynez Mountains, Santa Barbara County, California: American Association of Petroleum Geologists, v. 7, no. 1, p. 1–19.
- Laiming, B., 1939, Some foraminiferal correlations in the Eocene of the San Joaquin Valley, California: Pacific Science Congress, 6th, Proceedings, v. 2, p. 535–568.
- Lee-Wong, Florence, and Howell, D.G., 1977, Petrography of Upper Cretaceous sandstone in the Coast Ranges of central California, in Howell, D.G., Vedder, J.G., and McDougall, K.A., eds., Cretaceous geology of the California Coast Ranges, west of the San Andreas fault: Society of Economic Paleontologists and Mineralogists, Pacific Section, Pacific Coast Paleogeography Field Guide 2, p. 47–55.
- Luyendyk, B.P., 1991, A model for Neogene crustal rotations, transtension, and transpression, in southern California: Geological Society of America Bulletin, v. 103, no. 11, p. 1528–1536.
- MacKinnon, T.C., 1978, The Great Valley sequence near Santa Barbara, California, in Howell, D.G., and McDougall, K.A., eds., Mesozoic paleogeography of the western United States: Society of Economic Paleontologists and Mineralogists, Pacific Section, Pacific Coast Paleogeography Symposium 2, p. 483–491.
- Miall, A.D., 1993, Exxon global cycle chart: an event for every occasion?: Reply: Geology, v. 21, no. 3, p. 284–285.
- Nelson, R.N., 1925, Geology of the hydrographic basin of the upper Santa Ynez River, California: University of California Publications in Geological Sciences, v. 15, no. 10, p. 327–396.
- Nilsen, T.H., 1987, Paleogene tectonics and sedimentation of coastal California, in Ingersoll, R.V., and Ernst, W.G., eds., Cenozoic basin development of coastal California, Rubey Volume 6: Englewood Cliffs, N.J., Prentice-Hall, p. 81–123.

- Nilsen, T.H., and Clarke, S.H., Jr., 1975, Sedimentation and tectonics in the early Tertiary continental borderland of central California: U.S. Geological Survey Professional Paper 925, 64 p.
- Okada, Hisatake, and Bukry, David, 1980, Supplementary modification and introduction of code numbers to the low-latitude coccolith biostratigraphic zonation (Bukry, 1973, 1975): *Marine Micropaleontology*, v. 5, p. 321–325.
- Page, B.M., 1970, Sur-Nacimiento fault zone of California: continental margin tectonics: *Geological Society of America Bulletin*, v. 81, no. 3, p. 667–690.
- Page, B.M., and Engebretson, D.C., 1984, Correlation between the geologic record and computed plate motions for central California: *Tectonics*, v. 3, no. 2, p. 133–155.
- Page, B.M., Marks, J.G., and Walker, G.W., 1951, Stratigraphy and structure of mountains northeast of Santa Barbara, California: *Bulletin of the American Association of Petroleum Geologists*, v. 35, no. 8, p. 1727–1780.
- Reed, R.D., and Hollister, J.S., 1936, Structural evolution of southern California: Tulsa, Okla., American Association of Petroleum Geologists, 157 p.
- Ricci-Lucchi, F., 1975, Depositional cycles in two turbidite formations of northern Apennines (Italy): *Journal of Sedimentary Petrology*, v. 45, no. 1, p. 3–43.
- Robertson, A.H.F., 1989, Palaeoceanography and tectonic setting of the Jurassic Coast Range ophiolite, central California: evidence from the extrusive rocks and the volcanoclastic sediment cover: *Marine and Petroleum Geology*, v. 6, no. 3, p. 194–220.
- Saul, L.E., 1983, Turritella zonation across the Cretaceous-Tertiary boundary, California: Berkeley and Los Angeles, Calif., University of California Publications in Geological Sciences, v. 125, 164 p.
- 1986, Mollusks of latest Cretaceous and Paleocene age, Lake Nacimiento, California, in Grove, K. and Graham, S.A., *Geology of Upper Cretaceous and lower Tertiary rocks near Lake Nacimiento, California*: Society of Economic Paleontologists and Mineralogists, Pacific Section, p. 25–31.
- Schroeter, C.E., 1972, Local paleogeography of the Sierra Blanca Limestone (Eocene), in Weaver, D.W., ed., *Central Santa Ynez Mountains, Santa Barbara County, California*: American Association of Petroleum Geologists—Society of Economic Paleontologists and Mineralogists, Pacific Sections, Guidebook, p. 20–29.
- Schussler, S.A., 1981, Paleogene and Franciscan Complex stratigraphy, southwestern San Rafael Mountains, Santa Barbara County, California: Santa Barbara, University of California, M.A. thesis, 235 p.
- Sliter, W.V., McDougall, K.A., Vedder, J.G., and Whidden, K.J., 1994, Age and depositional history of Paleogene shallow-water limestone in the western Transverse Ranges [abs.]: *Geological Society of America Abstracts with Programs, Cordilleran Section*, v. 26, no. 2, p. 92.
- Squires, R.L., 1988, Geologic age refinements of west coast Eocene marine mollusks, in Filewicz, M.V., and Squires, R.L., eds., *Paleogene stratigraphy, west coast of North America*: Society of Economic Paleontologists and Mineralogists, Pacific Section, v. 58, p. 107–112.
- Stewart, J.H., and Crowell, J.C., 1992, Strike-slip tectonics in the Cordilleran region of the western United States, in Burchfiel, B.C., Lipman, P.W., and Zoback, M.L., eds., *The Cordilleran Orogen: conterminous U.S.*, v. G-3 of *The geology of North America*: Boulder, Colo., Geological Society of America, p. 609–628.
- Thompson, T.J., 1988, Outer-fan lobes of the lower to middle Eocene Juncal Formation, San Rafael Mountains, California, in Filewicz, M.V., and Squires, R.L., eds., *Paleogene stratigraphy, west coast of North America*: Society of Economic Paleontologists and Mineralogists, Pacific Section, v. 58, p. 113–127.
- Toumarkine, M., and Luterbacher, H., 1985, Paleocene and Eocene planktic foraminifera, in Bolli, H.M., Saunders, J.B., and Perch-Nielsen, K.E., eds., *Plankton stratigraphy*: Cambridge, U.K., Cambridge University Press, p. 87–154.
- Vedder, J.G., 1972, Revision of stratigraphic names for some Eocene formations in Santa Barbara and Ventura Counties, California: U.S. Geological Survey Bulletin 1354-D, p. D1–D12.
- Vedder, J.G., and Brown, R.D., Jr., 1968, Structural and stratigraphic relations along the Nacimiento fault in the southern Santa Lucia Range and San Rafael Mountains, California, in Dickinson, W.R., and Grantz, Arthur, eds., *Conference on Geologic Problems of San Andreas Fault System, Proceedings*: Stanford, Calif., Stanford University Publications in Geological Sciences, v. 11, p. 242–259.
- Vedder, J.G., Dibblee, T.W., Jr., and Brown, R.D., Jr., 1973, Geologic map of the upper Mono Creek-Pine Mountain area, California, showing rock units and structures offset by the Big Pine fault: U.S. Geological Survey Miscellaneous Geologic Investigations Map I-752, scale 1:48,000.
- Vedder, J.G., Gower, H.D., Clifton, H.E., and Durham, D.L., 1967, Reconnaissance geologic map of the central San Rafael Mountains and vicinity, Santa Barbara County, California: U.S. Geological Survey Miscellaneous Geologic Investigations Map I-487, scale 1:48,000.
- Vedder, J.G., Howell, D.G., and McLean, Hugh, 1977, Upper Cretaceous redbeds in the Sierra Madre-San Rafael Mountains, California, in Howell, D.G., Vedder, J.G., and McDougall, K.A., eds., *Cretaceous geology of the California Coast Ranges, west of the San Andreas fault*: Society of Economic Paleontologists and Mineralogists, Pacific Section, Pacific Coast Paleogeography Field Guide 2, p. 71–78.
- 1983, Stratigraphy, sedimentation, and tectonic accretion of exotic terranes, southern Coast Ranges, California, in Watkins, J.S., and Drake, C.L., eds., *Studies in continental margin geology*: American Association of Petroleum Geologists Memoir 34, p. 471–496.
- Vedder, J.G., McLean, Hugh, and Stanley, R.G., 1994, New 1:24,000-scale geologic maps show stratigraphic and structural relations that require reinterpretation of Cretaceous and Cenozoic tectonic events in the Sierra Madre-San Rafael Mountains area, California [abs.]: *Geological Society of America Abstracts with Programs, Cordilleran Section*, v. 26, no. 2, p. 100–101.
- Vedder, J.G., McLean, Hugh, Stanley, R.G., and Wiley, T.J., 1991, Paleogeographic implications of an erosional remnant of Paleogene rocks southwest of the Sur-Nacimiento fault zone, southern Coast Ranges, California: *Geological Society of America Bulletin*, v. 103, no. 7, p. 941–952.
- Walker, G.W., 1950, Sierra Blanca Limestone in Santa Barbara County, California: California Division of Mines Special Report 1-A, 5 p.
- Weaver, D.W., 1965, Summary of Tertiary stratigraphy, western Santa Ynez Mountains, in Weaver, D.W., and Dibblee, T.W., Jr., leaders, *Western Santa Ynez Mountains, Santa Barbara County, California*: Coast Geological Society—Society of Economic Paleontologists and Mineralogists, Pacific Section, Guidebook, p. 16–30.

- Whidden, K.J., Bottjer, D.J., Lund, S.P., and Sliter, W.V., 1993, Active margin carbonates as indicators of tectonism: evidence from Paleogene limestones in the Western Transverse Ranges, California [abs.]: Geological Society of America Abstracts with Programs, v. 25, no. 6, p. A-63.
- 1995a, Paleogeographic implications of Paleogene shallow-water limestones in southern San Rafael Mountains, California, *in* Fritsche, A.E., ed., Cenozoic paleogeography of the western United States—II: Society of Economic Paleontologists and Mineralogists, Pacific Section, Book 75, p. 193-211.
- Whidden, K.J., Lund, S.P., and Bottjer, D.J., 1995b, Extension of the western Transverse Ranges zone of Cenozoic tectonic block rotations north of the Santa Ynez fault, California, *in* Fritsche, A.E., ed., Cenozoic paleogeography of the western United States—II: Society of Economic Paleontologists and Mineralogists, Pacific Section, Book 75, p. 181-192.
- Williams, G.L., and Bujak, J.P., 1985, Mesozoic and Cenozoic dinoflagellates, *in* Bolli, H.M., Saunders, J.B., and Perch-Nielsen, K.E., eds., Plankton stratigraphy, Cambridge, U.K., Cambridge University Press, p. 847-965.
- Yaldezian, J.G., Popelar, S.J., and Fritsche, A.E., 1983, Movement on the Nacimiento fault in northern Santa Barbara County, California, *in* Anderson, D.W., and Rymer, M.J., eds., Tectonics and sedimentation along faults of the San Andreas system: Society of Economic Paleontologists and Mineralogists, Pacific Section, p. 11-15.



---

# SELECTED SERIES OF U.S. GEOLOGICAL SURVEY PUBLICATIONS

---

## Periodicals

**Earthquakes & Volcanoes** (issued bimonthly).

**Preliminary Determination of Epicenters** (issued monthly).

## Technical Books and Reports

**Professional Papers** are mainly comprehensive scientific reports of wide and lasting interest and importance to professional scientists and engineers. Included are reports on the results of resource studies and of topographic, hydrologic, and geologic investigations. They also include collections of related papers addressing different aspects of a single scientific topic.

**Bulletins** contain significant data and interpretations that are of lasting scientific interest, but are generally more limited in scope or geographic coverage than Professional Papers. They include the results of resource studies and of geologic and topographic investigations, as well as collections of short papers related to a specific topic.

**Water-Supply Papers** are comprehensive reports that present significant interpretive results of hydrologic investigations of wide interest to professional geologists, hydrologists, and engineers. The series covers investigations in all phases of hydrology, including hydrology, availability of water, quality of water, and use of water.

**Circulars** present administrative information or important scientific information of wide popular interest in a format designed for distribution at no cost to the public. Information is usually of short-term interest.

**Techniques of Water-Resources Investigations Reports** are papers of an interpretive nature made available to the public outside the formal USGS publications series. Copies are reproduced on request unlike formal USGS publications, and they are also available for public inspection at depositories indicated in USGS catalogs.

**Open-File Reports** include unpublished manuscript reports, maps, and other material that are made available for public consultation at depositories. They are a nonpermanent form of publication that may be cited in other publications as sources of information.

## Maps

**Geologic Quadrangle Maps** are multicolor geologic maps on topographic bases in 7 1/2- or 15-minute quadrangle formats (scales mainly 1:24,000 or 1:62,500), showing bedrock, surficial, or engineering geology. Maps generally include brief texts; some maps include structure and columnar sections only.

**Geophysical Investigations Maps** are on topographic or planimetric bases at various scales, showing the results of surveys using geophysical techniques, such as gravity, magnetic, seismic, or radioactivity, which reflect subsurface structures that are of economic or geologic significance. Many maps include correlations with the geology.

**Miscellaneous Investigations Series Maps** are on planimetric or topographic bases of regular and irregular areas at various scales; they present a wide variety of format and subject matter. The series also includes 7 1/2-minute quadrangle photogeologic maps on planimetric bases that show geology as interpreted from aerial photographs. The series also includes maps of Mars and the Moon.

**Coal Investigations Maps** are geologic maps on topographic or planimetric bases at various scales, showing bedrock or surficial geology, stratigraphy, and structural relations in certain coal-resource areas.

**Oil and Gas Investigations Charts** show stratigraphic information for certain oil and gas fields and other areas having petroleum potential.

**Miscellaneous Field Studies Maps** are multicolor or black-and-white maps on topographic or planimetric bases of quadrangle or irregular areas at various scales. Pre-1971 maps show bedrock geology in relation to specific mining or mineral-deposit problems; post-1971 maps are primarily black-and-white maps on various subjects, such as environmental studies or wilderness mineral investigations.

**Hydrologic Investigations Atlases** are multicolored or black-and-white maps on topographic or planimetric bases presenting a wide range of geohydrologic data of both regular and irregular areas; the principal scale is 1:24,000, and regional studies are at 1:250,000 scale or smaller.

## Catalogs

Permanent catalogs, as well as some others, giving comprehensive listings of U.S. Geological Survey publications are available under the conditions indicated below from USGS Map Distribution, Box 25286, Building 810, Denver Federal Center, Denver, CO 80225. (See latest Price and Availability List.)

“**Publications of the Geological Survey, 1879–1961**” may be purchased by mail and over the counter in paperback book form and as a set of microfiche.

“**Publications of the Geological Survey, 1962–1970**” may be purchased by mail and over the counter in paperback book form and as a set of microfiche.

“**Publications of the U.S. Geological Survey, 1971–1981**” may be purchased by mail and over the counter in paperback book form (two volumes, publications listing and index) and as a set of microfiche.

**Supplements** for 1982, 1983, 1984, 1985, 1986, and subsequent years since the last permanent catalog may be purchased by mail and over the counter in paperback book form.

**State catalogs**, “List of U.S. Geological Survey Geologic and Water-Supply Reports and Maps For (State),” may be purchased by mail and over the counter in paperback booklet form only.

“**Price and Availability List of U.S. Geological Survey Publications**,” issued annually, is available free of charge in paperback booklet form only.

**Selected copies of a monthly catalog** “New Publications of the U.S. Geological Survey” is available free of charge by mail or may be obtained over the counter in paperback booklet form only. Those wishing a free subscription to the monthly catalog “New Publications of the U.S. Geological Survey” should write to the U.S. Geological Survey, 582 National Center, Reston, VA 22092.

**Note.**—Prices of Government publications listed in older catalogs, announcements, and publications may be incorrect. Therefore, the prices charged may differ from the prices in catalogs, announcements, and publications.

